

University of Alberta

Hydrous Silicate Melts: A new Growth Medium for Diamond?

by

Andrew Jeffrey Fagan



A thesis submitted to the Faculty of Graduate Studies and Research
in partial fulfillment of the requirements for the degree of

Master of Science

Department of Earth and Atmospheric Sciences

Edmonton, Alberta
Spring 2009



Library and Archives
Canada

Published Heritage
Branch

395 Wellington Street
Ottawa ON K1A 0N4
Canada

Bibliothèque et
Archives Canada

Direction du
Patrimoine de l'édition

395, rue Wellington
Ottawa ON K1A 0N4
Canada

Your file *Votre référence*
ISBN: 978-0-494-54678-9
Our file *Notre référence*
ISBN: 978-0-494-54678-9

NOTICE:

The author has granted a non-exclusive license allowing Library and Archives Canada to reproduce, publish, archive, preserve, conserve, communicate to the public by telecommunication or on the Internet, loan, distribute and sell theses worldwide, for commercial or non-commercial purposes, in microform, paper, electronic and/or any other formats.

The author retains copyright ownership and moral rights in this thesis. Neither the thesis nor substantial extracts from it may be printed or otherwise reproduced without the author's permission.

AVIS:

L'auteur a accordé une licence non exclusive permettant à la Bibliothèque et Archives Canada de reproduire, publier, archiver, sauvegarder, conserver, transmettre au public par télécommunication ou par l'Internet, prêter, distribuer et vendre des thèses partout dans le monde, à des fins commerciales ou autres, sur support microforme, papier, électronique et/ou autres formats.

L'auteur conserve la propriété du droit d'auteur et des droits moraux qui protègent cette thèse. Ni la thèse ni des extraits substantiels de celle-ci ne doivent être imprimés ou autrement reproduits sans son autorisation.

In compliance with the Canadian Privacy Act some supporting forms may have been removed from this thesis.

While these forms may be included in the document page count, their removal does not represent any loss of content from the thesis.

Conformément à la loi canadienne sur la protection de la vie privée, quelques formulaires secondaires ont été enlevés de cette thèse.

Bien que ces formulaires aient inclus dans la pagination, il n'y aura aucun contenu manquant.


Canada

Table of Contents

		Page
Dedication		
Abstract		
Acknowledgements		
List of Tables		
List of Figures		
Chapter 1	Natural Diamonds and Experimental Research: a context for this study	
	Morphology	2
	Mineral Inclusions and geothermobarometry	5
	Fluid & melt inclusions	10
	Models of Diamond Formation	11
	Synthetic Diamonds	16
	Experimental Research	18
	Summary	30
	References	32
Chapter 2	Hydrous Silicate Melts: A new medium for diamond formation?	
	Introduction	42
	Diamond Formation studies	44
	Starting Materials	47
	Experimental Techniques	50
	Results	56
	Discussion	64
	Application to Natural growth	66
	Conclusions	70
	References	71
Chapter 3	An XRD and SEM catalogue of growth, resorbtion, surface features and morphology	
	Experimental Run tables	77
	XRD diffractograms	78
	Diamond Seed Images	81
	SEM photographs of diamond growth	82

Dediction

This thesis is dedicated to my Friends - all of you provided inspiration and help:

Sarah Shore, Alison Craig, Richard Waterworth, Walter Loogman, Hilary Corlett, Christine Dow & Heather Schijns

My deepest thanks goes out to you all.

Abstract:

Natural peridotitic diamonds form in the 'diamond window' (DFW), an area of the upper mantle bounded by temperatures of 900-1400°C and pressures between 4 and 7 GPa. This study has experimentally tested and shown the viability of a hydrous, halide bearing silicate melt as a possible diamond growth medium.

Many mechanisms have been suggested for diamond growth in the Earth's mantle, and despite much work in the last 40 years, this issue is still unresolved. Experimental petrology can help to determine the effect of different chemical constituents on diamond growth. Many systems have been investigated, including carbonate, sulphide and silicate. We have conducted experiments in the system MgO-SiO₂-C-H₂O to test the efficacy of a hydrous silicate melt (HSM) in nucleating and growing diamond, in a C-saturated system. Natural diamonds have been found to contain alkali halides within their fluid inclusions; these trapped 'brine-like' mantle fluids have been cited as 'diamond forming fluids'. For this reason, we have also evaluated the effect of alkali halides in catalyzing diamond-forming reactions by investigating the addition of KCl and NaCl. Previous studies in carbonate bearing systems have concluded that alkali halides have a catalytic effect on diamond formation reactions; this study tests the extension of this proposal to hydrous silicate melts.

Experiments were conducted in a multi-anvil apparatus housed within the C.M. Scarfe Laboratory for Experimental Petrology at the University of Alberta. In these experiments, diamond was successfully grown on seed crystals at temperatures of 1400-1600°C and pressures of 7 GPa, over 4 hour durations.

The HSM precipitated diamonds coexisting with enstatite and forsterite crystals in a simplified upper mantle assemblage. H₂O plays an important role in the diamond forming reaction. The presence of H₂O lowered the silicate solidus and allowed melting to occur at lower temperatures. This is especially relevant for experiments bounded by the physical conditions within the diamond window. Spontaneous nucleation of diamond was observed during the course of these experiments along with the formation of diamond coats, <10µm thick, created by the amalgamation of numerous single octahedral crystals. The addition of KCl, to the HSM system enabled diamond to form 200°C cooler than the previously published minimum experimental temperature. We observed that temperature is critical to the formation of diamond. The presence of the KCl likely affects the diffusion rate of carbon, allowing diamond growth to proceed at a lower temperature. KCl shows a clear effect on diamond growth, producing larger crystals at a lower temperature compared to an un-fluxed system. The NaCl system is different; in these experiments the diamond seed crystals show triangular and hexagonal etch pits, a common feature of resorption on natural stones and facets with small dissolution holes spread homogeneously over the surface of the seeds. Thus we suggest that NaCl is a possible diamond growth inhibitor within a silicate growth system.

This experimental study demonstrates that hydrous silicate melts, especially containing K-bearing alkali halides, are a viable medium for diamond growth in the Earth's upper mantle. We suggest that the necessary components used in this study could be present and can easily interact with one another in the sub-continental lithospheric mantle (SCLM), inside an imbricated oceanic slab. The gradual heating of the old slab will cause dehydration and eventually the generation of a HSM at P-T conditions inside the DFW.

Acknowledgements

I would like to acknowledge and thank the following people that provided assistance and help throughout my time at the University of Alberta.

Dr Robert W Luth is sincerely thanked for continually providing excellent supervision throughout the duration of this project. For never giving me an answer, but instead providing enough hints (and books!) for me to work things out for myself - the sign of an excellent graduate studies supervisor. Dr Thomas Stachel is also thanked for the numerous lengthy discussions and assistance he provided throughout the entirety of the project. My time in the DRG will be fondly remembered.

I also would like to thank Dr Jeff Harris for introducing me to the wonderful world of diamonds during my undergraduate at the University of Glasgow, and for persuading me to come to Edmonton for my MSc. Diane Caird for training and assistance using the multi-anvil apparatus and for running my XRD analyses. Sergei Matveev is acknowledged for his help and training in using the electron microprobe. George Braybrook and Rajeev Nair are also sincerely thanked for their efforts on the Scanning Electron Microscope. For her fantastic diamond photographic skills and generous heart in donating pictures for this thesis, Anetta Banas must also be acknowledged.

I must express thanks and sincere gratitude to Steven Creighton, Lucy Hunt, Sonja Aulbach and Katie Smart for numerous lengthy discussions on mantle geochemistry, diamonds and a fresh perspective on many other mantle related topics, your insights were invaluable.

And to my family, far away, but still close.

List of Tables

<i>Chapter 1</i>		<i>Page</i>
Table 1	COH fluid fluxed graphite re-crystallisation experiments	21
Table 2	Carbonate melt fluxed graphite re-crystallisation experiments	23
Table 3	S-bearing systems - graphite re-crystallisation and redox experiments	26
Table 4	Silicate bearing systems - graphite re-crystallisation and redox experiments	27
Table 5	Other diamond growth systems. Mantle catalysts - the effect of alkali halides	28
 <i>Chapter 2</i>		
Table 1	Starting compositions	47
Table 2	Electron microprobe results of experimental quench products	54
Table 3	SiO ₂ -MgO-H ₂ O system	56
Table 4	SiO ₂ -MgO-H ₂ O-C system	57
Table 5	SiO ₂ -MgO-H ₂ O-C-KCl	59
Table 6	SiO ₂ -MgO-H ₂ O-C-NaCl	61
Table 7	SiO ₂ -MgO-H ₂ O-C-KCl-NaCl	64
 <i>Chapter 3</i>		
Table 1	Experimental run table	77

List of Figures

<i>Chapter 1</i>		<i>Page</i>
Figure 1A	Spiral growth observed on a graphite crystal	4
Figure 1B	Resorption progression in natural diamonds	4
Figure 2	Mineral inclusion types	6
Figure 3	Peridotitic mineral inclusions within natural diamonds	6
Figure 4	Fluid inclusion compositions	11
Figure 5A	Haggerty's diamond formation model	14
Figure 5B	Taylor and Green's diamond formation model	14
Figure 5C	Kesson and Ringwood's diamond formation model	15
Figure 6	Phase diagram of selected experimental diamond growth studies	20
 <i>Chapter 2</i>		
Figure 1	P-T stability diagram with important phase relationships	43
Figure 2	Phase diagram of selected experimental diamond growth studies	45
Figure 3	Location of starting composition T vs. H ₂ O content	48
Figure 4	Seed diamond photographs	48
Figure 5	Cross-section through experimental assembly	50
Figure 6	Internal view of post-run capsule with layering	52
Figure 7	ternary diagram showing the composition of the quench crystals	55
Figure 8A	Diamond growth in the system SiO ₂ -MgO-H ₂ O-C	57
Figure 8B	Quench melt	57
Figure 9	The effect of KCl on diamond growth	59
Figure 10	Diamond growth in the system SiO ₂ -MgO-H ₂ O-C-KCl	60
Figure 11	Diamond growth in the system SiO ₂ -MgO-H ₂ O-C-NaCl	62
Figure 12	Resorption in system SiO ₂ -MgO-H ₂ O-C-NaCl	63
Figure 13	Dendritic patterns on surface of seed crystals	65
Figure 14	Diamond formation - Imbricated slab model	67
 <i>Chapter 3</i>		
XRD-1	Amorphous nature of the starting composition	78
XRD-2	Spectra of the starting compositions	79
XRD-3	Close-up of starting composition 8 (KCl bearing)	79
XRD-4 & 5	Comparison of start composition and quench composition	80

<i>Photograph</i>		<i>Page</i>
1	Synthetic diamond seeds	81
2	Synthetic diamond seeds	81
3	SiO ₂ -MgO-H ₂ O-C-KCl system growth overview	82
4	SiO ₂ -MgO-H ₂ O-C-KCl system growth overview	82
5	Close-up of new octahedral diamond layer	83
6	Extensive growth of new octahedral diamonds	83
7	New diamond growth layer - end-on view	84
8	Spiral growth observed on the new growth crystals	84
9	Growth occurring around steps on the seed crystal surface	85
10	Spiral growth and quenched melt	85
11	Large diamond feature forming under spiral growth conditions	86
12	New octahedral diamonds	86
13	Close-up of post-run diamond seed surface	87
14	Edge of cubo-octahedral crystal	87
15	Hole in diamond seed with new growth inside	88
16	Close-up of hole observed in Figure 15	88
17	Pits and fracturing along a crystal edge	89
18	Edge of a hole, showing new growth	89
19	Normal seed diamond surface	90
20	Growth occurring where rough crystal surface is exposed	90
21	Octahedral crystal growth alongside graphite	91
22	Irregular cubo-octahedral and octahedral growth	91
23	Smooth seed surface shows no growth	92
24	Edge growth of new diamond	92
25	Pre-existing dendritic texture on diamond seeds	93
26	Pre-existing dendritic texture on diamond seeds	93
27	Low magnification image of dendritic patterns and new growth	94
28	Sub micron growth of new diamonds	94
29	Smooth facets and rough edges	95
30	Octahedron crystallising on rough surface	95
31	Nano-layering of new diamonds and KCl crystals	96
32	Inside a post-run capsule, extensive layering	96
33	Negative Trignons, diamond dissolution and resorption	97
34	Very rough surface on diamond seed	97
35	No growth on the seed faces	98
36	Dissolution hexagonal pits	98

<i>Photograph</i>		<i>Page</i>
37	Graphitic coated lower seed surface	99
38	Stacked octahedral crystals making up new layer	99
39	Extensive growth of new octahedral diamonds	100
40	Close-up of new octahedral diamond layer and octahedra	100
41	Large octahedral diamond grown by spiral growth	101
42	Layer of graphite around new diamond growth area	101
43	Melt/diamond interface has rough surface and new crystals	102
44	Negative Trigons close-up	102
45	Negative trigon formation in NaCl bearing run	103
46	Dissolution holes on surface of diamond seed	103
47	Stacking of octahedral crystals to form new layers	104
48	Stacked octahedral crystals making up a new layer	104
49	Fracture surface with extensive new micron diamonds	105
50	Growth enhancing rough layer after experimentation	105
51	Isolated pod growth on the seed surface	106
52	New surface layer	106
53	Graphitic coated lower seed surface	107
54	Mixture of graphite and diamond coat	107
55	Close-up of seed surface	108
56	Two distinct layers of diamond growth on the seed surface	108
57	NaCl and KCl salts crystallised on the surface of the seed	109
58	Diamond formation inside a hole	109
59	Non catalysed system - with measurements of new growth	110
60	Quench phases seen under SEM	110

Chapter One

*Natural diamonds and experimental
research: a context for this study*

The genesis of natural diamonds remains an enigma. The results of studies of natural diamond can be used to constrain experimental research with an aim of simulating the formation of 'natural diamond' in a laboratory setting. To this end, this chapter will combine research from gemmology, geochemistry, high-pressure high-temperature experimental mineralogy and the study of mantle evolution to reassess the diamond formation question.

Diamond is the high-pressure polymorph of carbon. It is formed deep within the Earth's mantle and is only found at the surface within unusual igneous rocks or in sedimentary placers, remnants of these igneous hosts. These magmatic bodies entrained the diamonds on their ascent from the mantle, bringing them to the surface as xenocrysts. Exceptional diamond formation does occur, e.g. within ultra-high-pressure metamorphic belts (UHP) such as observed in Kazakhstan (Sobolev and Shatsky 1990) or Norway (Dobrzhinetskaya et al. 1995) or by impact of a bolide on Earth (DeCarli and Jamieson 1961); these however represent rare occurrences and the formation of diamond in the mantle should be considered the norm.

Diamond is valued both as a gemstone and as an industrial mineral and has a mining history that dates back into antiquity. It is the hardest naturally occurring mineral, making it useful as an industrial abrasive, e.g. for rotary drill-bits, rock-saws etc. It has excellent thermal conductivity, a key property used by the high-tech electronics industry where they use diamond as heat-sinks within computer chips. However, it is as a gemstone that the true 'value' of diamond is evident. Properties such as transparency, high refractive index and durability (because of its hardness) have made diamond the most highly prized of all gemstones.

There has been extensive research on diamond, and comprehensive review articles detailing

all of its properties are available in Harris (1992) and Meyer (1987). This chapter first looks at diamond as a mantle mineral, its morphology, its mineral and fluid inclusions, geothermobarometry and then will look at the various ways by which diamond may form, in nature and in the laboratory. We do not know how diamonds form in the Earth's mantle; this chapter will review current progress towards answering that question. By using the known properties on natural diamond and the pressure-temperature conditions of its origin as reference points, we can begin to test experimentally the various theories and models of diamond formation.

Morphology

Morphology was one of the first properties ever recorded about natural diamonds and is still one of the most important. Morphology, the description of the crystal shape, records information about the events that formed and changed the diamond – such as plastic deformation, resorption or the addition of a colour-centre. There are several major reference works for the morphology of diamond; the first written by Fersman and Goldschmidt (1911) entitled “Der Diamant” and another by Robinson (1979) as part of his unpublished PhD thesis from the University of Cape Town. To understand how natural diamond grows in the mantle we must understand how the crystal is formed and the various shapes that it can take.

The mechanism by which diamond crystals grow is no different to how other common mineral phases crystallise out of a fluid or a melt. Numerous authors have investigated the physical method by which diamonds nucleate and grow, these include Genshaft et al. (1977), Harrison and Tolansky (1964), Lang (1979), Seal (1962), Sunagawa (1984b) and a review paper by Bulanova (1995). The habit of the crystal reveals information on the mechanism

responsible for growth. Smooth diamond surface faces such as the {111} has very densely packed, slowly grown spiral layers, and is the only face on the diamond able to grow in this fashion (Hartman and Perdok 1955; Sunagawa 1984b). This method is dissimilar to the atomically 'rough' {100} face which is not expected to have largescale growth occurring by the slow spiral growth mechanism observed on the {111} face, but may have growth created by the faster 'rough' growth mechanism (Bulanova 1995; Sunagawa 1984b). This mechanism relies on the presence of dislocations on a surface; these dislocations are able to act as nucleation sites.

Diamond growth also requires the presence of a fluid or melt that is super-saturated in carbon; the degree of this super-saturation dictates the style of observed growth. This solution will form a highly reactive layer, or film, around a seed crystal, or newly forming diamond. In a weakly super-saturated solution the growth is tangential to the crystal faces and occurs on the {111} face, this growth is controlled by vacancies and crystal dislocations and forms interlocking layers by spiral growth. In strongly super-saturated conditions the growth is very rapid, enabling growth on atomically rough surfaces and creating 'dendritic' surface patterns. This growth style is easily observed on the surfaces of HPHT synthetic diamonds (Bulanova 1995) . Only slow spiral growth will create the smooth faces and perfect crystals seen on diamond gemstones (Sunagawa 1984a).

What does a newly grown diamond look like? To assess growth versus resorption and to enable the recognition of new diamond growth, knowledge of the primary diamond habits and the effect of resorption are crucial. Fersman and Goldschmidt (1911) and Robinson (1979) studied the morphology of natural diamonds and surface features related to growth and resorption and identified several key features. Growth is primarily observed as small individual octahedral crystals or as a thin growth layer on-top of a pre-existing diamond

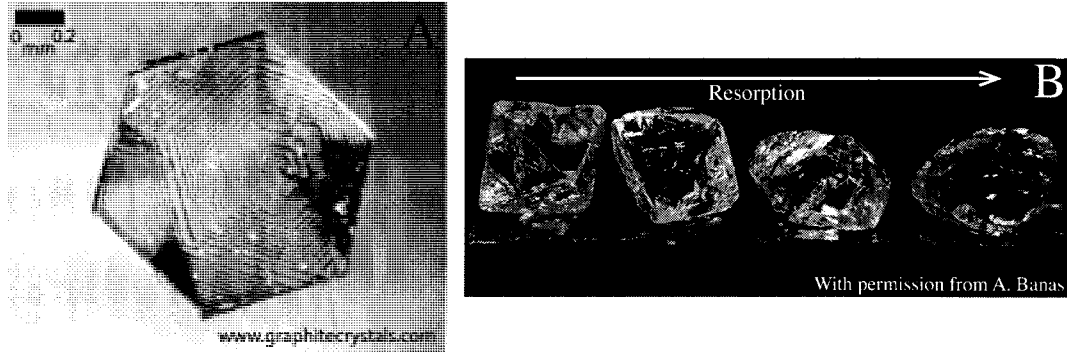


Figure 1A: Spiral Growth observed in a graphite crystal.

Figure 1B: Resorption progression, adapted from T Stachel, (personal comm, 2008). Arrow displays increasing resorption in octahedral crystals. Image taken by Anetta Banas, University of Alberta Diamond Research Group on samples from the DeBeers diamond display, University of Alberta.

substrate. These layers will be crystallographically aligned to the lattice of a seed crystal. Otherwise growth will form as a surface coat of stacked octahedral crystals similar to that observed in polycrystalline diamonds. Resorption, the dissolution of diamond, can be observed by the presence of trigons or dissolution holes in the diamond (Robinson 1979). ‘Trigons’ are equilateral triangular etch-pits with a pyramidal or flat base. They have been reproduced experimentally by chemical etching of the diamond surface (Frank and Lang 1965). It may be possible, however, for the same fluid to promote growth on a low-energy crystal face and cause resorption on a high-energy face at the same time. Fig 1 shows examples of growth and resorption features on natural diamond.

Fig 1B shows the commonest type of primary habit – an octahedron – although other primary habits exist, including cubes and surface coats. These coats represent thin layers of rapidly grown diamond and typically contain millions of sub-micron fluid inclusions, creating a cloudy surface on an otherwise gemmy diamond. The morphology of these coats is different

to any other type of diamond growth; instead of the slow spiral mechanism displayed on the {111} faces of gem diamonds, the coat will form as a series of stacked layers that are not aligned with the original diamond lattice. Examination of the diamond morphology within these fibrous overcoats has shown that they have affinity to the continuous growth regime, clearly seen by the lack of smooth interfaces and poor crystal shapes within the coat. Diamond growth in this form is likely to represent rapid crystallisation in a strongly oversaturated fluid or melt. We will return to the importance of this morphological evidence later in this chapter when we address fluid inclusions.

Cathodoluminescent studies on the internal morphology of natural diamonds have shown them to have complex histories of resorption and growth (Fitzsimons et al. 1999; Harte et al. 1999). However, these growth zones are often truncated by newer growth layers, showing that a period of non-growth or resorption occurred between the two growth events. Thus some macrodiamonds form in a very complex chemical system, which is capable of promoting and then inhibiting growth.

Mineral Inclusions

Mineral inclusions are small (typically less than 200 μm) fragments of mantle minerals trapped inside a diamond (Fig 2). These minerals have received extensive attention; notable reviews include those by Meyer (1987), Harris (1992) and Stachel et al. (2004). Debate still surrounds these inclusions and exactly what they may represent. They could be syngenetic (Fig 2a), i.e. forming at the same time as the diamond, or they could have formed before the diamond-forming event (Fig 2b). In most of the literature, the inclusions have been interpreted to be syngenetic.

Seminal work was undertaken in the 1970's to characterise the properties and geochemistry of these inclusions (Harris and Gurney 1979; Meyer and Boyd 1977; Sobolev 1977; Sobolev et al. 1976). This research led to the discovery of three distinct mineral associations, termed parageneses, two of which are related to the two main diamond bearing upper mantle rocks – peridotite and eclogite.

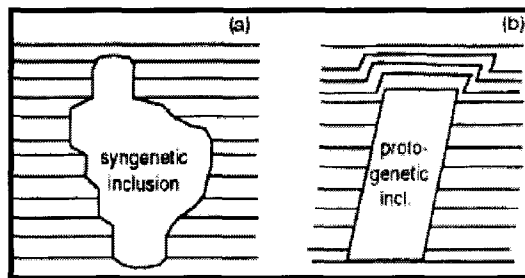


Figure 2: Types of mineral inclusions. After Bulanova (1995). Showing layers of diamond growth relative to the edges of the inclusion.

Diamonds of the peridotitic paragenesis (Fig. 3) make up the bulk of diamonds mined in the world today. This paragenesis is defined by inclusions of olivine, orthopyroxene, spinel, and garnet, which are similar in composition to minerals observed in peridotitic mantle rocks. The chemistry of these minerals is different to their counterparts in the eclogitic paragenesis,

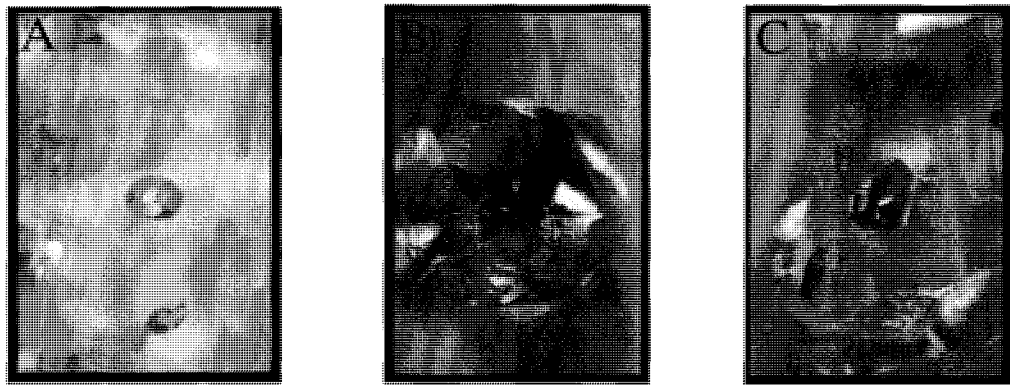


Figure 3: Photographs of South African peridotitic diamonds showing common inclusions, Photos from Fagan (unpub. BSc).

A) shows an peridotitic-olivine inclusion 0.5mm diameter

B) resorbed diamond with a sulphide inclusion at its core. Diamond is 2mm diameter.

C) semi-exposed p-type garnet inclusion, inclusion diameter ~0.25mm.

which usually consists of garnet, clinopyroxene and rutile. The eclogitic garnets have less Mg than their peridotitic counterparts. The lower Cr content of eclogitic clinopyroxenes leaves the mineral a pale green colour compared to the intense 'bottle' green typical of peridotitic clinopyroxenes, for review see Stachel and Harris (2008). The inclusions of peridotitic paragenesis can be subdivided further using classifications common to peridotites – the harzburgitic subdivision contains no clinopyroxene, whereas the lherzolithic one does. An unusual, and volumetrically minor, websteritic paragenesis occupies the compositional space low in olivine and high in clinopyroxene and orthopyroxene.

Both parageneses can contain inclusions of graphite, sulphide or diamond. A third, 'undetermined' paragenesis was defined by Harris (1992) to encompass a number of unusual mineral phases being discovered as diamond inclusions. These included known lower mantle and transition zone minerals such as ferropericlase and silicate perovskite; opening up the possibility of very deep diamond genesis, below the normal upper mantle formation window. The remainder of this review will concentrate on the majority of 'normal' upper mantle inclusions in diamonds, however for details on these unusual mineral inclusions see published review by Stachel et al. (2005).

As well as defining the chemistry of the diamond source regions, the mineral inclusions also allow the use of geothermometers and geobarometers to characterise the temperature and pressure at which the inclusion, and by inference, the diamond, was crystallising. This is useful because conducting experimental research to test the viability of the various mantle fluids or melts as diamond forming/diamond destructive agents requires constraining a region in P-T space that accurately reflects the actual P-T conditions at which natural diamonds are formed.

Geothermometers are temperature-dependant chemical reactions, where elements exchange between two or more distinct mineral phases depending on the temperature. Two types of geothermobarometer have been developed; the traditional multi-mineral, and the newer single mineral variety; both types rely on elemental exchange reactions. Elemental exchange geothermometers occur in two varieties, one involves the Fe-Mg exchange reaction between ferromagnesian minerals such as olivine, orthopyroxene and garnet (Ellis and Green 1979; Harley 1984; Krough 1988; O'Neill 1980; O'Neill and Wood 1979). For example, a commonly used geothermometer in diamond research is the exchange of Fe and Mg between opx and garnet (Harley 1984). This is strongly temperature dependant and provides a useful thermometer for use in garnet peridotite assemblages, a common diamond bearing rock and for use in diamond inclusion work, where inclusions of orthopyroxene and garnet co-exist within the same diamond.

The other common geothermometer uses the pyroxene solvus and calculates temperature based on the composition of coexisting orthopyroxene & clinopyroxene (Bertrand and Mercier 1985; Brey and Köhler 1990; Lindsay and Anderson 1983). The most commonly used pyroxene solvus geothermometer (Brey and Köhler 1990) has shown to be a powerful tool for assessing equilibration temperatures in lherzolite assemblages (Nimis and Taylor 2000). This thermometer is used in diamond research most effectively where a pair of clinopyroxene/orthopyroxene inclusions are in physical contact within the same diamond.

The single mineral exchange thermometer is based on the enstatite content in clinopyroxene and the barometer is based on the chrome content of clinopyroxene (Nimis and Taylor 2000). The thermometer assumes equilibration between clinopyroxene and orthopyroxene, although only the clinopyroxene composition is actually measured, thus increasing the

intrinsic error. Because of the assumed equilibration with garnet and orthopyroxene in the barometer it is only applicable to garnet peridotitic systems and unfortunately cannot be applied to eclogitic assemblages or to eclogitic mineral inclusions. However, despite these limitations, the single mineral technique provides the possibility of calculating P-T projections for diamonds with single peridotitic inclusions of clinopyroxene rather than relying on rare diamonds with ferromagnesian inclusion pairs.

After analysis of numerous diamond inclusion suites, from all over the world, Harris (1992) and Meyer (1987) concluded that the 'diamond window' or the 'diamond formation region' must lie between 900°C and 1400°C.

Appropriate reactions that act as geobarometers are more rare, but essentially rely on the same partitioning behaviour of elements as observed in geothermometers, except the key physical parameter is pressure, not temperature. To date, no appropriate pressure-dependant reactions have been identified for use in eclogitic assemblages. A commonly used and well-tested peridotitic barometer uses the partitioning of Al between orthopyroxene and garnet (Brey and Kohler 1990). Application of this geobarometer to diamond inclusions worldwide, including Canada (Tappert et al. 2005), Tanzania (Stachel et al. 2005) and South Africa (Phillips et al. 2004) have consistently defined a pressure window of 4-7GPa, corresponding to 130-220km depth.

In summary, the chemical characterisation of natural diamond inclusions, and the accurate pressure and temperature conditions recorded by the various exchange reactions, define where in the upper mantle natural diamonds formed. This "diamond window" exists between 900°C-1400°C and 5-7GPa.

Fluid / Melt inclusions:

Inclusions in diamond, other than minerals, have also been documented. Fluid and melt inclusions have also been studied from a number of localities including Canada, South Africa and Botswana (Izraeli et al. 2001; Klein-BenDavid et al. 2007; Schrauder and Navon 1994). These workers suggest that these fluids represent 'diamond forming fluids' (Navon 1998); and thus record the material from which diamond precipitated. These inclusions fall into two categories; the first – diamond coats - are found almost exclusively within cloudy or fibrous diamonds. These coated/fibrous diamonds have a thin layer of diamond around a pristine core, the coat itself contains millions of sub-micron fluid/melt inclusions, creating a white cloudy layer around the gem diamond. The second category are discrete inclusions, these are single inclusions that have a distinct shape, and are large enough to be analysed – much like the discrete solid-state inclusions discussed earlier. These commonly do not form cloudy coats, but instead represent pristine trapped fluids within the diamond (Navon 1991). The origins of the fibrous cloudy coat, and the fluids they contain have been linked to kimberlite entrainment and transport, i.e. they probably represent trapped volatiles associated with the kimberlite magma and developed upon entrainment.

Recently, the geochemistry of these inclusions was published (Izraeli et al. 2001; Klein-BenDavid et al. 2004; Kopylova et al. 2008; Navon et al. 2004; Navon et al. 2008; Weiss et al. 2008), Fig 4. These workers defined three end-member compositions; a K-Cl-H₂O 'brine', an Al-rich hydrous silicate melt, and a Na-Ca-Mg-Fe bearing carbonatitic fluid. These H₂O rich fluids span a large compositional range with the two distinct arrays representing a possible miscibility gap between the halide and silicate endmembers (Klein-BenDavid et al. 2004; Klein-BenDavid et al. 2007; Safonov et al. 2008).

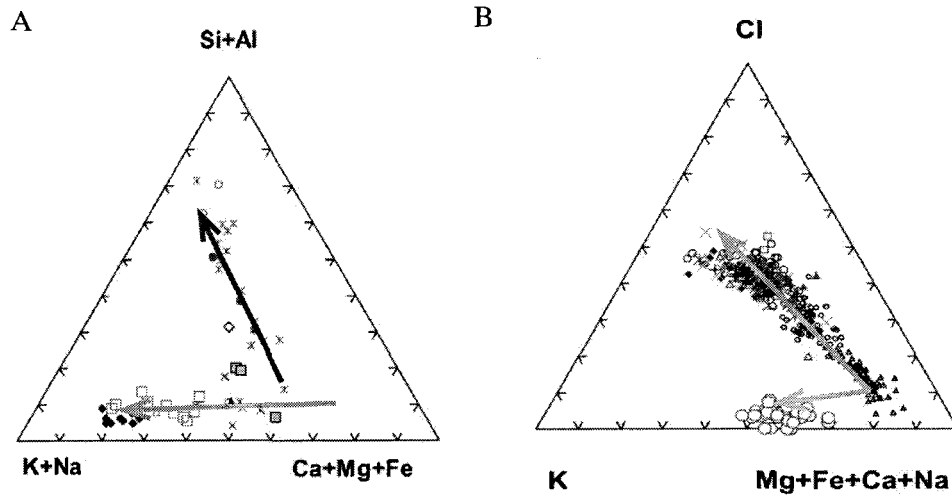


Figure 4: Adapted from Klein Ben-David (2007).

A: Fluid compositions from inclusions in diamonds. Two distinct arrays are shown by arrows, projecting from a carbonatitic endmember towards a K+Cl endmember (green), and an aluminous-hydrous silicate endmember (red).

B: Blue arrows shows the high levels of both K and Cl in these diamond fluids.

Models of Diamond Formation

Models of diamond formation are abundant in the literature, most of which derive from observations on natural stones – morphology, isotopes, geothermobarometry, mineral and fluid inclusion geochemistry etc. Key models began to enter the literature in the mid-1980's. The first of these was by Boyd and Gurney (1986) for the Kaapvaal craton of southern Africa, and modelled its relationship to the diamond stability field and the numerous kimberlite localities on the cratonic surface. They furthered a proposal (Jordan 1979), in which an Archean craton has a deep underlying keel, analogous to an iceberg in the ocean. This model is simple, it suggests that over-thickened lithosphere keels form under ancient cold cratons, and in some areas these keels descend below the graphite

to diamond transition (Kennedy and Kennedy 1976) and thus are potentially diamond stable. This is important because the cratonic keels offer a stable environment in which the diamonds can grow. How diamonds may form in this 'cratonic root' environment was addressed by numerous authors in the following few years.

The Haggerty (1986) diamond formation model (Fig 5a) takes the cratonic root zones of Boyd and Gurney (1986) and suggests that overall the keel is reduced relative to a more oxidised asthenosphere. The influx of oxidised partial melts or fluids from the asthenosphere into the lower parts of the lithospheric keel causes reduction of carbonate bearing melts or fluids upon contact with the lithosphere, releasing carbon, which at the right P, T and oxygen fugacity (fO_2) conditions would form diamond. The source of the oxidised fluid/melt was not specified.

In contrast, Taylor and Green (1988) proposed a reduced asthenosphere underlying a relatively oxidised lithosphere (Fig 5b). These reactions would still be controlled by the fO_2 of the surrounding assemblage. Their model invokes CH_4 fluids entering the cratonic keel, where they would be oxidised, releasing C to form cratonic diamonds. Problems also exist with this model; for example the CH_4/H_2O ratio will dictate the temperatures at which melting would begin. If this ratio were low, melting would occur at temperatures greater than normal continental geotherms, even in the presence of a hydrous phase. These two models are essentially arguing the same point from different sides – that the fO_2 of the surrounding assemblage controls the redox formation of diamond in the cratonic keels and that diamond precipitates from the fluid or melt because of a redox reaction.

In 1989, as part of their 'slab-mantle interactions' series of papers, Ringwood and Kesson proposed a new environment for diamond genesis, away from the cratonic keels of the

previous models – a subduction zone (Fig 5c) (Kesson and Ringwood 1989). Their original model tried to explain the eclogitic paragenesis mineral inclusions by having the diamonds precipitate directly in the subducting slab, or in the overlying peridotitic mantle that would be rich in ‘eclogitic’ fluids. A subduction zone enables serpentine minerals within the ultramafic part of the subducting slab to be transported deep into the upper mantle (Ulmer and Trommsdorff 1995). The eventual dehydration of these minerals would release significant volumes of water into the overlying eclogitic part of the slab and the mantle wedge, causing refertilisation of the peridotites and lowering the solidus of the entire silicate assemblage, transforming carbon into diamond at the same time. Kesson & Ringwood (1989) suggest the source of the carbon to be biogenic carbonate from the subducted oceanic plate.

Another new model was generated with the discovery of cloudy and fibrous natural diamonds, rich in fluid micro-inclusions (Navon 1991). In this model, the fluid inclusions trapped within the diamonds directly represent the original diamond-forming medium. These fluids represent a brine-like substance with three definite end-member compositions – a carbonatitic fluid, a Cl-rich brine and a hydrous silicate melt (Izraeli et al. 2001). The interaction between these fluid/melt end-members with the surrounding lithospheric keel assemblage (Haggerty 1986; Taylor and Green 1988) directly precipitates diamond (Fig. 4). However, cloudy and fibrous diamonds are not typical natural samples and are not representative of mantle diamonds generally. These fibrous diamond coats grew rapidly, trapping the fluids, and the internal morphology shows no evidence of the slow ‘spiral-growth’ mechanisms typical of macroscopic gem diamonds (Stachel 2008). Instead, it is likely that these fluids were generated from the kimberlitic magma as it intruded through the cratonic lithosphere (Klein-BenDavid et al. 2007). Thus it appears that using the geochemistry of these coated diamond fluids, as the mantle diamond formation medium is, at this stage, premature.

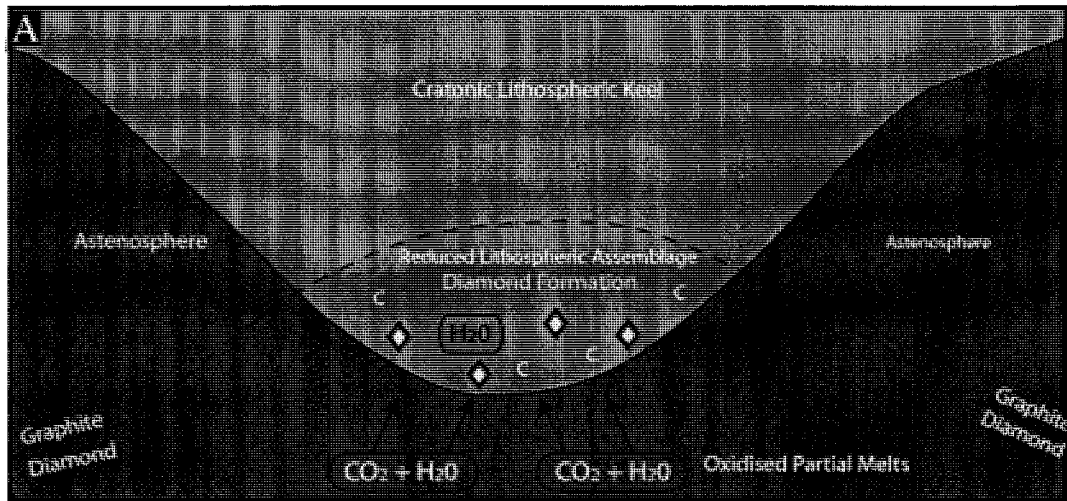
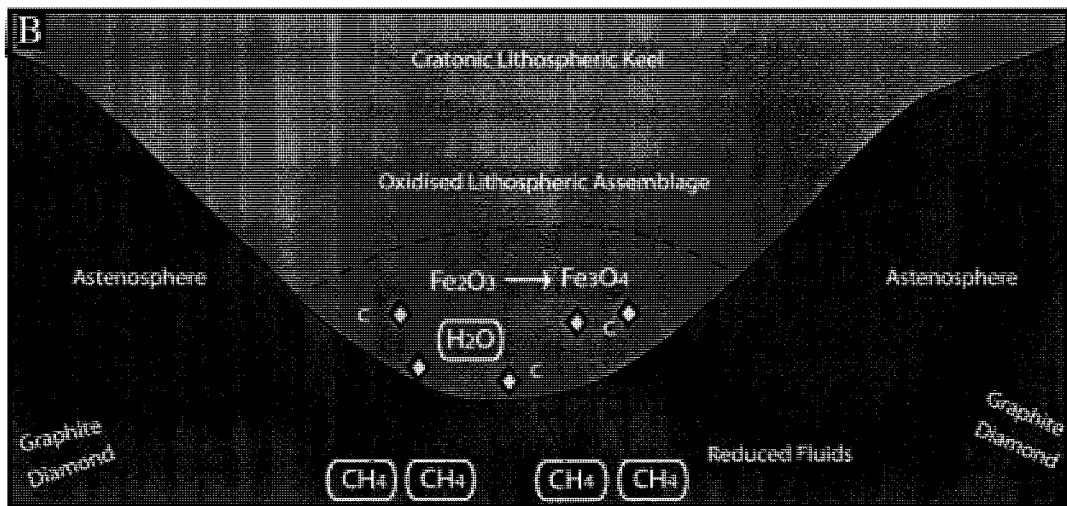


Figure 5: Formation models after Gurney and Boyd, (1986).

A) - Haggerty (1986). Influx of relatively oxidised COH fluids into the reduced cratonic keel.

B): Taylor and Green (1987) - Reduced Mantle assemblage and oxidised lithospheric component.

Both models are heavily reliant on oxygen fugacity and redox exchanges to facilitate diamond growth in the lithospheric keel.



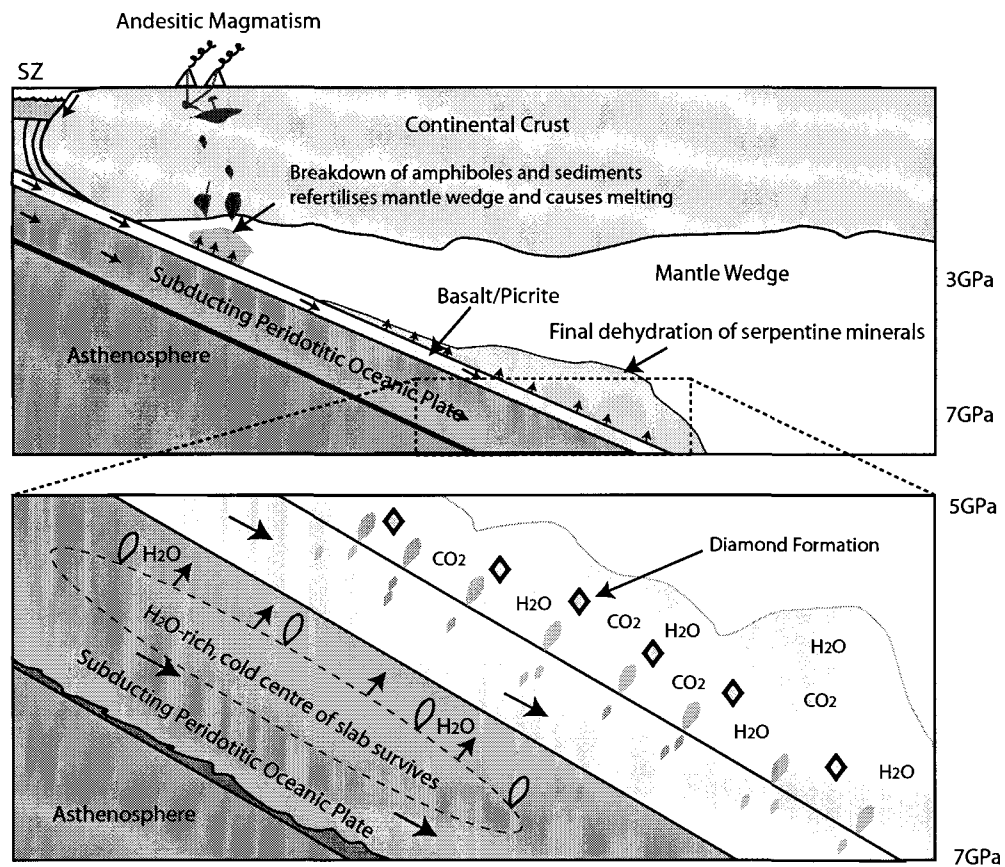


Fig 5c: Kesson and Ringwood (1989) subduction zone model. Dehydration of serpentine in oceanic lithosphere create fluids and promote diamond growth.

The most recent model for the formation of diamond is from Stachel and Harris (2008). Their imbrication model for the formation of cratonic keels, adapted from a model first proposed by Helmstaedt and Schultze (1989), has subducted oceanic plate collecting under stable cratonic crust; providing a place for diamonds and their corresponding fluids to generate and reside. Haggerty (1986) suggested that interstitial sulphide melt in the silicate mantle assemblage may play a crucial role in catalysing diamond formation. The research in this thesis shows the relevance of this imbrication model to diamond formation from hydrous silicate melts as well.

One way to test these models is with experimental petrology, first in simple experimental systems and later, in more complex ‘pseudo-mantle’ assemblages. The use of experimental apparatus for this purpose is not new, key work was begun on the stability and synthesis of diamond in the General Electric laboratories in the 1950’s (Bovenkirk et al. 1959). The first ‘diamonds’ produced experimentally were known as ‘synthetics’ and their production is well documented in both the scientific literature (Bovenkirk 1961; Bovenkirk et al. 1959) and in a popular press book by Hazen (1999).

Synthetic Diamonds

Initially, total synthetic diamond production amounted to a few carats; however, as high pressure-high temperature apparatus design improved, the technique was greatly refined, allowing the production of large gem-quality stones. The drive behind these early experimental studies was financial rather than scientific and was not aimed at reproducing natural conditions of diamond formation, but rather to make good quality large stones that could be sold. The High-Pressure High-Temperature (HPHT) setup required the use of a molten transition metal flux, typically Fe and Ni, and vastly overstepped pressure and temperature conditions before the spontaneous diamond crystals could form. In the mantle, Fe and Ni would have partitioned dominantly into the core during the formation of the earth, e.g. Fei and Lee (2003), and would thus be unavailable to flux diamond genesis. Thus, HPHT grown synthetic diamonds are grown differently to natural samples. Recent developments in commercial diamond growth have introduced a new way to grow industrial diamond – carbon vapour deposition (CVD). This technique layers individual carbon atoms on top of a seed substrate and subsequently on top of each other, building up wafers of diamond. Each layer is precipitated from a carbon plasma, usually heated by a

laser to the required temperature in a near vacuum (Markovic et al. 2002). This metastable growth of diamond at low pressure, as useful as it may be for industrial applications, does not reflect the way natural diamonds can precipitate.

Akaishi et al. (1990) documented diamond growth in a new experimental system without the use of a transition metal flux; instead they used a carbonate system to re-crystallise graphite into diamond. These experiments sparked renewed interest in diamond formation in the mantle and its link to wider mantle processes. At this stage it is important to make the distinction between experimental research aimed at producing diamond, and research aimed at producing diamond *in the same way it is formed within the mantle*. The former process has great application in the field of materials science; however, their results cannot be directly applied to a mantle environment. For mantle researchers, the knowledge that diamond forms at 1900°C and 7.7GPa (e.g. Sato et al. 1999) is not relevant, because the natural diamond window never reaches temperatures this high. The possibility does exist however, that it is simply not possible to generate diamond at the low temperatures recorded by the geothermometry of natural samples in normal experimental timescales. Thus the elevated temperatures simply speed up diamond growth kinetics to a measurable level. With this in mind, the rest of this chapter will try and focus on specific experiments tasked with investigating diamond formation under the physical conditions recorded in natural samples by geothermobarometry, but will include experiments that can show slow growth kinetics.

Experimental Research

The mantle has a very complex chemical environment; to directly model this, taking into account all of the available degrees of freedom would be almost impossible. As a result, simple chemical systems were developed to model the fundamental chemistries of the mantle. These enable researchers to test diamond formation models in a chemical system with lesser complexity (e.g. Litvin and Zharikov 1999). Fig 6 shows the “diamond formation window” (red box), as defined by geothermobarometry on natural samples, this is the ‘P-T target’ area for experimental studies aiming to reproduce natural diamond growth. Plotted on this is a selection of studies taken from Tables 1-5, in various chemical settings that show where most of the diamond growth research has concentrated in P-T space. Importantly, only a few studies have achieved spontaneous diamond growth at P and T conditions within the bounding DFW box.

The location in P-T space of an individual diamond source region, its relationship to its own hydrous solidus and its second critical endpoint are key factors in establishing whether diamond formation occurred in a melt or a fluid phase (Stachel and Harris 2008). To this end, the forsterite+enstatite+H₂O solidus (Stalder et al. 2001) – a simplified peridotitic system - is also shown for reference, as is a ‘normal’ continental geotherm and the mantle adiabat.

Gunn and Luth (2006) categorized studies of diamond growth into three basic types: 1) The re-crystallisation of graphite into diamond using a variety of solvents (COH fluids; carbonate, sulphide or silicate melts), 2) Oxidation of a reduced fluid (such as CH₄) and 3) The reduction of carbonate by a reduced fluid. These latter two can be directly correlated with the diamond formation models of Haggerty (1986) and Taylor and Green (1988).

The first of these types of systems, the re-crystallisation of graphite to diamond, has received the most attention in the literature to date, with numerous solvents being tested. In the absence of a flux, the direct conversion of graphite to diamond (e.g. Yusa et al. 1998) occurs only at very high T, well in excess of mantle conditions (Table 5), lower temperature growth requires a fluid or melt. Previous studies include C-O-H fluids (Table 1) or carbonate melts (both of which can be rich in CO₂, H₂O or CH₄ as shown in Table 2), sulphide melts (Table 3) and silicate melts – both hydrous and anhydrous (Table 4). The effect of various mantle catalysts and the fluxes used in current experimental research is shown in Table 5, with special emphasis on alkali chlorides.

The second and third systems highlighted by Gunn & Luth (2006) show diamond growth by redox-controlled chemical reactions, where the interaction of the lithosphere with infiltrating oxidised fluids (CO₂+H₂O) or reduced ones (CH₄), alter the stability of the carbon phase, rather than trying to directly flux the graphite to diamond transition (Kennedy and Kennedy 1976). These have received little attention compared to the graphite re-crystallisation studies.

A sulphide melt may absorb enough O₂ to reduce carbonate to elemental carbon (Gunn and Luth, 2006). Other studies (Pal'yanov et al. 2002b) also linked sulphide-silicate systems to diamond growth. These studies (Table 3) are significant because they offer a way of reducing carbonate without the need for reduced fluids, and because sulphides are very common inclusions within natural diamonds (Harris 1992; Harris and Gurney 1979; Meyer 1987). These experiments were incorporated into the 'sulphide droplet' model of Stachel and Harris (2008), where small pervasive droplets of immiscible sulphide liquid are trapped in the silicate mantle matrix, unable to move, but present to act as a diamond forming catalyst.

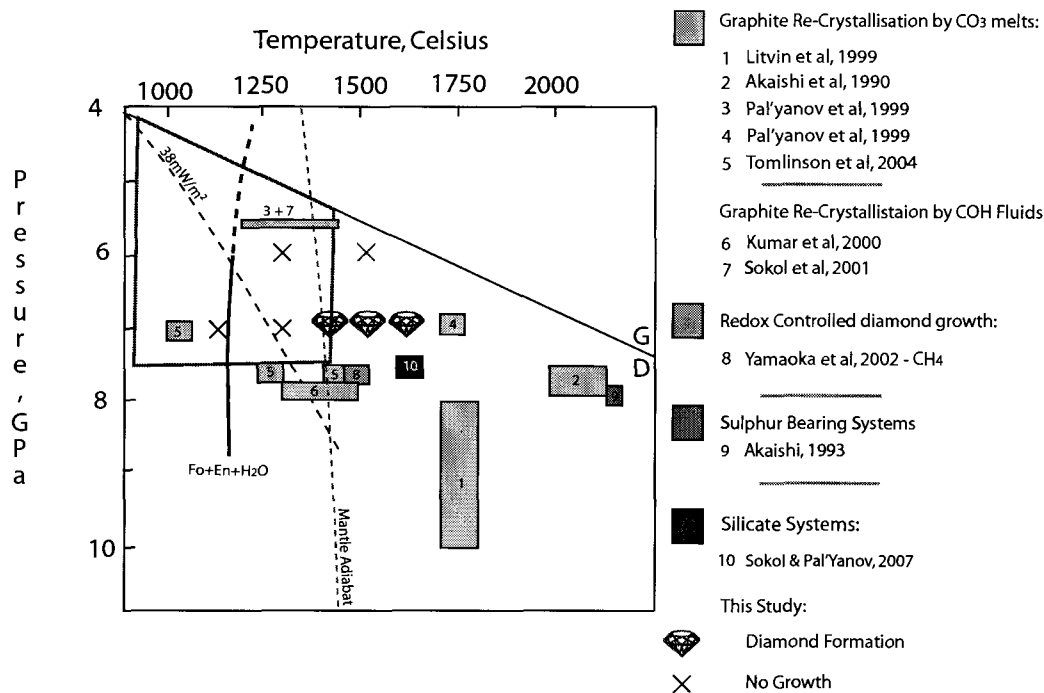


Figure 6: Selected diamond formation studies in P-T space, full list in Tables 1-5. Red box is the diamond formation window. Also shown is the solidus for Fo+En+H₂O from Stalder et al. (2001); the 38mW/m² cratonic geotherm and the graphite to diamond transition from Kennedy and Kennedy (1976).

Experiments utilising alkali halides such as KCl (Table 5), have recently received significant attention, and have been documented to exist in the mantle both as xenocrysts within kimberlites (Sharygin et al. 2008) and as inclusions in natural diamond (Ben-David. et al. 2004). Tomlinson et al. (2004) used KCl as a catalyst in a carbonate bearing experimental system. The temperatures in this study produced diamonds at amongst the lowest temperature ever in a laboratory setting (1050°C). They believed that KCl had an effect on the diffusion rates of carbon, allowing diamond to form faster and at a lower temperature than previously recorded (Tomlinson et al. 2004). The effect of KCl on diamond formation in a silicate assemblage, such as the one found within the natural diamond formation window, was unknown until recently (Fagan and Luth 2007).

System	T		P		Duration hrs	Type	Diamond Growth	Size μm	Study
	Low $^{\circ}\text{C}$	high $^{\circ}\text{C}$	low GPa	high GPa					
$\text{Mg}(\text{OH})_2 + \text{gr}$	2150	2150	7.7	7.7	0.3	Gr-recryx	no seeds	20	Akaishi et al, 1990
$\text{Ca}(\text{OH})_2 + \text{gr}$	2000	2150	7.7	7.7	0.3	Gr-recryx	no seeds	20	Akaishi et al, 1990
$\text{Mg}(\text{OH})_2 + \text{gr}$	2150	2150	7.7	7.7	?	Gr-recryx	?	?	Akaishi, 1993
$\text{Na}_2\text{CO}_3 + \text{H}_2\text{C}_2\text{O}_4 \cdot 2\text{H}_2\text{O} + \text{gr}$	1150	1420	5.7	5.7	20-120	Gr-recryz	seeded	65	Pal'Yanov et al, 1999
$\text{K}_2\text{CO}_3 + \text{H}_2\text{C}_2\text{O}_4 \cdot 2\text{H}_2\text{O} + \text{gr}$	1150	1420	5.7	5.7	20-120	Gr-recryz	seeded	25	Pal'Yanov et al, 1999
$\text{H}_2\text{O} + \text{gr} + \text{di}$	1600	2200	7.7	7.7	0.5-4	Gr-recryz	seeded	20	Hong et al, 1999
$\text{H}_2\text{O} + \text{gr}$	1600	2200	7.7	7.7	0.5-4	Gr-recryz	no seeds	10	Hong et al, 1999
$(\text{COOH})_2 + \text{gr}$	1300	1500	7.7	7.7	24-240	Gr-recryz	?	10	Kumar et al, 2000
$\text{C}_2\text{H}_2\text{O}_4 + \text{gr}$	1500	1500	7.7	7.7	24	Gr-recryz	?	10	Kumar et al, 2000
$(\text{COOH})_2 \cdot 2\text{H}_2\text{O} + \text{gr}$	1400	2000	7.7	7.7	0.5-360	Gr-recryz	?	30	Akaishi et al, 2000

Table 1: COH fluxed Graphite re-crystallisation experiments

Table 1: COH fluxed Graphite re-crystallisation experiments (cont.)

CaMg(CO ₃) ₂ +gr+H ₂ O	1300	1420	5.7	7	2-42	Gr-recryz	seeded	<60	Sokol et al, 2000
CaMg(CO ₃) ₂ +gr+H ₂ O+CO ₂	1300	1420	5.7	7	2-42	Gr-recryz	seed only	<60	Sokol et al, 2000
H ₂ O+gr	1200	1500	5.5	7.7	24	Gr-recryz	seeded	10	Yamaoka et al, 2000
CO ₂ +gr	1200	1420	5.7	5.7	?	Gr-recryz	seeded	?	Sokol et al, 2001
CO ₂ +H ₂ O+gr	1200	1420	5.7	5.7	?	Gr-recryz	seeded	?	Sokol et al, 2001
H ₂ O+gr	1200	1420	5.7	5.7	?	Gr-recryz	seeded	?	Sokol et al, 2001
CH ₄ +gr	1200	1420	5.7	5.7	?	Gr-recryz	seeded	?	Sokol et al, 2001
C ₁₈ H ₃₆ O ₂ + gr	1500	1500	7.7	7.7	1-48	Gr-recryz	?	10	Akaishi et al 2001
C ₂ H ₆ O ₆ + gr	1500	1500	7.7	7.7	1-49	Gr-recryz	?	10	Akaishi et al 2001
Ag ₂ C ₂ O ₄ + gr + di	1200	1420	5.7	5.7	42-84	Gr-recryz	seeded	40	Sokol et al, 2001
H ₂ C ₂ O ₄ .2H ₂ O + gr + di	1200	1420	5.7	5.7	42-136	Gr-recryz	seeded	50	Sokol et al, 2001
H ₂ O + gr + di	1200	1420	5.7	5.7	42-135	Gr-recryz	seeded	80	Sokol et al, 2001
C ₁₄ H ₁₀ + gr + di	1200	1420	5.7	5.7	42-84	Gr-recryz	seeded	<1	Sokol et al, 2001

Table 1: Key:

System = experimental starting composition

Type = style of experiment being conducted, recrystallisation, redox etc

Spon = Spontaneous diamond growth was achieved, can be completed with or without seed diamonds

Gr-recryz = graphite recrystallisation

? = unknown property - no further information

System	T		P		Duration hrs	Type	Diamond Growth	Size μm	Study	
	Low	high	low	high						
	$^{\circ}\text{C}$	$^{\circ}\text{C}$	GPa	GPa						
$\text{Li}_2\text{CO}_3 + \text{gr}$	2150	2150	7.7	7.7	0.3	Gr-recryz	spn	no seeds	20	Akaishi et al, 1990
$\text{Na}_2\text{CO}_3 + \text{gr}$	2150	2150	7.7	7.7	0.3	Gr-recryz	spn	no seeds	20	Akaishi et al, 1990
$\text{SrCO}_3 + \text{gr}$	2150	2150	7.7	7.7	0.3	Gr-recryz	spn	no seeds	20	Akaishi et al, 1990
$\text{MgCO}_3 + \text{gr}$	2150	2150	7.7	7.7	0.3	Gr-recryz	spn	no seeds	20	Akaishi et al, 1990
$\text{CaCO}_3 + \text{gr}$	1800	2000	7.7	7.7	0.3	Gr-recryz	no growth	no seeds	0	Akaishi et al, 1990
$\text{MgCO}_3 + \text{gr}$	2150	2150	7.7	7.7	?	Gr-recryx	spn	?	?	Akaishi, 1993
$\text{MgCO}_3 + \text{gr}$	1600	1650	9	10	?	Gr-recryz	?	?	?	Taniguchi et al, 1997
$\text{K}_2\text{Mg}(\text{CO}_3)_2 + \text{gr}$	1600	1650	9	10	?	Gr-recryz	?	?	?	Taniguchi et al, 1997
$\text{Li}_2\text{CO}_3 + \text{gr}$	1700	1750	7	7	2-18	Gr-recryz	spn + layering	seeded	90	Pal'yanov et al, 1999
$\text{Na}_2\text{CO}_3 + \text{gr}$	1700	1750	7	7	0.1-16.5	Gr-recryz	spn + layering	seeded	300	Pal'yanov et al, 1999
$\text{K}_2\text{CO}_3 + \text{gr}$	1700	1750	7	7	0.1-11.5	Gr-recryz	spn + layering	seeded	180	Pal'yanov et al, 1999

Table 2: Carbonate Melt fluxed Graphite re-crystallisation experiments

$\text{Cs}_2\text{CO}_3 + \text{gr}$	1700	1750	7	7	0.5-18	Gr-recryz	spn + layering	seeded	160	Pal'yanov et al, 1999
$\text{MgCO}_3 + \text{CaCO}_3 + \text{gr}$	1600	2000	7.7	7.7	1	Gr-recryz	spn	seeded	>20	Sato et al, 1999
$\text{MgCO}_3 + \text{gr}$	1800	2000	7.7	7.7	1	Gr-recryz	spn	seeded	?	Sato et al, 1999
$\text{CaCO}_3 + \text{gr}$	1800	2000	7.7	7.7	1	Gr-recryz	spn	seeded	?	Sato et al, 1999
$\text{Na}_2\text{Mg}(\text{CO}_3)_2 + \text{gr}$	1700	1800	8	10	?	Gr-recryz	spn	Seeded	150	Litvin et al, 1999
$\text{NaKMg}(\text{CO}_3)_2 + \text{gr}$	1700	1800	8	10	?	Gr-recryz	spn	Seeded	150	Litvin et al, 1999
$\text{Na}_2\text{CO}_3 + \text{gr}$	1360	1420	5.7	5.7	20-40	Gr-recryz	spn	seeded	40	Pal'yanov et al, 1999
$\text{K}_2\text{CO}_3 + \text{gr}$	1250	1420	5.7	5.7	30-40	Gr-recryz	seed growth	seeded	15	Pal'yanov et al, 1999
$\text{CaMg}(\text{CO}_3)_2 + \text{gr}$	1300	1420	5.7	7	2-42	Gr-recryz	spn	seeded	<60	Sokol et al, 2000
$\text{Ag}_2\text{CO}_3 + \text{gr}$	1500	2000	7.7	7.7	0.5-27	Gr-recryz	spn	no seeds	5-20	Sun et al, 2000
$\text{Na}_2\text{CO}_3 + \text{gr}$	1250	1700	5.7	7	0.3-40	Gr-recryz	spn + layering	seeded	450	Pal'yanov et al, 2002
$\text{K}_2\text{CO}_3 + \text{gr}$	1250	1700	5.7	7	0.3-41	Gr-recryz	spn + layering	seeded	75	Pal'yanov et al, 2002

Table 2: Carbonate Melt fluxed Graphite re-crystallisation experiments (cont.)

CaCO ₃ +CH ₄	1500	1500	7.7	7.7	0.5-48	redox	spn	no seed	>40	Yamaoka et al, 2002
Carbonatic Melts	1200	2315	5.5	8.5	?	redox	spn+ layering	seeded	?	Spivak and Litvin, 2004
K ₂ CO ₃ +KCl	1050	1420	7	7.7	1	Gr-recryz	seed growth	seeded	30	Tomlinson et al, 2004
K ₂ CO ₃ +KCl+gr	1600	1800	7.5	7.5	10-20	Gr-recryz	spn	seeded	60	Pal'yanov et al 2007
CaMg(CO ₃) ₂ + gr	1570	1820	7	8.5	0.1 -0.9	Gr-recryz	spn	Seeded	?	Litvin et al, 2008
K ₂ CO ₃ + gr	1570	1820	7	8.5	0.1 -0.9	Gr-recryz	spn	Seeded	?	Litvin et al, 2008
Eclogite- Dolomite systems	1570	1820	7	8.5	0.1 -0.9	Gr-recryz	spn	Seeded	?	Litvin et al, 2008
K ₂ CO ₃ + gr	1400	1600	7.5	7.5	15	Gr-recryz	spn	seeded	?	Pal'yanov et al, 2007
K ₂ CO ₃ + H ₂ O + gr	1500	1600	7.5	7.5	15	Gr-recryz	spn	seeded	?	Pal'yanov et al, 2007
KCl+H ₂ O+gr	1500	1600	7.5	7.5	15	Gr-recryz	spn	seeded	30	Pal'yanov et al, 2007
K ₂ CO ₃ +KCl+H ₂ O+gr	1500	1500	7.5	7.5	15	Gr-recryz	spn	seeded	?	Pal'yanov et al, 2007

Table 2: Carbonate Melt fluxed Graphite re-crystallisation experiments (cont.)

System	T		P		Duration	Type	Diamond Growth	Size	Study
	Low °C	high °C	low GPa	high GPa					
Na ₂ SO ₄ +gr	2150	2150	7.7	7.7	0.3	Gr-recryx	spn	no seeds	Akaishi et al, 1990
MgSO ₄ +gr	2150	2150	7.7	7.7	0.3	Gr-recryx	spn	no seeds	Akaishi et al, 1990
CaSO ₄ ·0.5H ₂ O+gr	2150	2150	7.7	7.7	0.3	Gr-recryx	spn	no seeds	Akaishi et al, 1990
gr+MgSO ₄	2150	2150	7.7	7.7	?	Gr-recryx	spn	?	Akaishi, 1993
gr+Na ₂ SO ₄	1600	2200	6.5	7.7	?	Gr-recryx	spn	?	Akaishi, 1993
Fe+S+O melt	1300	1300	6	7.5	24	redox	spn gr	no seed	Gunn and Luth, 2006
MgCO ₃ +Mg ₂ Si ₂ O ₆	1300	1300	6	7.5	6-48	redox	spn gr	no seed	Gunn and Luth, 2006
MgCO ₃ +Fe-S-O melt+Mg ₂ Si ₂ O ₆	800	1300	6	7.5	2	redox	spn gr	no seed	Gunn and Luth, 2006
MgCO ₃ +SiO ₂ +Al ₂ O ₃ +FeS	1250	1800	6.3	6.3	8-44	redox	< spn	seeded	Pal'yanov et al 2007

Table 4: Silicate bearing systems - graphite recrystallisation and redox controlled

System	T	P low	P	Duration	Type	Diamond	Size	Study
	Low °C	high °C	high GPa	hrs		Growth	µm	
Kimberlite Melt	1800	2200	7	7.7	0.3-15	redox	seeded	200 Arima et al, 1993
Fe ₂ SiO ₄ + gr	1300	1400	5	5.5	1-6	Gr-recryz	?	200 Chepurov et al, 1999
MgCO ₃ +SiO ₂	1400	1450	6	6	43	redox	seeded	>25 Pal'yanov et al, 2002
MgCO ₃ +SiO ₂ +Na ₂ CO ₃	1400	1800	6	7	18-42	redox	seeded	>25 Pal'yanov et al, 2002
CaMg(CO ₃) ₂ +Si	1500	1800	7.7	7.7	1-4	redox	seeded	50 Arima et al, 2002
CaMg(CO ₃) ₂ +SiC	1500	1800	7.7	7.7	1-24	redox	seeded	90 Arima et al, 2002
MgCO ₃ -SiO ₂	1200	1800	5.2	7	18-91	redox	seeded	? Pal'yanov et al, 2005
CaMg(CO ₃) ₂ +SiO ₂	1500	1500	6	6	20-40	redox	seeded	? Pal'yanov et al, 2005

Table 4 cont...

$\text{MgCO}_3 + \text{SiO}_2 + \text{Al}_2\text{O}_3$	1200	1600	5.2	6	20-90	redox	< spon	seeded ?	Pal'yanov et al, 2005
$\text{SiO}_2 + \text{H}_2\text{O} + \text{gr}$	1600	1600	7.5	7.5	15-40	Gr-recryz	spon	seeded 50	Sokol & Pal'yanov, 2008
$\text{Mg}_2\text{SiO}_4 + \text{H}_2\text{O} + \text{gr}$	1600	1600	7.5	7.5	15-40	Gr-recryz	spon	seeded 50	Sokol & Pal'yanov, 2008
$\text{Mg}(\text{OH})_2 + \text{SiO}_2 \cdot 0.3\text{H}_2\text{O} + \text{gr}$	1300	1600	5.5	7	0.5-48	Gr-recryz	spon	seeded 50	Fagan & Luth, 2008

Table 5: Other Diamond growth systems. Mantle Catalysts - The effect of Alkali Halides

System	T	T	P	P	Duration	Type	Diamond Growth	Size	Study
	Low °C	high °C	low GPa	high GPa	hrs			µm	
graphite only	2700	2700	10	14	?	Direct gr	spon	no seed 10	Yusa et al, 1998
<i>Alkali Halides</i>									
LiCl + gr	1400	1620	6	6.6	5	Gr-recryz	seed only	seeded ?	Wang et al, 1997

NaCl + gr	1400	1620	6	6.6	5	Gr-recryz	seed only	seeded	?	Wang et al, 1997
KCl + gr	1400	1620	6	6.6	5	Gr-recryz	seed only	seeded	?	Wang et al, 1997
RbCl + gr	1400	1620	6	6.6	5	Gr-recryz	seed only	seeded	?	Wang et al, 1997
CsCl + gr	1400	1620	6	6.6	5	Gr-recryz	seed only	seeded	?	Wang et al, 1997
NaF + gr	1400	1620	6	6.6	5	Gr-recryz	seed only	seeded	?	Wang et al, 1997
NaBr + gr	1400	1620	6	6.6	5	Gr-recryz	seed only	seeded	?	Wang et al, 1997
NaI + gr	1400	1620	6	6.6	5	Gr-recryz	seed only	seeded	?	Wang et al, 1997
Fe ₃ O ₄ + gr	1300	1400	4.5	5.5	0.5-6	Gr-recryz	spon	?	10	Chepurov et al, 1999
FeTiO ₄ + gr	1300	1300	5	5	1	Gr-recryz	no growth	?	0	Chepurov et al, 1999
Ag ₂ O + gr	1500	2000	7.7	7.7	0.5-27	Gr-recryz	spon	no seeds	5-20	Sun et al, 2000
K ₂ CO ₃ +KCl	1050	1420	7	7.7	1	redox CO ₃	seed growth	seeded	30	Tomlinson et al, 2004

Silicate systems have been relatively understudied compared to their counterparts in other melt/fluid systems (Table 4). Early theoretical work (Sunagawa 1984b), showed the potential for a silicate system to act as the diamond-forming medium. One problem with using a silicate assemblage is that the dry solidus for lherzolite occurs at temperatures well in excess of the diamond formation window and thus could not generate diamonds at the appropriate P and T. However, the presence of H₂O lowers the melting temperature of hydrous peridotite such that a hydrous silicate melt would exist in the DFW (Kawamoto and Holloway 1997). Thus, hydrous-peridotite is an option with regards to the diamond formation medium. Sokol and Pal'yanov (2007) successfully grew diamond in the SiO₂-MgO-H₂O system at 7.5GPa, 1600°C. After testing the various starting compositions and H₂O-silicate ratios, they concluded that H₂O-C rich fluids were the more effective at producing new diamond growth than hydrous silicate melts. Given its effect in carbonate systems and its presence in nature (Navon 1998; Sharygin et al. 2008; Tomlinson et al. 2004), KCl would appear to be an ideal addition to a silicate system.

Summary:

How natural diamond grows still remains unsolved. The relatively low pressure and temperatures recorded by geothermobarometry on natural diamond inclusions caused large difficulties for experimental petrologists trying to recreate the natural growth system. At reduced temperatures carbon nucleation and growth kinetics may be very slow; this may not be an issue in the mantle, but it represents a significant issue on laboratory time-scales. This requires the use of seed diamonds and the 'overstepping' of the reactions by increasing the temperature and pressure of the apparatus well above those observed in nature. Therefore it is possible that growing micron-sized crystals in a few hours within a laboratory is significant. We currently have little evidence to determine the speed at

which natural diamonds grow. Their zonation, observed by cathodoluminescence studies (Fitzsimons et al. 1999; Harte et al. 1999) clearly demonstrate that diamond grows from a fluid medium, and the growth itself takes place in a series of events rather than one all-encompassing growth phenomenon. For diamond growth to occur several physical conditions must be met:

- The availability of a carbon source
- The presence of a fluid or melt
- Lack of perturbation or influx of compounds inconducive to diamond growth

Natural diamond studies provided an excellent base for experimental work on the formation of diamond. The characterisation of the morphology and growth styles of natural diamond, its elemental makeup and isotopes, its fluid and mineral inclusions and their associated geochemistry, and most importantly, the geothermobarometry, can be used to assess the characteristics of the source fluid/melt from which the diamonds crystallised. Experimental research has primarily focussed on re-crystallisation of graphite to diamond. Little work has been completed on reduction of carbonates or oxidation of reduced (CH_4) bearing assemblages. Diamond formation in a silicate melt or fluid is the least tested of all the chemical systems and perhaps holds the key to the formation to natural diamond.

To address this, this study concentrates on the re-crystallisation of graphite by a hydrous silicate melt (HSM). The water-saturated silicate solidus lies within the natural diamond formation window, thus a HSM, offers an ideal, and little tested, candidate as the diamond formation medium. The use of chemical fluxes, such as KCl in carbonate studies also required extension into silicate systems to ensure the catalytic effects previously recorded can also be expanded into these hydrous silicate melt systems.

References

- Akaishi M (1993) New non-metallic catalysts for the synthesis of high pressure, high temperature diamond. *Diamond and Related Materials* 2(2-4):183-189
- Akaishi M, Kanda H, Yamaoka S (1990) Synthesis of diamond from graphite carbonate systems under very high-temperature and pressure. *Journal of Crystal Growth* 104(2):578-581
- Akaishi M, Kumar MDS, Kanda H, Yamaoka S (2001) Reactions between Carbon and a reduced COH fluid under diamond stable conditions. *Diamond and Related Materials* 10:2125-2130
- Akaishi M, Yamaoka S (2000) Crystallization of diamond from C-O-H fluids under high-pressure and high-temperature conditions. *Journal of Crystal Growth* 209(4):999-1003
- Arima M, Kozai Y, Akaishi M (2002) Diamond nucleation and growth by reduction of carbonate melts under high-pressure and high-temperature conditions. *Geology* 30(8):691-694
- Arima M, Nakayama K, Akaishi M, Yamaoka S, Kanda H (1993) Crystallization of diamond from a silicate melt of kimberlite composition in high-pressure and high-temperature experiments. *Geology* 21(11):968-970
- Ben-David. OK, S. IE, Hauri. E, O. N (2004) Mantle fluid interaction: a tale of one diamond. *Lithos* 77:243-253
- Bertrand P, Mercier JCC (1985) The mutual solubility of coexisting ortho- and clinopyroxene: toward an absolute geothermometer for the natural system? *Earth and Planetary Science Letters* 76:109-122
- Bovenkirk HP (1961) Some observations on the morphology and crystal characteristics of synthetic diamonds. *American Mineralogist* 46:952-963
- Bovenkirk HP, Bundy FP, Hall T, Strong HM, Wentorf RHj (1959) Preparation of diamond. *Nature* 184:1094-1098
- Boyd SR, Gurney JJ (1986) Diamonds and the African lithosphere. *Science* 232(4749):472-477
- Brey GP, Köhler T (1990) Geothermobarometry in four-phase lherzolites 2: New thermobarometers and practical assessment of existing thermometers. *Journal of Petrology* 31(6):1353-1378

Bulanova GP (1995) The formation of diamond. *Journal of Geochemical Exploration* 53:1-23

Chepurov AI, Fedorov II, Sonin VM, Bagryantsev DG, Osorgin YN (1999) Diamond formation during reduction of oxide and silicate carbon systems at high P-T conditions. *European Journal of Mineralogy* 11:355-362

DeCarli PS, Jamieson JC (1961) Formation of diamond by explosive shock. *Science* 133(3467):1819-1820

Dobrzhinetskaya LF, Eide EA, Larsen R, Sturt B, Tronnes R, Smith D, Taylor W, Posukhova T (1995) Microdiamond in high-grade metamorphic rocks of the Western gneiss region, Norway. *Geology* 23:597-600

Ellis DJ, Green DH (1979) An experimental study of the effect of Ca upon garnet-clinopyroxene Fe-Mg exchange equilibria. *Contributions to Mineralogy and Petrology* 71(13-22)

Fagan AJ, Luth RW (2007) Growth of diamond from a carbonaceous hydrous silicate melt: An Experimental Study. In: AGU Fall Meeting, abstracts, San Francisco

Fersman AE, Goldschmidt V (1911) *Der Diamant*, Winter, Heidleberg, Germany

Fitzsimons WC, Harte B, Chinn IL, Gurney JJ, Taylor WR (1999) Extreme chemical variation in complex diamonds from George Creek, Colorado: a SIMS study of Carbon isotopic composition and nitrogen abundance. *Mineralogical Magazine* 63(6): 857-878

Frank FC, Lang AR (1965) X-ray topography of diamond. In: Berman R (ed) *Physical properties of diamond*, vol. Clarendon Press, London, p 69-115

Genshaft YS, Yakubova SA, Volkova LM (1977) Internal morphology of natural diamond, In: Genshaft, Yu.S, *Investigation of High Pressure Minerals*, Institute of Physics of the Earth, Moscow, P5-131

Gunn S, Luth RW (2006) Carbonate reduction by Fe-S-O melts at high pressure and high temperature. *American Mineralogist* 91: 1110-1116

Haggerty SE (1986) Diamond genesis in a multiply-constrained model. *Nature* 320:34

Harley SL (1984) An experimental study of the partitioning of Fe-Mg between garnet and orthopyroxene. *Journal of Petrology* 86: 359-373

Harris JW (1992) *Diamond Geology*, In: *The properties of natural and synthetic diamonds*, Vol 58A. Academic Press, London: 345-392

- Harris JW, Gurney JJ (1979) Inclusions in diamond. In: Field JE (ed) *The properties of Diamond*, Academic press, London: 345-393
- Harrison ER, Tolansky S (1964) Growth history of a natural octahedral diamond. *Proceedings of the Royal Society of London (A279)*:490-496
- Harte B, Fitzsimons WC, Harris JW, Otter ML (1999) Carbon isotope ratios and nitrogen abundances in relation to cathodoluminescence characteristics for some diamonds from Kaapvaal province, S. Africa. *Mineralogical Magazine* 63(6):829-856
- Hartman P, Perdok WG (1955) On the relation between structure and morphology of crystals. *Acta Crystallographica* 8:49-52
- Hazen RM (1999) *The Diamond Makers*, Cambridge University Press, Cambridge, p 244
- Helmstaedt HH, Schulze DJ (1989) Southern African kimberlites and their mantle sample: implications for Archean tectonics and lithosphere evolution. In: Ross. J et al (eds) *Kimberlites and Related Rocks*, vol 1. Blackwell, Carlton, pp 358-368
- Hong SM, Akaishi M, Yamaoka S (1999) Nucleation of diamond in the system of carbon and water under very high pressure and temperature. *Journal of Crystal Growth* 200:326-328
- Izraeli ES, Harris JW, Navon O (2001) Brine inclusions in diamonds: a new upper mantle fluid. *Earth and Planetary Science Letters* 187(3-4):323-332
- Jordan TH (1979) In: Boyd FR, Meyer HOA (eds) *Proceedings of the 2nd International Kimberlite Conference*, Vol 2. American Geophysical Union, p 1-14
- Kawamoto T, Holloway JR (1997) Melting Temperature and partial melt chemistry of water-saturated mantle peridotite to 11GPa. *Science* 276:240-243
- Kennedy CS, Kennedy GC (1976) Equilibrium boundary between graphite and diamond. *Journal of Geophysical Research* 81(14):2467-2470
- Kesson SE, Ringwood AE (1989) Slab-mantle interactions - 2. *Chemical Geology* 78:97-118
- Klein-BenDavid O, Izraeli ES, Hauri E, Navon O (2004) Mantle fluid evolution-a tale of one diamond. *Lithos* 77:243-253
- Klein-BenDavid O, Izraeli ES, Hauri. E, Navon O (2007) Fluid inclusions in diamonds

from the Diavik mine, Canada and the evolution of diamond forming fluids. *Geochimica et Cosmochimica Acta* 71:723-744

Kopylova M, Navon O, Dubrovinsky L, Khachatryan G, Kopylov P (2008) Mineralogy of natural diamond-forming fluids. In: 9th International Kimberlite Conference, Frankfurt, Germany, extended abstracts, 3p.

Krough EJ (1988) The garnet clinopyroxene Fe-Mg exchange geothermometer - a reinterpretation of existing experimental data. *Contributions to Mineralogy and Petrology* 99:44-48

Kumar MDS, Akaishi M, Yamaoka S (2000) Formation of diamond from supercritical H₂O-CO₂ fluid at high pressure and high temperature. *Journal of Crystal Growth* 213(1-2):203-206

Lang AR (1979) Internal Structure. In: Field JE (ed) *The properties of diamond*, Academic Press, London, pp 425-469

Li J, Fei Y (2003) Experimental constraints on core composition. In: Turekian KK, Holland HD (eds) *Treatise on Geochemistry*, vol 2. Elsevier, Amsterdam, p 522-552

Lindsay DH, Anderson DJ (1983) A two pyroxene thermometer. *Proc. Lunar & Planet. Sci. Conf. Part 2: Journal of Geophysical Research*. 88:A887-906

Litvin VY (2007) High pressure mineralogy of diamond genesis. In: Ohtani E (ed) *Advances in High-Pressure Mineralogy*, Special paper 421. Geological Society of America, Boulder, CO, pp 83-103

Litvin YA, Litvin VY, Kadik AA (2008) Experimental characterisation of diamond crystallisation in melts of mantle silicate-carbonate-carbon systems at 7.0-8.5GPa. *Geochemistry International* 46(6):531-553

Litvin YA, Zharikov VA (1999) Primary fluid carbonatite inclusions in diamond: experimental modelling in the system K₂O-Na₂O-CaO-MgO-FeO-CO₂ as a diamond forming medium at 7-9GPa. *Doklady Earth Sciences* 391:388-391

Markovic Z, Todorovic-Markovic B, Marinkovic M, Nenadovic T (2002) Temperature measurement of carbon arc plasma in helium. *Carbon* 41(2):369-371

Meyer HOA (1987) Inclusion in Diamond. In: Nixon PH (ed) *Mantle Xenoliths*, Wiley, Chichester, pp 501-522

Meyer HOA, Boyd SR (1977) The Mantle Sample: Inclusions in Kimberlites and other Volcanics. In: 2nd International Kimberlite Conference, American Geophysical Union, Santa Fey, N.M, p 432

- Navon O (1991) High internal pressures in diamond fluid inclusions determined by infrared absorption. *Nature* 353:746-749
- Navon O (1998) Diamond Formation in the Earth's mantle. In: 7th International Kimberlite Conference, vol 2. Cape Town, SA
- Navon O, Klein-BenDavid O, Izraeli ES (2004) Diamond-forming fluids. *Geochimica et Cosmochimica Acta* 68(11):A277-A277
- Navon O, Klein-BenDavid O, Weiss Y (2008) Diamond Forming Fluids: their origin and evolution. In: 9th International Kimberlite Conference, Frankfurt, Germany, extended abstracts, 3p.
- Nimis P, Taylor WR (2000) Single clinopyroxene thermometry for garnet peridotites. Part 1. Calibration and testing of a Cr-in-clinopyroxene barometer and an enstatite-in-clinopyroxene thermometer. *Contributions to Mineralogy and Petrology* 139:541-554
- O'Neill HSC (1980) An experimental study of Fe-Mg partitioning between garnet and olivine and its calibration as a geothermometer: corrections. *Contributions to Mineralogy and Petrology* 72:337
- O'Neill HSC, Wood BJ (1979) An experimental study of Fe-Mg partitioning between garnet and olivine and its calibration as a geothermometer. *Contributions to Mineralogy and Petrology* 70:59-70
- Pal'yanov YN, Borzdov YM, Bataleva YV, Sokol AG, Palyanova GA, Kupriyanov IN (2007a) Reducing role of sulphides and diamond formation in the Earth's Mantle. *Earth and Planetary Science Letters* 260:242-256
- Pal'yanov YN, Shatsky VS, Sobolev NV, Sokol AG (2007b) The role of ultrapotassic fluids in diamond formation. In: Proceedings of the National Academy of Science of the USA, High-Pressure Geoscience Special Feature. p 1-6
- Pal'yanov YN, Sokol AG, Borzdov YM, Khokhryakov AF (2002a) Fluid-bearing alkaline carbonate melts as the medium for the formation of diamonds in the Earth's mantle: an experimental study. *Lithos* 60(3-4):145-159
- Pal'yanov YN, Sokol AG, Borzdov YM, Khokhryakov AF, Shatsky AF, Sobolev NV (1999a) The diamond growth from Li_2CO_3 , Na_2CO_3 , K_2CO_3 and Cs_2CO_3 solvent-catalysts at $P=7$ GPa and $T=1700-1750$ degrees C. *Diamond and Related Materials* 8(6):1118-1124

Pal'yanov YN, Sokol AG, Borzdov YM, Khokhryakov AF, Sobolev NV (1999b) Diamond formation from mantle carbonate fluids. *Nature* 400(6743):417-418

Pal'yanov YN, Sokol AG, Borzdov YM, Khokhryakov AF, Sobolev NV (2002b) Diamond formation through carbonate-silicate interaction. *American Mineralogist* 87(7):1009-1013

Pal'yanov YN, Sokol AG, Tomilenko AA, Sobolev NV (2005) Conditions of diamond formation through carbonate-silicate interaction. *European Journal of Mineralogy* 17:207-214

Phillips D, Harris JW, Viljoen KS (2004) Mineral chemistry and thermobarometry of inclusions from De Beers Pool diamonds, Kimberley, South Africa. *Lithos* 77(1-4):155-179

Robinson DK (1979) Surface textures and other features of diamonds. In: *Geology*, Unpublished PhD. University of Cape Town, Cape Town, RSA, p 161

Safonov OG, Perchuk LL, Litvin YA, Chertkova NV (2008) Experimental model for alkalic chloride-rich mantle liquids. In: 9th International Kimberlite Conference, Frankfurt, Germany, extended abstracts, 3p.

Sato K, Akaishi M, Yamaoka S (1999) Spontaneous nucleation of diamond in the system MgCO₃-CaCO₃-C at 7.7 GPa. *Diamond and Related Materials* 8(10):1900-1905

Schrauder M, Navon O (1994) Hydrous and carbonatitic mantle fluids in fibrous diamonds from Jwaneng, Botswana. *Geochimica et Cosmochimica Acta* 58(2):761-771

Seal M (1962) The growth history of natural diamond as revealed by etching experiments. In: 1st International congress on Diamond in Industry, London, Paris, pp 361-375

Sharygin VV, Kamenetsky VS, Kamenetsky MB, Golovin AV (2008) Mineralogy and genesis of kimberlite-hosted chloride containing nodules from Udachnya-East pipe, Yakutia, Russia. In: 9th International Kimberlite Conference, Frankfurt, Germany, extended abstracts, 3p.

Sobolev NV (1977) Deep seated inclusions in kimberlites and the problem of the composition of the upper mantle (Translated from Russian, 1974), AGU San Francisco, 1p.

Sobolev NV, Efimova ES, Koptil VI, Lavrentiev YG, Sobolev VC (1976) Inclusions of coesite, garnet and omphacite in diamonds from Yakutia - first find of the coesite paragenesis. *Doklady Earth Sciences USSR* 230:1442-1444

- Sobolev NV, Shatsky VS (1990) Diamond inclusions in garnets from metamorphic rocks: a new environment for diamond formation. *Nature* 343:742-746
- Sokol AG, Pal'yanov YN (2007) Diamond formation in the system MgO-SiO₂-H₂O-C at 7.5GPa and 1600 celcius. *Contributions to Mineralogy and Petrology* 155(1):33-43
- Sokol AG, Pal'yanov YN, Pal'yanova GA, Khokhryakov AF, Borzdov YM (2001) Diamond and graphite crystallization from C-O-H fluids under high pressure and high temperature conditions. *Diamond and Related Materials* 10(12):2131-2136
- Sokol AG, Tomilenko AA, Pal'yanov YN, Borzdov YM, Pal'yanova GA, Khokhryakov AF (2000) Fluid regime of diamond crystallisation in carbonate-carbon systems. *European Journal of Mineralogy* 12(2):367-375
- Spivak AV, Litvin YA (2004) Diamond syntheses in multicomponent carbonate-carbon melts of natural chemistry: elementary processes and properties. *Diamond and Related Materials* 13(3):482-487
- Stachel T (2008) Personal Communication - MSc thesis meeting, Edmonton, Canada
- Stachel T, Aulbach S, Brey GP, Harris JW, Leost I, Tappert R, Viljoen KS (2004) The trace element composition of silicate inclusions in diamonds: a review. *Lithos* 77(1-4):1-19
- Stachel T, Brey GP, Harris JW (2005) Inclusions in sublithospheric diamonds: Glimpses of the deep Earth. *Elements* 1(2):73-78
- Stachel T, Harris JW (2008) The origin of Cratonic diamonds - constraints from mineral inclusions. *Ore Geology Reviews* 34(1-2):5-32
- Stalder R, Ulmer P, Thompson AB, Gunther D (2001) High Pressure fluids in the system MgO-SiO₂-H₂O under upper mantle conditions. *Contributions to Mineralogy and Petrology* 140:607-618
- Sun LL, Akaishi M, Yamaoka S (2000) Formation of diamond in the system of Ag₂CO₃ and graphite at high pressure and high temperatures. *Journal of Crystal Growth* 213(3-4):411-414
- Sunagawa I (1984a) Growth of crystals in nature. *Bulletin of Mineralogy*, 104:81-87
- Sunagawa I (1984b) Morphology of natural and synthetic diamond crystals. In: Sunagawa. I (ed) *Materials Science of the Earths Interior*, Terrapub, Tokyo, pp 303-331
- Taniguchi T, Dobson D, Jones AP, Rabe R, Milledge HJ (1996) Synthesis of cubic diamond

in the graphite-magnesium carbonate and graphite- $K_2Mg(CO_3)_2$ systems at high pressure of 9-10 GPa region. *Journal of Materials Research* 11(10):2622-2632

Tappert R, Stachel T, Harris JW, Shimizu N, Brey GP (2005) Mineral inclusions in diamonds from the Panda kimberlite, Slave Province, Canada. *European Journal of Mineralogy* 17(3):423-440

Taylor WR, Green DH (1988) Measurement of reduced peridotite C-O-H fluids and implications for redox melting of the mantle. *Nature* 332:349-353

Tomlinson E, Jones A, Milledge J (2004) High-pressure experimental growth of diamond using C-K₂CO₃-KCl as an analogue for Cl-bearing carbonate fluid. *Lithos* 77(1-4):287-294

Ulmer P, Trommsdorff V (1995) Serpentine stability to mantle depths and subduction related magmatism. *Science* 268(5212):5

Wang Y, Kanda H (1998) Growth of HPHT diamonds in alkali halides: possible effects of oxygen contamination. *Diamond and Related Materials* 7:57-63

Weiss Y, Kessel R, Griffin WL, Kiflawi I, Bell DR, Harris JW, Navon O (2008) Diamond forming fluids from Kankan, Guinea: major and trace element study. In: 9th International kimberlite Conference, Frankfurt, Germany, extended abstracts, 2p.

Yamaoka S, Kumar MDS, Kanda H, Akaishi M (2002) Crystallization of diamond from CO₂ fluid at high pressure and high temperature. *Journal of Crystal Growth* 234:5-8

Yamaoka S, Kumar S, Akaishi M, Kanda H (2000) Reaction between carbon and water under diamond-stable high pressure and high temperature conditions. *Diamond and Related Materials* 9(8):1480-1486

Yusa H, Takemura K, Morishima H, Watanabe K (1998) Direct transformation of graphite to cubic diamond observed in a laser-heater diamond anvil cell. *Applied Physics Letters* 72(15):1843-1845

Chapter Two

*Hydrous silicate melts:
A new medium for diamond formation?*

Introduction:

The mechanism by which diamond forms is a problem that numerous workers in the last century have tried to solve. To date, research has focussed on the chemical makeup of the fluids or melts from which diamond precipitates in the Earth's Mantle. By analysing natural diamonds, brought to the Earth's surface in kimberlite eruptions, a large set of diamond properties have been recorded. This dataset includes information on diamond morphology, mineral and fluid inclusions, isotope and trace-element geochemistry and geothermobarometry (Harris 1992; Klein-BenDavid et al. 2004; Navon 1998; Robinson 1979; Stachel et al. 2003, 2004; Tappert et al. 2005). The latter is important because the temperatures and pressures recorded by the geochemistry of mineral inclusions within diamond constrains a 'diamond formation window' (Harris 1992); a region in pressure-temperature space in which the diamond was growing when it enclosed its mineral inclusions. This window exists between 130 km and 220 km depth (4.3-7GPa, 900-1400°C). By recreating these conditions within a laboratory, we can test the various chemical systems in which diamond will be produced - as if it were in the mantle. Commercial laboratory grown 'synthetic' diamonds are typically produced by methods that have no correlation with nature (Bovenkirk 1961; Bovenkirk et al. 1959; Hazen 1999), usually involving molten transition metal catalysts or a high-T carbon plasma, neither of which can exist in the mantle.

Figure 1 shows the important solidi in P-T space pertaining to diamond formation (Dasgupta and Hirschmann 2006; Iwamori 1998; Kawamoto and Holloway 1997; Kessel et al. 2005; Stalder et al. 2001). In a silicate assemblage the dry solidus exists at temperatures too high to form a melt in the DFW. However, the addition of H₂O to the silicate assemblage lowers the silicate solidus dramatically. The fo+en+H₂O and lherzolite-H₂O solidii are shown for reference (Iwamori 1998; Stalder et al. 2001). The lherzolite solidus is shown as

a broad-band representing where the solidus would lie with changes in the major element composition of the lherzolite. The solidus of Kawamoto and Holloway (1997) lies in agreement with the one calculated by Iwamori (1998) exists below 1000°C at 3GPa and will be present up to 1100°C at 8GPa. In a hydrous assemblage, any sub-solidus fluids would exist as an independent pervasive fluid, rich in H₂O (Kawamoto and Holloway 1997). Above the silicate solidus, these fluids would enter a melt phase, creating a hydrous silicate melt. Because the DFW exists between 900 and 1400°C, only a very small area at the lower end of diamond stable P-T conditions exists within the H₂O-fluid stability field. However, once the lherzolite-H₂O solidus is crossed (Kawamoto and Holloway 1997)

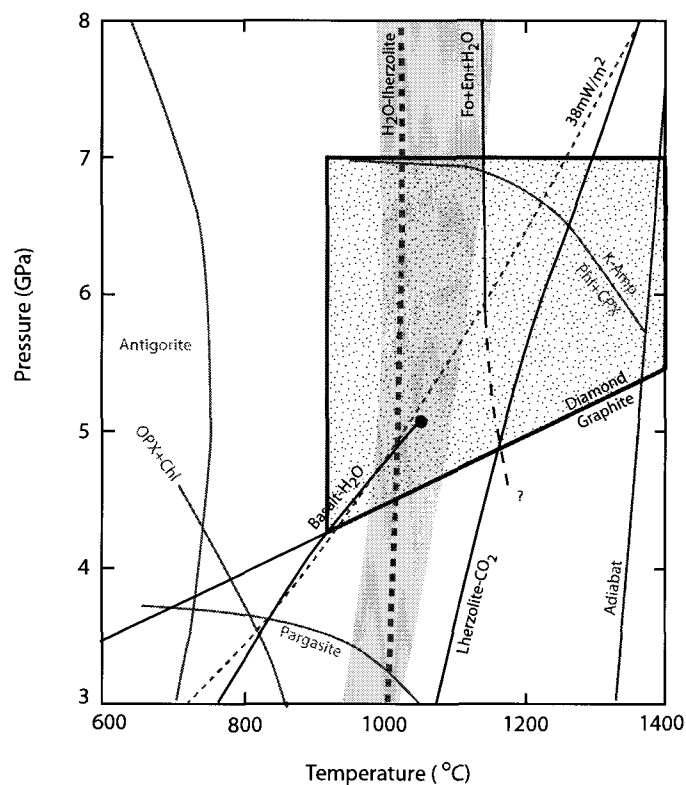


Figure 1: P-T stability diagram. Shown are important reactions for the generation of a hydrous silicate melt or a COH fluid. These include the lherzolite-H₂O solidus - green area - Iwamori (1998), lherzolite-CO₂ from Dasgupta and Hirschmann (2006), Fo-En-H₂O from Stalder et al. (2001), Basalt-H₂O from Kessel et al. (2005). The H₂O saturated, KLB-1 lherzolite solidus (orange) and various hydrous dehydration reactions are from Kawamoto and Holloway (1997). Red bounded stippled box represents the Diamond Formation Window.

only a harzburgitic composition remains subsolidus. The fo-en-H₂O solidi (Stalder et al, 2001) represents the harzburgitic solidus; above this a hydrous silicate melt would occur in both harzburgite and lherzolite, within the DFW. No second critical endpoint has yet been located for the lherzolite-H₂O system, which is important because it will define where the silicate system will cease to be distinguishable as a fluid or a melt (Stachel and Harris 2008). Because a free H₂O fluid has been shown to be stable at P-T conditions below the silicate solidus (Kawamoto and Holloway 1997), the dehydration of antigorite and other hydrous phases (see Fig. 1) would provide the necessary H₂O to lower the solidus and generate diamonds from the resulting HSM. The basalt-H₂O solidus and its second critical endpoint (2EP) is also shown in Fig. 1 (Kessel et al. 2005). Beyond the 2EP, no distinction between the fluid or melt phases can be determined. Experimentation in this eclogite-H₂O system, especially the possibility of diamond formation beyond the basalt-H₂O 2EP, would make a good expansion of this current study.

Diamond Formation Studies:

Significant advances in experimental petrology enabled Bovenkirk et al. (1959), and others, to form synthetic diamonds in a HPHT laboratory. However, their use of Fe-Ni catalysts and P-T conditions well in excess of natural systems make these studies irrelevant for application to the mantle genesis of diamond. Since 1990, most of the diamond synthesis studies have been completed using COH fluids and carbonate melts to flux the graphite to diamond transition. Such melts and fluids (Fig. 2) have been demonstrated by numerous authors to successfully make diamond (Akaishi et al. 2001; Akaishi and Yamaoka 2000; Litvin et al. 1999a; Litvin et al. 1999b; Pal'yanov et al. 2007; Pal'yanov et al. 2000; Safonov et al. 2008; Sokol et al. 2001), however many of these studies required reaction overstepping in their P-T conditions. This moved the results further and further away from nature in an attempt to induce diamond growth. Diamond was successfully grown within

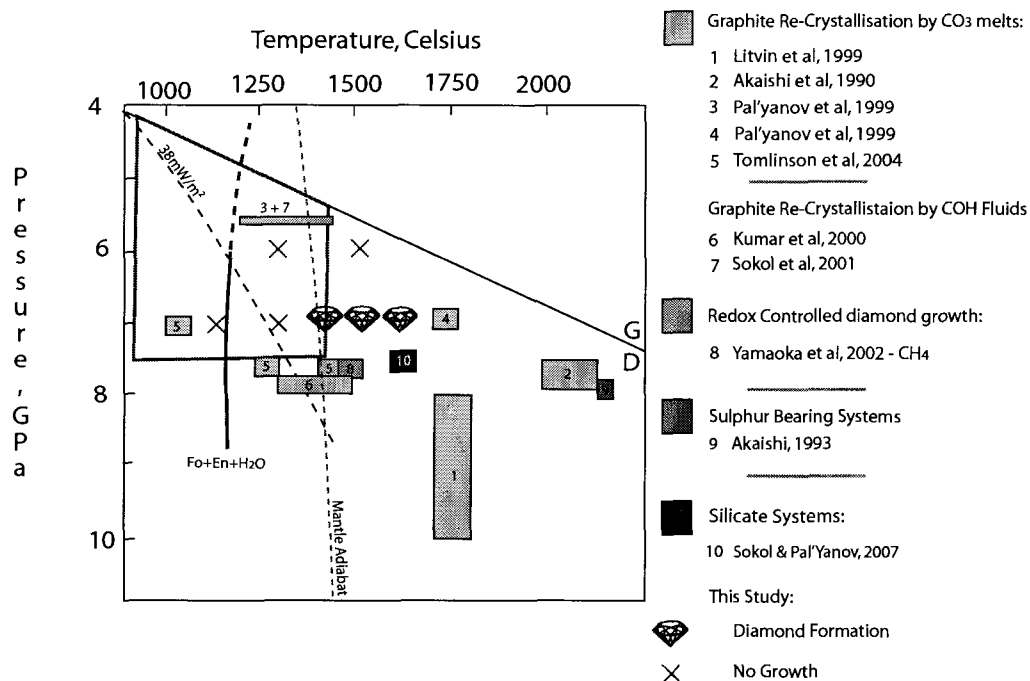


Figure 2: Temperature-Pressure phase diagram showing the results of numerous workers experimental research for comparison to this study. For reference the graphite-diamond transition of Kennedy & Kennedy (1976) is shown, along with the red bounding box illustrating the Natural Diamond Formation Window (Harris, 1992). The mantle adiabat, Fo+En+H₂O solidus (Stalder et al, 2001) and a continental geotherm of 38mW/m² are also displayed.

the diamond formation window using a carbonate-melt (Pal'yanov et al. 1999), a carbonate-halide melt (Tomlinson et al. 2004) and a COH fluid (Sokol et al. 2001). These experiments, and many more (e.g. Sun et al. 2000; Yamaoka et al. 2002a; Yamaoka et al. 2000) have shown that diamond genesis is possible using these solvents, but that achieving it under natural conditions still remains difficult. Many studies rely on the presence of graphite within the starting compositions as a source for carbon; this style of experimentation has become standard across numerous research groups. Tomlinson et al. (2004) demonstrated the ability of alkali halides to aid the graphite to diamond transition, reporting diamond growth at 1050°C in the presence of KCl.

Other than experiments designed to re-crystallise graphite, there are others that rely on redox reactions to either a) reduce a carbonate bearing assemblage or b) oxidise a reduced (CH_4) assemblage. These clearly are not only dependent on lying within the P-T diamond formation window but are also heavily dependent on the $f\text{O}_2$ conditions (reviewed in detail by Luth 1999). The formation of diamond by reduction of a carbonate assemblage was successfully attempted (Gunn and Luth 2006; Spivak and Litvin 2004), the former used a sulphide melt as their reduction agent, forming metastable graphite rather than diamond, however. The source of either of the redox fluids/melts needed to release the C for diamond production is still under examination, although sulphide represents a likely candidate (Gunn and Luth 2006). The antonym to this formation method is the oxidation of a reduced assemblage (assumed usually to be CH_4 bearing) by oxidised fluids or melts. To the authors' knowledge, little work has been conducted on CH_4 bearing systems (Yamaoka et al. 2002b) as a method of forming diamond. Most of the studies on reduced fluids have been aimed at characterising phase equilibria under reducing conditions (Eggler and Baker 1982; Frost 2006; Green et al. 1987; Taylor and Green 1988).

To date, only one other study has tested a hydrous silicate system (Sokol and Pal'yanov 2007). Results from this study show that the $\text{MgO-SiO}_2\text{-H}_2\text{O-C}$ system is capable of growing diamond, especially when melt-water ratios are >0.5 ($\text{H}_2\text{O}/\text{H}_2\text{O}+\text{silicate}$). A pure $\text{H}_2\text{O-C}$ fluid system was shown to be the most successful at spontaneously nucleating diamonds. All of the experiments in this study were designed to test the effect of H_2O concentration on diamond genesis, rather than to form diamond at the low P-T conditions found within the DFW, as a result the P-T conditions (1600°C , 7.7GPa) greatly exceed those recorded in natural diamonds.

To compliment the work of Sokol and Pal'yanov (2007) and Tomlinson et al. (2004), we

examined whether an alkali-halide rich hydrous silicate melt could grow diamonds at the P-T conditions inside the DFW.

Starting materials:

Starting compositions (Table 1) were produced from a combination of silicic acid (a hydrous silicate compound containing structural water), brucite and graphite; later experiments added KCl and NaCl to their starting compositions. The starting materials were selected

Starting composition chemical makeup (molar basis)	No. of experiments
$\text{SiO}_2 \cdot 0.36\text{H}_2\text{O} + \text{Mg}(\text{OH})_2$	2
$\text{SiO}_2 \cdot 0.36\text{H}_2\text{O} + \text{Mg}(\text{OH})_2 + 2\text{C}$	5
$\text{SiO}_2 \cdot 0.36\text{H}_2\text{O} + \text{Mg}(\text{OH})_2 + 2\text{C} + \text{KCl}$	18
$\text{SiO}_2 \cdot 0.36\text{H}_2\text{O} + \text{Mg}(\text{OH})_2 + 2\text{C} + \text{KCl} + \text{NaCl}$	4
$\text{SiO}_2 \cdot 0.36\text{H}_2\text{O} + \text{Mg}(\text{OH})_2 + 2\text{C} + 0.5\text{KCl} + 0.5\text{NaCl}$	4
$\text{SiO}_2 \cdot 0.36\text{H}_2\text{O} + \text{Mg}(\text{OH})_2 + 2\text{C} + \text{NaCl}$	8
Total	41

Table 1: Composition of the various starting materials tested in this study and the number of experiments completed in each system.

for use as a starting composition because of the difficulty in reliably and reproducibly sealing known volumes of liquid water into platinum capsules of the size used in these experiments. By using chemicals with defined structural water content, we were able to construct a starting composition that, when at high pressure and temperature, would yield crystalline forsterite and enstatite coexisting with a hydrous silicate melt; and at lower temperatures a forsterite + enstatite + fluid mixture. All chemical starting components were purchased from Sigma Aldrich and Alfa Aesar and have a purity of >99%. The starting composition was formulated to give a Mg:Si ratio in the experiment of 1:1.5 – the elemental ratio needed to produce forsterite and enstatite as run products. Thus, once at experimental P and T above the wet silicate solidus, the carbon-bearing hydrous silicate

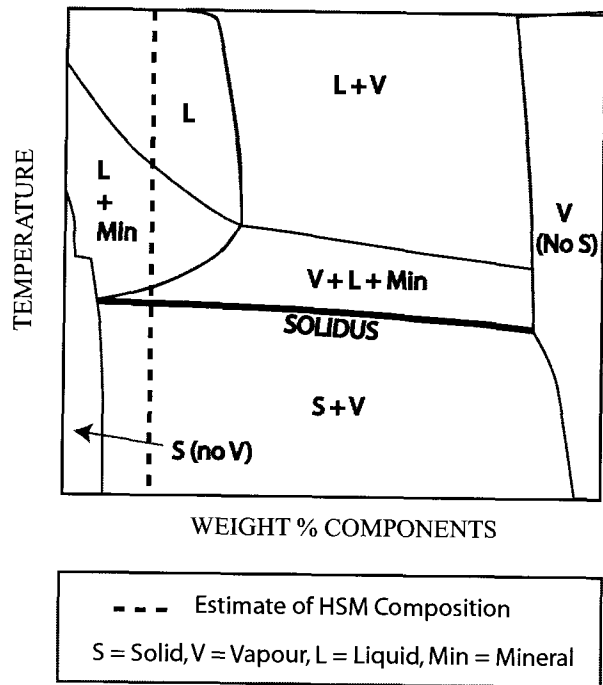


Figure 3:

Generalised phase diagram showing the location of a HSM with 16.7 wt% H₂O and where that lies in relation to other possible phases.

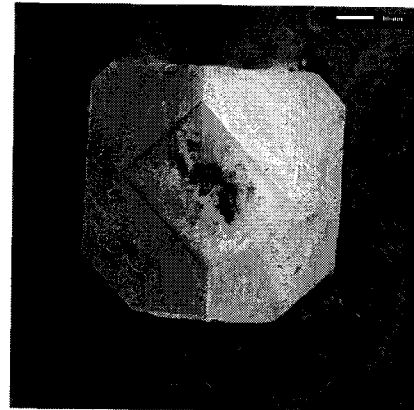
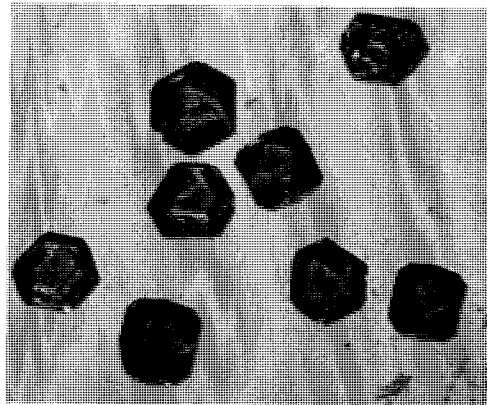


Figure 4: Seed Diamonds.

Left: pictures shows the styles of diamonds used as seeds. Fe-Ni inclusions can be seen inside the diamonds. Diameter = 1mm

Right: SEM image of a Cr-coated seed prior to experimental run, each surface is atomically smooth. Some minor contaminants are visible, these were later removed.

melt would be in equilibrium with a harzburgitic residue. Any diamond formation would thus occur in a simplified upper mantle compositional melt. Loss-on-heating experiments were conducted to determine the amount of structural water in brucite and silicic acid. We heated these experiments up to 1500°C, well in excess of the dehydration temperature at 1bar. XRD analyses were also obtained to show complete dehydration had been obtained. Based on these loss-on-heating experiments, the starting composition contained ~16.7 wt% H₂O (Fig. 3).

Seed diamonds (Fig. 4) were used in this study to provide nucleation sites for new diamond growth. The inclusion of such seeds lowers the potential energy required before new crystals can begin to form, and is a standard crystal growth technique. A number of small (<2mm) synthetic diamonds were obtained from Element Six via Thomas Stachel; these diamonds were grown using HP-HT techniques and in Fe-Ni metal catalysts. As a result, many of the crystals have inclusions of these transition metals within them as remnants of their highly catalysed rapid growth. The seeds used in this study were selected from a batch of over 1000 synthetic micro-diamonds; they were examined under a binocular reflected light microscope and only diamonds displaying good crystal morphology, i.e. ones with no cracks or surface blemishes, and ones with no Fe-Ni inclusions breaching their surface, were selected as seed diamonds for this study. This winnowing process enabled the selection of ~50 synthetic diamonds for use as seeds in experiments. To assess the results of diamond growth on these seeds, each was photographed with a SEM from multiple angles, in an attempt to document the pre-existing surfaces of the seed crystals. The seed diamonds themselves were not coated prior to insertion into the SEM, instead they were mounted on a simple carbon stub, and as a result the photograph magnification could only resolve the seeds down to 10µm. Analytical disruption caused by crystal charging effects stopped the analyses at this point. To accurately document the nature of the diamond seed surfaces on

a μm or nm scale, 8 seeds were Cr coated and imaged on the SEM at high magnification. These give a general representation of the surface of the crystals and are shown in Fig. 4. The Cr-coated seeds were never used in HP-HT diamond growth experimentation.

Experimental Techniques:

Capsules were produced from (99.99% purity) Pt tubing, with an outer diameter of 1.5mm, 0.1mm wall thickness and total length of 4.5mm. After cleaning and annealing, the base

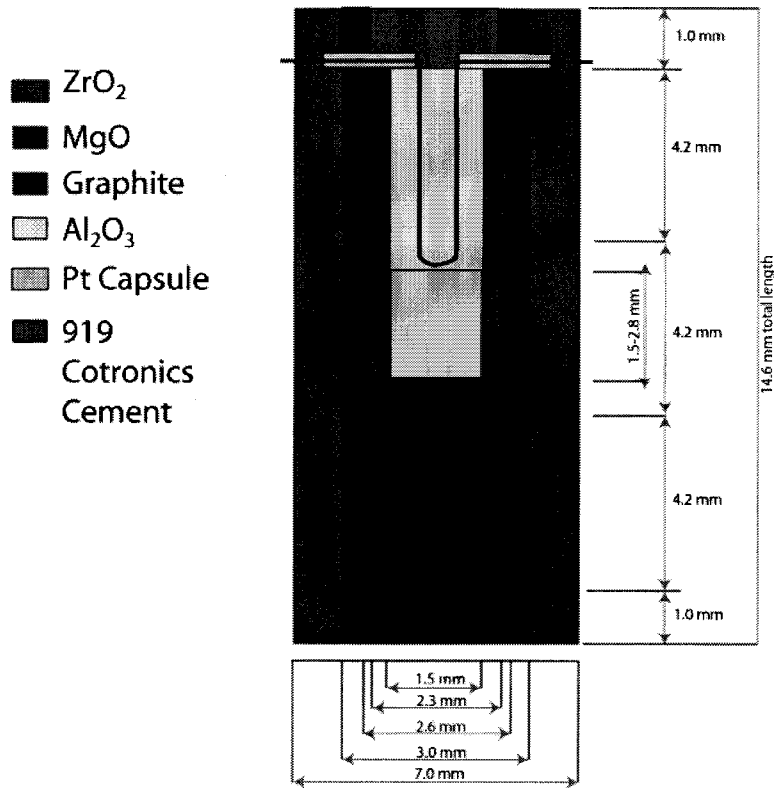


Figure 5: Cross section through the experimental assembly. Graphite furnaces, Pt capsule and thermocouples are shown. All measurements in mm. Thermocouple shown housed within the 4-bore T/C alumina.

of each capsule was triple crimped and welded shut using a carbon rod arc welder. The base was then flattened and a small experimental charge was loaded. For experiments containing diamond seed crystals, ~1 mg of sample was loaded, then the seed crystal inserted, followed by the remaining ~ 2 mg, covering the diamond seed and producing a capsule volumetrically filled to about $\frac{3}{4}$ of its height. The top of the capsule was cleaned to remove any excess powder; triple crimped and sealed using the welder. The sealed capsule was then carefully reshaped into a compact cylinder with the assistance of a brass mould.

The capsule was run in a sample assembly consisting of an 18mm edge-length MgO+5% Cr₂O₃ octahedron. The sample was centred within this octahedron, inside a stepped graphite furnace using MgO spacers and sleeves (Fig 5). The graphite furnace was surrounded by a ZrO₂ sleeve to reduce thermal conductivity within the assembly. A W₉₅Re₅-W₇₄Re₂₆ thermocouple was inserted axially into the furnace assembly in a four-bore 99.99% alumina ceramic. The octahedron, with Pt capsule removed, was then dried at 1000°C for 1hr in a 2% H₂-98% N₂ gas furnace. After removal and cooling, the capsule was re-inserted. The entire octahedron was placed into the centre of pre-arranged WC cubes with 11mm truncations and centred within the high-pressure apparatus. Pyrophyllite was used as a pressure gasket membrane between the anvils. This assembly is identical to that used by previous studies from this laboratory (Buob 2003; Gunn and Luth 2006; Luth 2001).

The complete assembly was run in the USSA-2000 split-sphere multi-anvil press, housed in the C.M Scarfe Laboratory for Experimental Petrology, at the University of Alberta. The pressure calibration of this apparatus was based on the quartz-coesite reaction at 2.95 GPa, 1000°C (Bohlen 1984) garnet-pervoskite transition in CaGeO₃ at 6.1 GPa, 1000°C (Susaki et al. 1985) and the coesite-shishovite transition at 9.1 GPa, 1000°C from Yagi and Akimoto (1976). The pressure uncertainty of the apparatus is ~0.5 GPa. All details on the calibration of the multi-anvil press can be found in Walter et al. (1995).

The experiment was brought to pressure over a period of 3 hrs, and heated at 70°C/min to the desired run temperature and held there ($\pm 5^\circ\text{C}$) for the duration of the run. The thermocouple *emf* was not corrected for pressure, and thermal gradients within the capsule are believed to be $\sim 50^\circ\text{C}$ (Domanik and Luth 1999). The run was quenched by shutting off the power to the graphite furnaces; temperatures below 300°C was achieved in typically <5 seconds. The experiment was then decompressed over 4-6 hours.

The Pt capsule was removed from the sample assembly by cracking open the ceramic octahedra and its inner layers. The capsule was opened carefully, whereupon the powder and any diamond seed were recovered. The seed crystal was first removed and cleaned in acetone before being placed into a small glass vial with de-ionised water and sealed with a cork lid. This vial was placed into the ultrasonic bath for 20 minutes, which removed any loose quench material from the surface of the seed diamond. The diamond was then extracted, air-dried and placed on a carbon stub for SEM analyses. The stubs were coated with a fine chrome coating in a powder-arc coater to prevent the sample charging under the SEM electron beam.

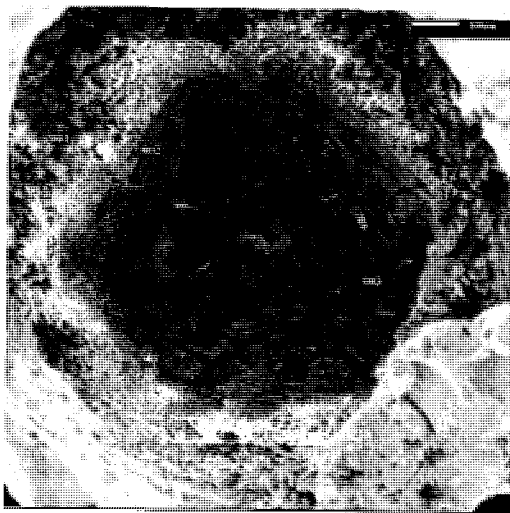


Figure 6: Internal view of a Pt capsule after an experimental run and after the removal of the diamond seed crystal. Layering is present, crystalline Fo+En+gr lie at the bottom (003) with the uppermost layers being made of quench melt (002), the top layer (001) contains a significant amount of H₂O. No part of the seed diamond appears to be in contact with the Pt capsule upon quench. Run AJF11-1, 1500°C, 7GPa.

Because the individual seed diamonds were imaged prior to the run, we were able to compare the seed diamond morphology before and after experimentation. As explained previously, resolution difference between the two sets of images occurred because we were unable to Cr coat the diamonds prior to their use in a run. Thus we relied on lower magnification shots of the seeds and looked for areas on the surface of the diamond that clearly differed. It must be noted that if an entire surface layer was added to the diamond face, this visual analysis technique could not detect it. Usually however, the growth was restricted to a set of faces on the diamond seed that were easily seen both with the SEM and on the wide-angle control photographs.

The material left in the capsule after removal of the seed was also analysed. It was typically layered, with the hydrous silicate material at the top of the capsule, and probably represents a quench texture. The more crystalline graphite, enstatite and forsterite-rich layer lies at the base of the capsule (Fig. 6). The uppermost white, more silicious material has a consistency not unlike toothpaste, and is clearly the material housing the remaining water. All of these layers were sampled and the fine-grained product was placed onto a quartz slide and analysed on a Rigaku Geigerflex 2173 powder x-ray diffractometer. Finally, the powder was placed into a small vial and stored for future analysis in a dessicator.

A series of control experiments were run without a diamond seed. These experiments were prepared for qualitative analyses using the JEOL 8900J electron microprobe at the University of Alberta. To do this, the Pt capsules were cleaned and mounted into plugs of epoxy (Petropoxy 154). These plugs were then ground on a Buehler manual grinding machine using 400 grit SiC paper until the platinum wall of the capsule was breached. More epoxy was then vacuum impregnated into the capsule, sealing the friable run products into a solid block. Several cycles of grinding and vacuum impregnation were required before a

Run Number	SiO₂	MgO	K₂O	Na₂O	H₂O	Total
<i>Olivine</i>						
AJF 8-3	42.88	57.17	0.00	0.01	-	100.06
AJF 8-3	42.49	56.56	0.01	0.00	-	99.08
AJF 8-4	42.22	57.19	0.00	0.00	-	99.42
AJF 8-5	41.68	57.56	0.00	0.00	-	99.24
AJF 8-5	41.20	57.46	0.00	0.01	-	98.67
AJF 8-7	42.32	57.08	0.00	0.02	-	99.42
AJF 8-7	42.21	57.28	0.00	0.00	-	99.49
AJF 8-14	42.21	57.03	0.02	0.01	-	99.27
AJF 8-14	42.18	57.29	0.02	0.01	-	99.51
AJF 8-16	42.20	56.32	0.02	0.02	-	98.56
AJF 8-16	42.45	56.08	0.00	0.00	-	98.53
AJF 8-18	42.16	56.70	0.01	0.00	-	98.96
<i>Enstatite</i>						
AJF 4-1	59.53	40.44	0.00	0.00	-	100.10
AJF 4-1	58.81	39.32	0.03	0.16	-	98.78
AJF 7-1	59.13	40.12	0.01	0.03	-	99.88
AJF 7-1	59.11	39.86	0.01	0.03	-	99.66
AJF 7-2	59.44	39.91	0.00	0.01	-	99.48
AJF 7-2	59.45	39.79	0.00	0.02	-	99.34
AJF 8-1	59.36	40.01	0.01	0.00	-	99.57
AJF 8-1	59.55	39.90	0.02	0.02	-	99.61
AJF 8-3	59.14	39.72	0.02	0.03	-	98.90
AJF 8-3	59.47	40.06	0.01	0.00	-	99.54
AJF 8-4	59.41	40.65	0.01	0.03	-	100.29
AJF 8-18	59.35	39.89	0.04	0.08	-	99.55
<i>Quenched Liquids</i>						
AJF 4-1	54.22	5.03	2.16	2.00	25.33	74.67
AJF 7-2	15.51	39.56	0.00	0.04	44.00	56.00
AJF 8-1	24.42	40.95	0.00	0.03	34.49	65.50
AJF 8-4	20.89	21.94	0.02	0.01	57.06	42.94
AJF 8-18	2.58	23.57	1.64	0.83	56.20	43.80

Table 2: Representative samples of electron microprobe analyses. Water calculated as a difference from 100%. Top section shows the production of forsteritic olivine and enstatite opx, the lower section are the quench melt phases shown in Fig 7 (Blue Dots).

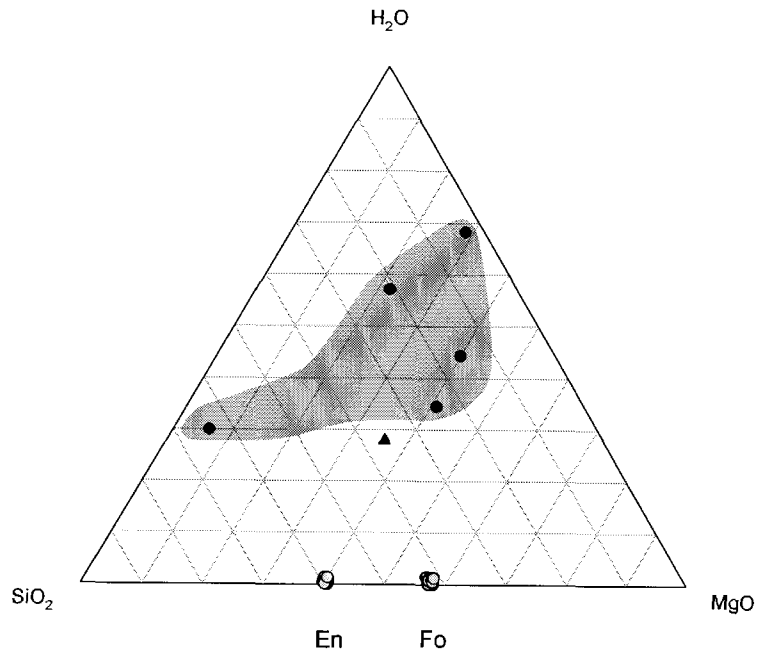


Figure 7: Ternary diagram showing the composition of the quench crystals (yellow dots), the starting composition (red triangle) and the quench melt residue (blue dots) plotted in wt %. Blue area, highlights the variability of the water and mineral contents of the melt.

solid cross-section through the capsule was exposed. A small volume of the experimental powder was inevitably lost during this process. In order to get the fully polished surface required for microprobe analyses a series of successively finer SiC paper was used from 400 grit down to 1200. Samples were then polished on a manual lapping wheel using deionised water and 5 μ m, 1 μ m and 0.05 μ m Al₂O₃ polishing solution. After cleaning and drying, the samples were carbon coated in preparation for electron microprobe analyses.

BSE and SE images were obtained of the experimental charges and the single and multi-phase relationships observed within them. Quantitative EPMA analyses on olivine and orthopyroxene were conducted using a 1 μ m wide beam diameter; 20kV-accelerating

voltage; 20nA beam current and the count times were 20sec/10sec seconds (peak/background). A $\phi\rho Z$ correction (Armstrong 1995) was applied to the data before final output. Quench and melt residue textures were analysed using a 10 μ m beam diameter, 15kV accelerating voltage, 15nA beam current and the count times were 20 seconds peak/10 seconds background. H₂O content was then calculated by the difference between the analysis total and 100%. Thus assuming perfect calibration of the microprobe the H₂O contents outlined in Table 2 should be treated as maximum H₂O contents.

Finally, one last set of control experiments were conducted; these were prepared without the addition of a seed diamond or graphite. Results from these ensured that the C played no role in the generation of a HSM, or the production of stable forsterite and enstatite as quench products.

Results:

System SiO₂-MgO-H₂O:

These experiments were conducted to enable analyses of the melt quench products using the electron microprobe. With no seed diamond, the capsule and contents were thus substantially easier to prepare and polish. Only two experiments were conducted in this system (table 3); neither was carbon bearing. Reaction of the starting composition was

Table 3: SiO₂-MgO-H₂O system

Run ID	Temp (°C)	Pressure (GPa)	Duration (hrs)	Nucleation	Seed Growth
7-2	1300	6	24	no C	no seed
7-1	1300	7	24	no C	no seed

confirmed by powder x-ray diffraction, which showed the presence of crystalline forsterite and enstatite and no silicic acid or brucite. As expected, no observable difference was determined between the C-bearing and the non C-bearing forsterite and enstatite crystals.

System SiO₂-MgO-H₂O-C

This system is the base system for the study, adding graphite to the HSM composition described above (Table 4). Seed diamonds were used in all experiments. No diamond was

Table 4: SiO₂-MgO-H₂O-C system

Run ID	Temp (°C)	Pressure (GPa)	Duration (hrs)	Nucleation	Seed Growth
5-5	1300	6	24	none	none
4-1	1300	7	4	none	no seed
5-4	1300	7	9.5	none	none
6-1	1300	7	24	none	no growth
6-2	1300	7	24	none	no growth
6-4	1500	6	4	none	no growth
6-3	1500	7	4	possible	yes, <1µm
6-5	1600	7	4	yes	yes, >10µm

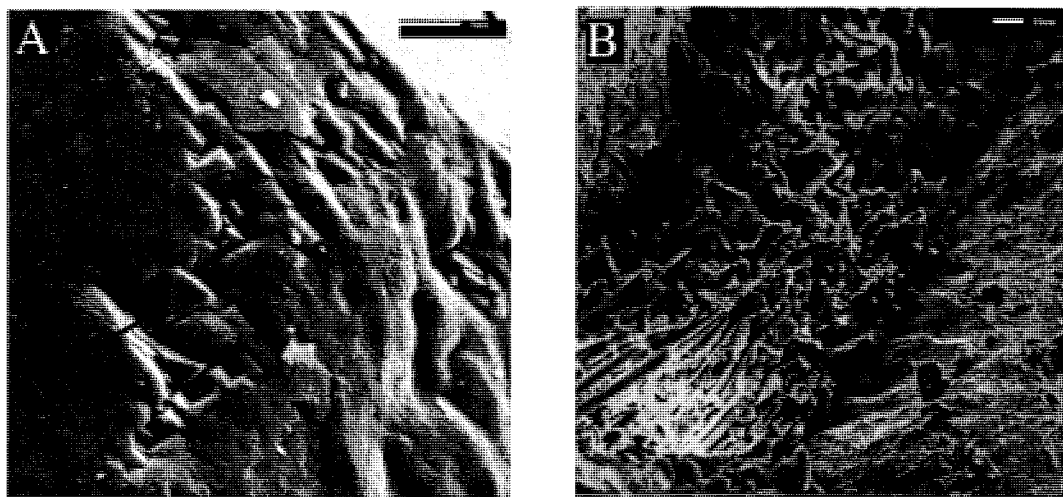


Figure 8: Diamond growth in the system MgO-SiO₂-H₂O-C

A - Shows distinctive octahedral morphology, crystallisation occurs in/along a surface crack. Arrow shows spontaneous growth in AJF6-3.

B - displays a section of acicular quench melt Fo+En crystals inside a hole on the seed crystal in run AJF6-3.

spontaneously grown below 1600°C. There was the possibility that a very fine coat of diamond was grown on the outer surface of the seed at 1500°C, however, clear growth of new crystals can be observed at 1600°C. This system was tested down to 1100°C without seeing diamond growth occurring in the timescale of these experiments. This suggests that either growth will not occur, or an induction period of >24 hrs exists in the hydrous silicate system at these low temperatures.

Fig 8 shows the formation of new diamond crystals in defects on a seed diamond at 1500°C, 7GPa (run AJF6-3). Figure 8B shows the style of melt quench products, acicular forsterite and enstatite coexisting with quenched melt, now amorphous hydrated phases. All newly grown diamonds exhibited octahedral morphology; this is consistent with growth and morphology studies in natural diamonds (Bulanova 1995; Robinson 1979; Sunagawa 1984).

System SiO_2 -MgO- H_2O -C-KCl

At lower T (<1400°C) with added KCl, we observed no diamond growth, as in the KCl absent system. However, formation of crystals at 1400°C at 7GPa (run AJF8-18) was observed; which to the authors' knowledge is the first time that a silicate experimental system has formed diamond within the natural DFW. Upon increasing the T to 1500°C the diamond growth occurred more rapidly (Table 5) and produced larger, better quality octahedral and coat layer growths (Fig. 10).

Figure 9 illustrates the catalytic abilities of KCl in diamond genesis. Both of these experiments were conducted under the same P-T-t conditions, the only difference being the addition of KCl. The scale-bars are 1 micron; there is at least two or three orders of magnitude difference in growth between the two sets of experiments.

Table 5: SiO₂-MgO-H₂O-C-KCl system

Run ID	Temp (°C)	Pressure (GPa)	Duration (hrs)	Nucleation	Seed Growth
8-7	1100	7	24	none	no growth
8-10	1300	6	8	none	no growth
8-2	1300	7	24	none	no seed
8-4	1300	7	24	none	no growth
8-5	1300	7	3	none	no growth
8-8	1300	7	8	none	no growth
8-18	1400	7	4	possible	yes, <1μm
8-17	1500	5.5	4	possible	?
8-14	1500	7	4	yes	yes, <1μm
8-16	1500	7	4	none	yes, <10μm
8-3	1500	7	3	yes	yes, >10μm

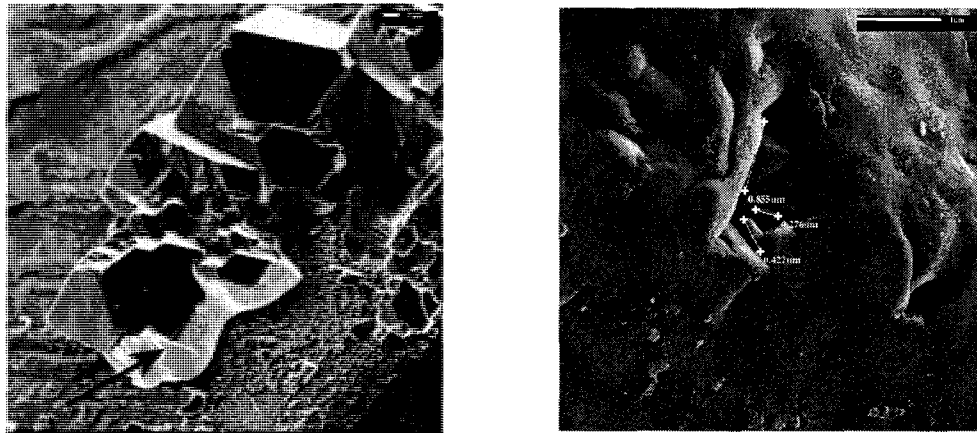


Figure 9: The effect of KCl. Left picture is a KCl bearing system, the right is KCl free. Both of these experiments were conducted under the same P-T conditions of 1500°C, 7GPa. Scalebars are the same (1um). Arrow in left image displays quenched HSM.

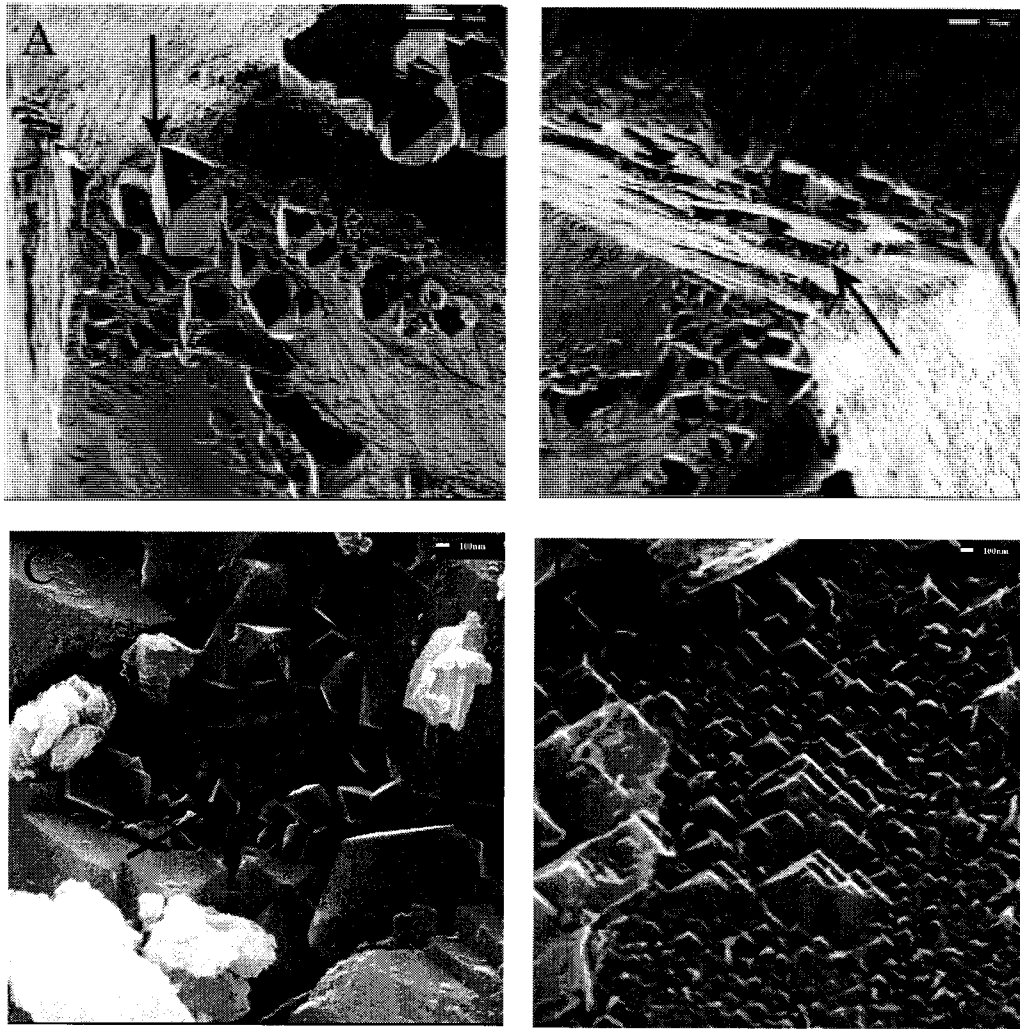


Figure 10: MgO-SiO₂-H₂O-C-KCl

- A) Extensive octahedral growth on the surface of seed crystal in run AJF8-3.*
- B) Amalgamation of octahedral crystals form new diamond layers in AJF8-3.*
- C) Randomly orientated spontaneous growth inside a crystal defect, run AJF8-16.*
- D) Close-up picture of a growing diamond seed surface, run AJF8-14.*

An attempt to characterise the effects of pressure on diamond genesis was also attempted in this system, but the results at 5.5 and 6 GPa were inconclusive. We therefore concentrated on characterising the effect of temperature. Fig. 10 shows the various styles of growth observed in all positive experiments conducted in this system, from large octahedra (A), to growth layers (B). The layers are important because it shows micron scale surface growth, which amalgamate into a series of very complex layers. It is also important to note that the entire face of the seed appears to be growing in runs >1500°C, right down to the nm scale (Fig. 9D).

System SiO₂-MgO-H₂O-C-NaCl [\pm KCl]

Three systems containing NaCl were tested, a pure NaCl system (no KCl) and two 50:50 ratio mixes of KCl and NaCl, one at 0.5 mol each, the other at 1.0 mol each (table 1). Table 6 shows the pure NaCl runs, which at T>1600°C grew large octahedral diamonds on several faces of the seed crystal (Fig. 11). Areas of surface coat development can be seen (A+C), where octahedra have amalgamated and formed stacked columns, i.e. a fibrous layer. Diamond growth was not restricted to defects or cracks as observed in the SiO₂-MgO-H₂O system, instead operates on the faces of the crystal (D). In contrast, the presence

Table 6: SiO₂-MgO-H₂O-C-NaCl system

Run ID	Temp (°C)	Pressure (GPa)	Duration (hrs)	Nucleation	Seed Growth
12-4	1400	7	24	dissolution	no growth
12-5	1400	7	4	none	no growth
12-9	1400	7	4	none	no growth
12-2	1500	7	4	none	no growth
12-6	1500	7	4	dissolution	no growth
12-8	1500	7	4	none	yes, <1µm
12-7	1600	7	4	yes	yes, >10µm

of NaCl below 1600°C caused the opposite effect – resorption (Fig. 12). Clear dissolution features, as first documented by Fersman and Goldschmidt (1911), were observed on the seed diamonds. These included negative trigons, hexagonal and circular pits. No growth was observed on the seeds. Given that NaCl has been documented as a fluid inclusion in natural diamond samples (Izraeli et al. 2001), its effect as either a diamond dissolution

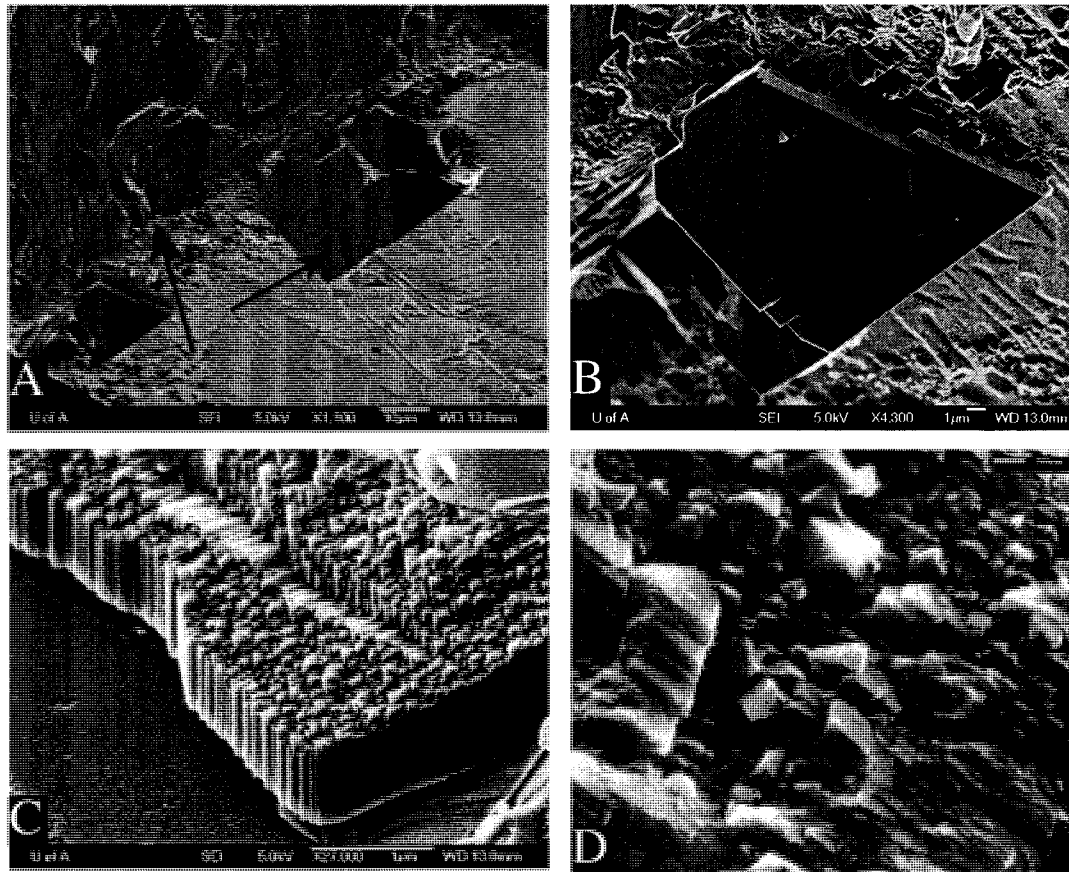


Figure 11: Growth in a Na-bearing system. Once temperatures exceed 1600°C diamond formation can proceed. No resorption was noted.

A) Extensive octahedral diamond growth showing excellent faces and smooth intersects (AJF12-7). Also shown is the formation of a diamond coat on the vertical face.

B) Closeup of the perfectly formed diamond octahedral crystal (AJF12-7)

C) Nano-layering of octahedra creating a fibrous coat (AJF12-6)

D) Nanometer sized spontaneous octahedral diamond growth - shows the entire seed is growing - not just where large octahedra are observed (AJF11-4).

compound or a diamond growth enhancer requires further assessment.

Systems of mixed NaCl-KCl [SiO₂-MgO-H₂O-C-NaCl-KCl]

In these experimental systems (Table 7) the seed diamonds show no signs of dissolution or resorption. Growth was observed at 1400°C, 7GPa, the same conditions as the pure KCl system. Thus we must tentatively suggest that the resorption and diamond dissolution effects of NaCl are mitigated by the presence of KCl; this suggests that KCl is a powerful diamond growth enhancer.

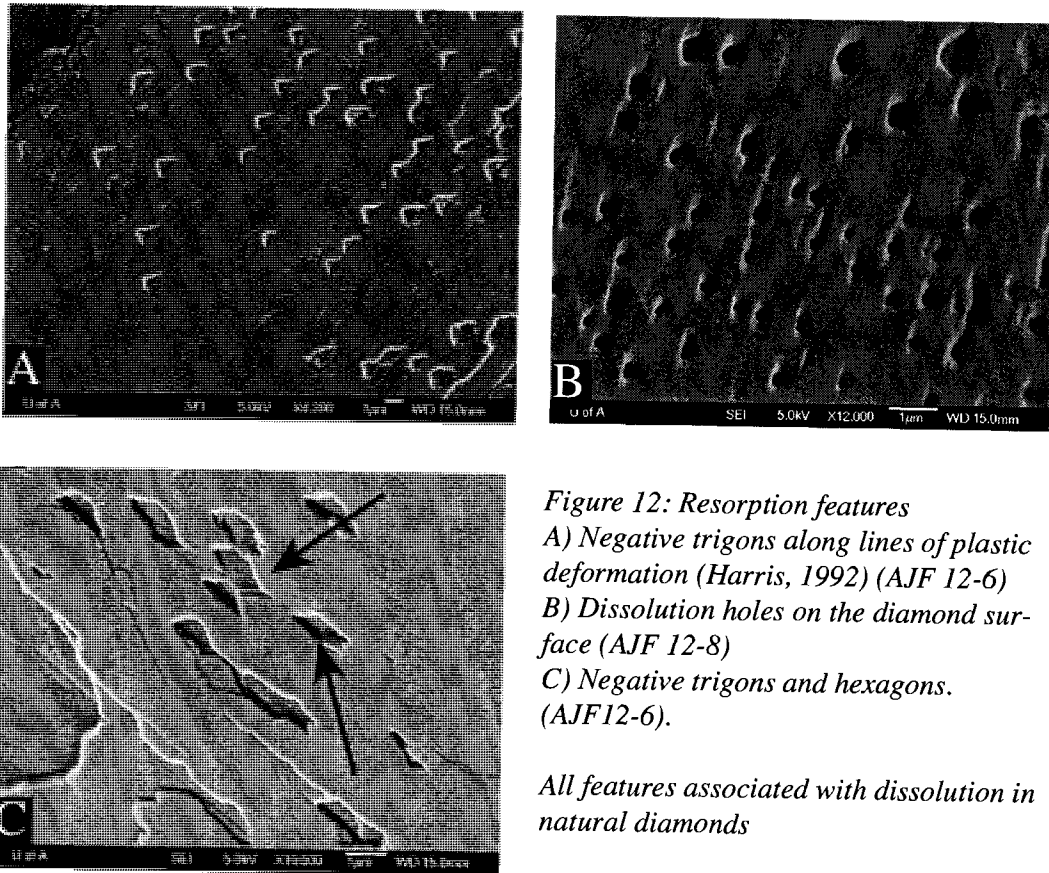


Figure 12: Resorption features
A) Negative trigons along lines of plastic deformation (Harris, 1992) (AJF 12-6)
B) Dissolution holes on the diamond surface (AJF 12-8)
C) Negative trigons and hexagons. (AJF 12-6).

All features associated with dissolution in natural diamonds

Table 7: SiO₂-MgO-H₂O-C-NaCl-KCl system

Run ID	Temp (°C)	Pressure (GPa)	Duration (hrs)	Nucleation	Seed Growth
11-3	1400	7	4	possible	yes, <1μm
11-1	1500	7	4	possible	yes, <1μm
11-4	1500	7	4	yes	yes, >1μm
13-1	1500	7	4	none	no growth
13-4	1500	7	4	possible	no growth

Discussion

The style of growth observed on the diamond seeds is similar in the various chemical systems studied. The original surfaces of the seed crystals commonly had pronounced “dendritic” looking patterns (Fig. 13), which is a common surface feature of synthetic diamonds. Its presence, however, added difficulty in assessing diamonds for new layer growth. In numerous cases, growth was observed as small individual octahedra attached to the surface of the seed by one or more crystal faces. These octahedral crystals often occur in clusters, sometimes on the faces of the seed diamonds, but more commonly on the crystal edges or surface defects of the seed crystal. Due to high levels of carbon oversaturation in the experiments, we observed diamond growth by spiral growth, giving rise to the prominent octahedral crystals (Bulanova 1995; Sunagawa 1984). We observed greater quantities and sizes of diamond at higher temperature experiments. With the lower temperature runs, there was slower growth causing smaller crystals. This may also explain why we typically see certain areas of the seed crystal that have grown diamond much more successfully than others. This feature is not restricted to these experiments; Pal’yanov et al. (2002) also showed development of full octahedral micro-diamonds on the surface of the seed crystal as well as pronounced surface coat development.

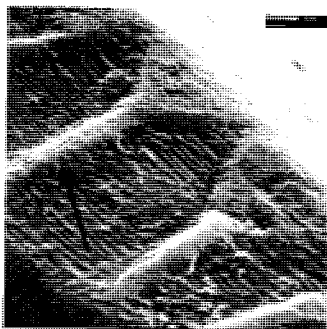


Figure 13: Dendritic patterns on original seed crystal prior to use in HPHT experiment.

The reference works for the morphology and surface features of natural diamonds was completed by Fersman and Goldschmidt (1911) and Robinson (1979). To the authors' knowledge, no similar extensive study has yet been published for high pressure – high temperature synthetic diamonds, like the ones used as seed crystals in this study. Because of the qualitative method used in this study to assess if growth of diamond has occurred – i.e. the diamonds were visually inspected under the SEM - only experiments displaying obvious growth were recorded as positive. Thus it is possible that samples with minor surface growth, rather than the more obvious spot-growth were missed during assessment. It was found that the growth layers, if present, were so small that it was impossible to conduct CL imaging on them to assess surface growth conditions or any zonations within the new diamond layers. However, some of the growth layers were thicker, and can easily be seen on the SEM. These appear to be forming by the amalgamation of octahedral habit diamond crystals, creating a polycrystalline coat along the seed diamond surface (Fig 10B).

Application to natural diamond growth

This study demonstrated that HSM can flux the graphite to diamond reaction at P-T akin to the diamond formation window and that the generated melt was in equilibrium with a simplified mantle mineral assemblage, thus it seems appropriate to apply our results to a new natural diamond formation model.

We agree with Kesson and Ringwood (1989), that the supra-subduction zone mantle could be a crucial area for diamond formation. In their model, fluids released by the dehydration of serpentine minerals ascend into the overlying mantle wedge and are responsible for diamond formation and mantle metasomatism in the wedge (Kesson and Ringwood 1989).

It is not only in this subduction zone setting that the HSM model would apply; it may also be relevant to diamond genesis within the cratonic keels and the sub-continental lithospheric mantle (SCLM) beneath the continents. Stachel and Harris (2008) modified a SCLM model first proposed by Helmstaedt and Schultze (1989). This 'imbrication' model provides an ideal environment to apply the HSM diamond formation model.

Shallow dehydration of oceanic plates is restricted to the upper levels of a subduction zone and gives rise to its associated plate boundary volcanism. However, other hydrous minerals are present within the oceanic slab that do not dehydrate until greater depths, well inside the natural diamond formation window (Ulmer and Trommsdorff 1999). In the SiO_2 -MgO- H_2O system, the H_2O bearing minerals would completely dehydrate upon reaching 8GPa (~250km) (Ulmer and Trommsdorff 1999). The thermal conditions required for generation of a hydrous melt inside the DFW exist in subduction zones that are similar in structure to modern-day Izu-Bonin subduction zone (Peacock 2000).

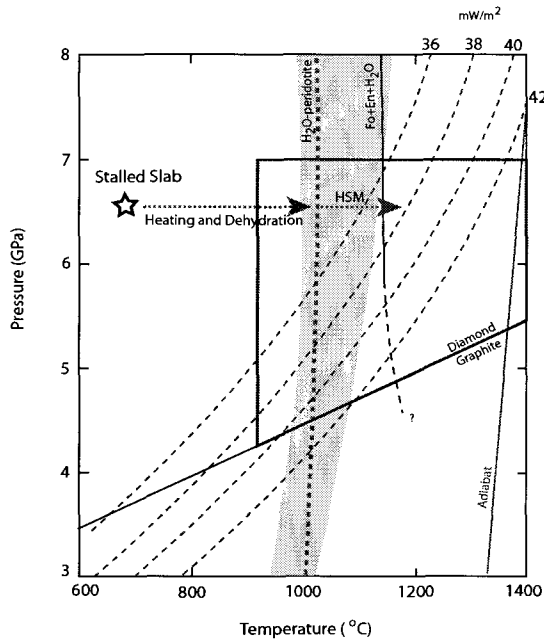
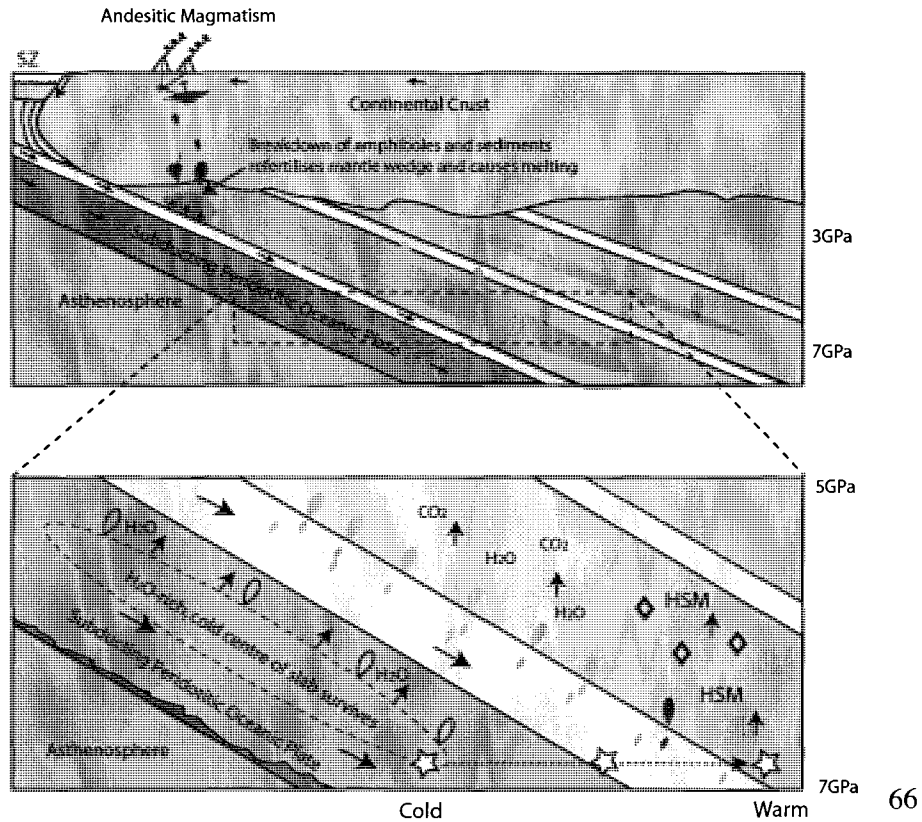


Figure 14: Imbrication Model
 Top: Phase diagram showing the generation of a Hydrous Silicate Melt from a stalled subducted slab. Blue arrow represents dehydration in a fluid stable environment, orange arrow represents dehydration in hydrous melt environment. Typical continental geotherms, and a simplified model solidus (Stalder et al. 2001; Kawamoto & Holloway, 1997) are also shown.

Bottom: Simplified model (after Stachel and Harris, 2008) showing the generation of a HSM and diamond genesis. Stars represent the heating path shown in the top figure.



A new model (Helmstaedt and Schulze 1989; Stachel and Harris 2008) requires that a subducted oceanic slab imbricate against an older slab and break off upon reaching a particular depth or density. Due to the high spreading rates at Archean oceanic ridges, the oceanic crust did not have time to cool before being subducted, and thus, was buoyant in the upper mantle below the sub-continental lithospheric mantle (SCLM). The broken slab would be added to the imbrication package and a newer oceanic slab would begin to occupy the space to the side of the slab, see Fig. 14. This imbrication process would build-up an area in the upper mantle where old slabs would reside, typically at a depth similar to the DFW. The stalled slabs still hold their hydrous minerals, typically with more volatiles surviving towards the centre portions of the slab rather than those exposed to the mantle temperatures around the slab-edges. As the mantle conditions begin to heat up the centre of the old slab, the dehydration boundaries of the hydrous minerals would be crossed, releasing significant volumes of water into the stalled slab material and the surrounding mantle. We envisage this occurring at $T \sim 700^{\circ}\text{C}$ after the breakdown of antigorite and other serpentine minerals has occurred around 5GPa (Fig. 1 and Ulmer and Trommsdorff 1999). The source of carbon is enigmatic and there are several possibilities. These include carbonate fluids or melts generated from the subducted slab and the sediments trapped along with it. Diamond formation would then require interaction of these oxidised fluids or melts with a reduced mantle assemblage. Alternatively, these fluids or melts, once introduced into the mantle, may interact with ascending reduced fluids to produce elemental carbon. The final possibility is that the carbon is primordial, thus is present as a stable phase within the upper mantle already.

The slab's heating regime is dictated by the ambient heat-flow of the surrounding mantle; typical cratonic geotherms ($36\text{-}42\text{mW/m}^2$) would exist in this mantle area. Heating of the

slab by the surrounding rocks would continue until a steady state geotherm was reached, no further subduction is required to generate the conditions required for dehydration. If we assume a model geotherm of 38mW/m^2 , a standard diamond bearing geotherm documented in many areas of the world, then the wet-lherzolite solidus is crossed at $950\text{-}1100^\circ\text{C}$ at $4.8\text{-}5.5\text{GPa}$ depending on the precise location of the wet solidus (Fig 11). Thus at the deeper imbrication depths of 7GPa , break down of any hydrous phases would trigger melting at the wet solidus. The genesis of diamond from this HSM would then be controlled by the presence of a carbon source and catalysts such as KCl. The presence of KCl in the mantle has been demonstrated by its presence in diamond fluid inclusions as a KCl-NaCl-H₂O brine (Izraeli et al. 2001). If this brine resides at DFW depth and is able to percolate through a garnet lherzolite assemblage, Na would be preferentially removed, as it partitions into the surrounding clinopyroxene; Cl and K would partition into any hydrous phases, such as phlogopite, or would remain in the fluid in a phlogopite absent assemblage. Thus over time the brine would evolve, gradually becoming more K and Cl rich. The melting of an imbricated oceanic slab would result in a hydrous silicate melt rich in H₂O and KCl, similar to the compositions used to form diamond in this study.

Conclusions:

We have shown that a hydrous silicate melt is capable of fluxing the graphite to diamond transition under pressures and temperatures akin to the natural diamond formation region. This study agrees with work conducted by Sokol and Pal'yanov (2007), in a similar experimental system. The addition of KCl to a HSM system enables diamond growth at lower temperatures. We suggest that NaCl is a diamond inhibitor in hydrous silicate melts. We believe that a stalled subducted oceanic plate, lying within the DFW for a long period of time represents the ideal location for diamond growth from a HSM.

References:

Akaishi M, Kumar MDS, Kanda H, Yamaoka S (2001) Reactions between carbon and a reduced COH fluid under diamond stable conditions. *Diamond and Related Materials* 10:2125-2130

Akaishi M, Yamaoka S (2000) Crystallization of diamond from C-O-H fluids under high-pressure and high-temperature conditions. *Journal of Crystal Growth* 209(4):999-1003

Armstrong JT (1995) A Package of correction programs for the quantitative electron microbeam X-ray analysis of thick polished materials, thin films, and particles, *Microbeam Analysis* 4:177-200

Bohlen SR (1984) Equilibria for precise pressure calibration and a frictionless furnace assembly for the piston-cylinder apparatus. *Neues Jahrbuch Mineralogie Monatshefte H* 9:404-412

Bovenkirk HP (1961) Some observations on the morphology and crystal characteristics of synthetic diamonds. *American Mineralogist* 46:952-963

Bovenkirk HP, Bundy FP, Hall T, Strong HM, Wentorf RHj (1959) Preparation of diamond. *Nature* 184:1094-1098

Bulanova GP (1995) The formation of diamond. *Journal of Geochemical Exploration* 53:1-23

Buob A (2003) The system $\text{CaCO}_3\text{-MgCO}_3$: experiments and thermodynamic modelling of the trigonal and orthorhombic solid solutions at high pressures and temperatures. Dr Nat Sci thesis, Swiss Federal Institute of Technology, unpublished, p 107

Dasgupta R, Hirschmann MM (2006) Melting in the Earth's deep upper mantle caused by carbon dioxide. *Nature* 440:P 659-662

Domanik K, Luth RW (1999) The effect of pressure on thermal gradients in multianvil apparatus. In: AGU spring meeting abstracts, p2.

Eggler DH, Baker DR (1982) Reduced volatiles in the system COH: implications to mantle melting, fluid formation and diamond genesis. In: Akimoto S, Manghnami MH (eds) High-pressure research in geophysics, vol 12. Centre for Academic Publications, Tokyo, pp 237-250

Fersman AE, Goldschmidt V (1911) *Der Diamant*, Winter, Heidleberg, Germany

Frost BJ (2006) Investigation of the behaviour of reduced COH fluids at conditions of the Earths transition zone. Bayerisches Forschungsinstitut fur Experimentelle Geochemie und Geophysik, Universität Bayreuth, Annual Report 1:106-108

- Green DH, Falloon TJ, Taylor WR (1987) Mantle derived magma roles of variable source peridotite and variable carbon-oxygen-hydrogen fluid compositions, In: Mysen BO (ed) Magmatic processes: physiochemical principles, Geochemical Society Special Publication 1, p139-154
- Gunn S, Luth RW (2006) Carbonate reduction by Fe-S-O melts at high pressure and high temperature. *American Mineralogist* 91:1110-1116
- Harris JW (1992) Diamond Geology, In: Field, J.E. The properties of natural and synthetic diamonds, Special Publication. Academic Press, London
- Hazen RM (1999) *The Diamond Makers*, Cambridge University Press, Cambridge, p 244
- Helmstaedt HH, Schulze DJ (1989) Southern African kimberlites and their mantle sample: implications for Archean tectonics and lithosphere evolution. In: Ross. J et al (eds) *Kimberlites and Related Rocks*, vol 1. Blackwell, Carlton, pp 358-368
- Iwamori H (1998) Transportation of H₂O and melting in subduction zones. *Earth and Planetary Science Letters* 160(1-2):65-80
- Izraeli ES, Harris JW, Navon O (2001) Brine inclusions in diamonds: a new upper mantle fluid. *Earth and Planetary Science Letters* 187(3-4):323-332
- Kawamoto T, Holloway JR (1997) Melting Temperature and partial melt chemistry of water-saturated Mantle peridotite to 11GPa. *Science* 276:240-243
- Kessel R, Ulmer P, Pettke T, Schmidt MW, Thompson A (2005) The water-basalt system at 4 to 6 GPa: Phase relations and second critical endpoint in a K-free eclogite at 700 to 1400 degrees celsius. *Earth and Planetary Science Letters* 237:873-892
- Kesson SE, Ringwood AE (1989) Slab-mantle interactions - 2. *Chemical Geology* 78:97-118
- Klein-BenDavid O, Izraeli ES, Hauri E, Navon O (2004) Mantle fluid evolution-a tale of one diamond. *Lithos* 77:243-253
- Litvin YA, Aldushin KA, Zharikov VA (1999a) Synthesis of diamond at 8.5-9.5 GPa in the system K₂Ca(CO₃)₂-Na₂Ca(CO₃)-C corresponding to the composition of fluid carbonatite in diamonds from kimberlites. *Doklady Akademii Nauk* 367(4):529-532
- Litvin YA, Chudinovskikh LT, Saporin SK, Obyden SK, Chukichev MV, Vavilov VS (1999b) Diamonds of new alkaline carbonate-graphite HP synthesis: SEM morphology,

CCL-SEM and CL spectroscopy studies. *Diamond and Related Materials* 8:267-272

Luth DR (1999) Carbon and Carbonates in the Mantle. In: Fei, Y et al (eds) *Mantle Petrology: Field Observations and High pressure Experimentation : A Tribute to Francis R. (Joe) Boyd*, vol No 6. The Geochemical Society, pp 297-321

Luth RW (2001) Experimental determination of the reaction aragonite plus magnesite = dolomite at 5 to 9 GPa. *Contributions to Mineralogy and Petrology* 141(2):222-232

Navon O (1998) Diamond Formation in the Earth's mantle. In: *Proceedings of the 7th International Kimberlite Conference*, vol 2. Cape Town, SA

Pal'yanov YN, Shatsky VS, Sobolev NV, Sokol AG (2007) The role of ultrapotassic fluids in diamond formation. In: *Proceedings of the National Academy of Science of the USA, High-Pressure Geoscience Special Edition*. pp 1-6

Pal'yanov YN, Sokol AG, Borzdov YM, Khokhryakov AF, Sobolev NV (1999) Diamond formation from mantle carbonate fluids. *Nature* 400(6743):417-418

Pal'yanov YN, Sokol AG, Borzdov YM, Khokhryakov AF, Sobolev NV (2002) Diamond formation through carbonate-silicate interaction. *American Mineralogist* 87(7):1009-1013

Pal'yanov YN, Sokol AG, Khokhryakov AF, Pal'yanova GA, Borzdov YM, Sobolev NV (2000) Diamond and graphite crystallization in COH fluid at PT parameters of the natural diamond formation. *Doklady Earth Sciences* 375(9):1395-1398

Peacock SM (2000) Thermal structure and metamorphic evolution of subducting slabs. In: Eiler J (ed) *Inside the Subduction Factory*, vol 138. American Geophysical Union, Washington DC, pp 7-23

Robinson DK (1979) Surface textures and other features of diamonds. Unpublished PhD thesis. University of Cape Town, Cape Town, RSA. p 161

Safonov OG, Perchuk LL, Litvin YA, Chertkova NV (2008) Experimental model for alkalic chloride-rich mantle liquids. In: *9th International Kimberlite Conference*, Frankfurt, Germany, extended abstract, 3p.

Sokol AG, Borzdov YM, Pal'yanov YN, Khokhryakov AF, Sobolev NV (2001) An experimental demonstration of diamond formation in the dolomite-carbon and dolomite-fluid-carbon systems. *European Journal of Mineralogy* 13(5):893-900

Sokol AG, Pal'yanov YN (2007) Diamond formation in the system MgO-SiO₂-H₂O-C at

- 7.5GPa and 1600 celcius. *Contributions to Mineralogy and Petrology* 155(1):33-43
- Spivak AV, Litvin YA (2004) Diamond syntheses in multicomponent carbonate-carbon melts of natural chemistry: elementary processes and properties. *Diamond and Related Materials* 13(3):482-487
- Stachel T, Aulbach S, Brey GP, Harris JW, Leost I, Tappert R, Viljoen KS (2004) The trace element composition of silicate inclusions in diamonds: a review. *Lithos* 77(1-4):1-19
- Stachel T (2007) Diamonds. In: Groat LA (ed) *Geology of Gem Deposits*, Special Publication, Mineralogical Association of Canada
- Stachel T, Harris JW (2008) The origin of Cratonic diamonds - constraints from mineral inclusions. *Ore Geology Reviews* 34(1-2):5-32
- Stachel T, Harris JW, Tappert R, Brey GP (2003) Peridotitic diamonds from the Slave and the Kaapvaal cratons - similarities and differences based on a preliminary data set. *Lithos* 71(2-4):489-503
- Stalder R, Ulmer P, Thompson AB, Gunther D (2001) High Pressure fluids in the system MgO-SiO₂-H₂O under upper mantle conditions. *Contributions to Mineralogy and Petrology* 140:607-618
- Sun LL, Akaishi M, Yamaoka S (2000) Formation of diamond in the system of Ag₂CO₃ and graphite at high pressure and high temperatures. *Journal of Crystal Growth* 213(3-4):411-414
- Sunagawa I (1984) Morphology of natural and synthetic diamond crystals. In: Sunagawa. I (ed) *Materials Science of the Earths Interior*, Terrapub, Tokyo, pp 303-331
- Susaki J, Akaogi M, Akimoto S, Shimomura O (1985) Garnet-pervoskite transformation in CaGeO₃: insitu xray measurements using synchotron radiation. *Geophysical Research Letters* 12:729-732
- Tappert R, Stachel T, Harris JW, Muehlenbachs K, Ludwig T, Brey GP (2005) Diamonds from Jagersfontein (South Africa): messengers from the sublithospheric mantle. *Contributions to Mineralogy and Petrology* 150(5):505-522
- Taylor WR, Green DH (1988) Measurement of reduced peridotite COH solidus and implications for redox melting of the mantle. *Nature* 332:349-352
- Tomlinson E, Jones A, Milledge J (2004) High-pressure experimental growth of diamond using C-K₂CO₃-KCl as an analogue for Cl-bearing carbonate fluid. *Lithos* 77(1-4):287-

Ulmer P, Trommsdorff V (1999) Phase relations of hydrous mantle subducting to 300km. In: Fei Y, Bertka CM, Mysen BO (eds) *Mantle Petrology: Field observations and High Pressure Experimentation*, The Geochemical Society, Washington DC

Walter MJ, Thibault Y, Wei K, Luth RW (1995) Characterizing experimental pressure and temperature conditions in multi-anvil apparatus. *Canadian Journal of Physics* 73(5-6):273-286

Yagi T, Akimoto S (1976) Direct determination of coesite-stishovite transition by in-situ X-ray measurements. *Tectonophysics* 35:259-270

Yamaoka S, Kumar MDS, Kanda H, Akaishi M (2002a) Crystallization of diamond from CO₂ fluid at high pressure and high temperature. *Journal of Crystal Growth* 234:5-8

Yamaoka S, Kumar MDS, Kanda H, Akaishi M (2002b) Formation of diamond from CaCO₃ in a reduced C-O-H fluid at HP-HT. *Diamond and Related Materials* 11(8):1496-1504

Yamaoka S, Kumar S, Akaishi M, Kanda H (2000) Reaction between carbon and water under diamond-stable high pressure and high temperature conditions. *Diamond and Related Materials* 9(8):1480-1486

Chapter 3

Experimental results illustrating
diamond growth in a hydrous
silicate melt system

An XRD & SEM catalogue of
growth, resorption, surface fea-
tures and morphology

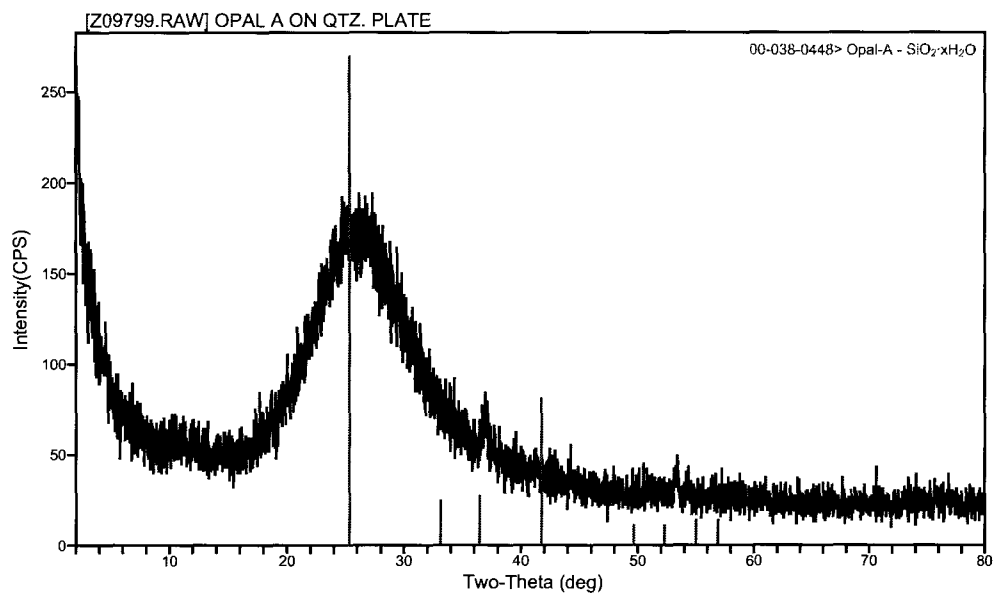
Contents:

Experimental run tables	Pages 77-78
X-ray results	Pages 79-80
Diamond seed images	Page 81
SEM photographs of diamond growth	Pages 82-111

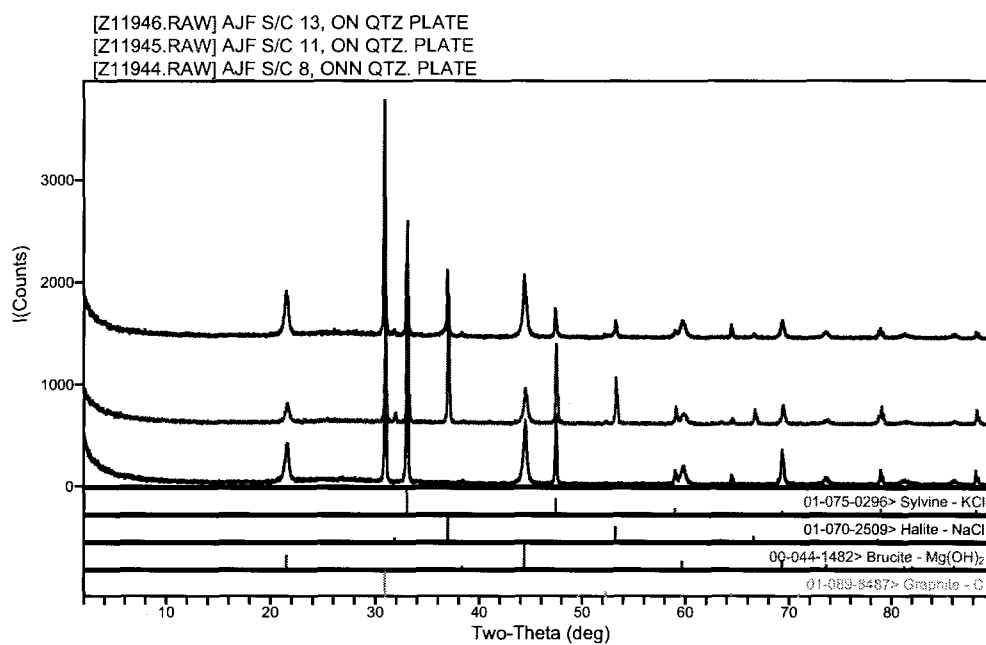
Experimental Run Table

Run ID	Temp (°C)	Pressure (GPa)	Duration (hrs)	System
7-2	1300	6	24	SiO ₂ -MgO-H ₂ O
7-1	1300	7	24	SiO ₂ -MgO-H ₂ O
5-5	1300	6	24	SiO ₂ -MgO-H ₂ O-2C
4-1	1300	7	4	SiO ₂ -MgO-H ₂ O-2C
5-4	1300	7	9.5	SiO ₂ -MgO-H ₂ O-2C
6-1	1300	7	24	SiO ₂ -MgO-H ₂ O-2C
6-2	1300	7	24	SiO ₂ -MgO-H ₂ O-2C
6-4	1500	6	4	SiO ₂ -MgO-H ₂ O-2C
6-3	1500	7	4	SiO ₂ -MgO-H ₂ O-2C
6-5	1600	7	4	SiO ₂ -MgO-H ₂ O-2C
8-7	1100	7	24	SiO ₂ -MgO-H ₂ O-2C-KCl
8-10	1300	6	8	SiO ₂ -MgO-H ₂ O-2C-KCl
8-2	1300	7	24	SiO ₂ -MgO-H ₂ O-2C-KCl
8-4	1300	7	24	SiO ₂ -MgO-H ₂ O-2C-KCl
8-5	1300	7	3	SiO ₂ -MgO-H ₂ O-2C-KCl
8-8	1300	7	8	SiO ₂ -MgO-H ₂ O-2C-KCl
8-18	1400	7	4	SiO ₂ -MgO-H ₂ O-2C-KCl
8-17	1500	5.5	4	SiO ₂ -MgO-H ₂ O-2C-KCl
8-14	1500	7	4	SiO ₂ -MgO-H ₂ O-2C-KCl
8-16	1500	7	4	SiO ₂ -MgO-H ₂ O-2C-KCl
8-3	1500	7	3	SiO ₂ -MgO-H ₂ O-2C-KCl
11-3	1400	7	4	SiO ₂ -MgO-H ₂ O-2C-KCl-NaCl
11-1	1500	7	4	SiO ₂ -MgO-H ₂ O-2C-KCl-NaCl
11-4	1500	7	4	SiO ₂ -MgO-H ₂ O-2C-KCl-NaCl

Run ID	Temp (°C)	Pressure (GPa)	Duration (hrs)	System
12-4	1400	7	24	SiO ₂ -MgO-H ₂ O-2C-NaCl
12-5	1400	7	4	SiO ₂ -MgO-H ₂ O-2C-NaCl
12-9	1400	7	4	SiO ₂ -MgO-H ₂ O-2C-NaCl
12-2	1500	7	4	SiO ₂ -MgO-H ₂ O-2C-NaCl
12-6	1500	7	4	SiO ₂ -MgO-H ₂ O-2C-NaCl
12-8	1500	7	4	SiO ₂ -MgO-H ₂ O-2C-NaCl
12-7	1600	7	4	SiO ₂ -MgO-H ₂ O-2C-NaCl
13-1	1500	7	4	SiO ₂ -MgO-H ₂ O-2C-0.5KCl-0.5NaCl
13-4	1500	7	4	SiO ₂ -MgO-H ₂ O-2C-0.5KCl-0.5NaCl

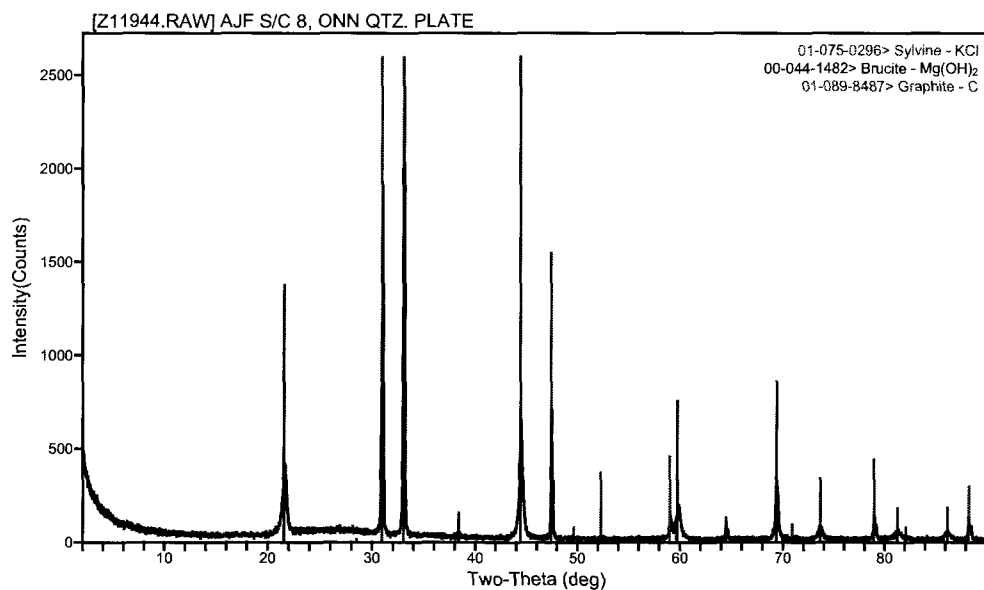


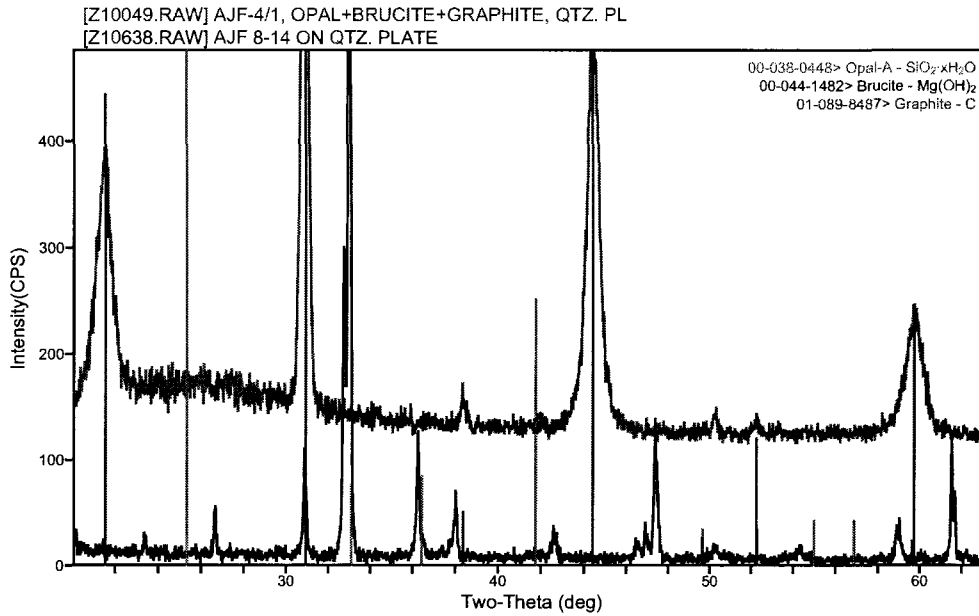
XRD 1: Showing the amorphous nature of the starting composition. This run was performed on Silicic Acid. Since this compound is not located in the University of Alberta Jade 7.0 XRD interpretation program, we found that the Opal-A XRD database card was the best fit.



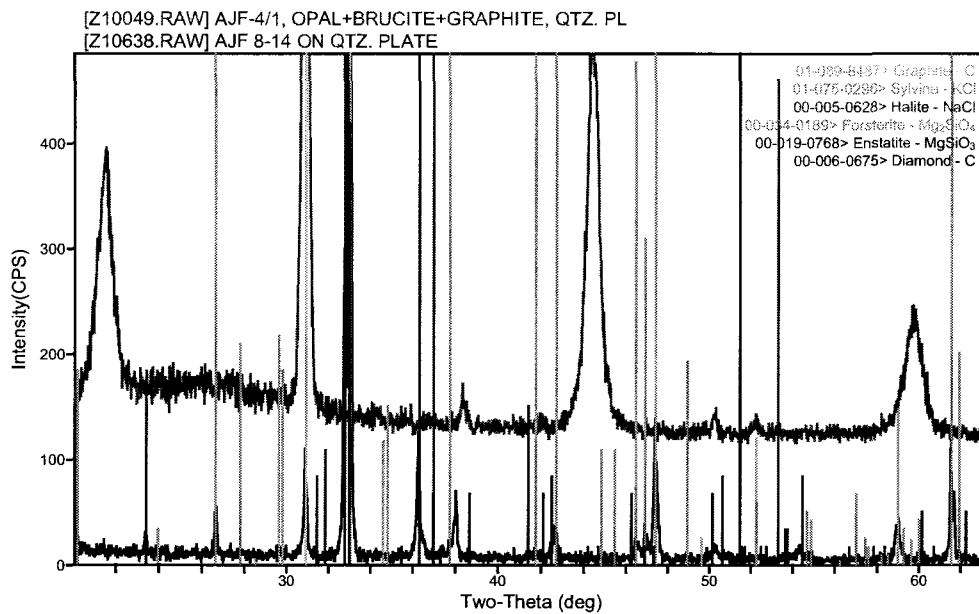
XRD-2 (above): Three important starting compositions, increasing in complexity from black, to red to blue. For full compositions see table 1 (page 47).

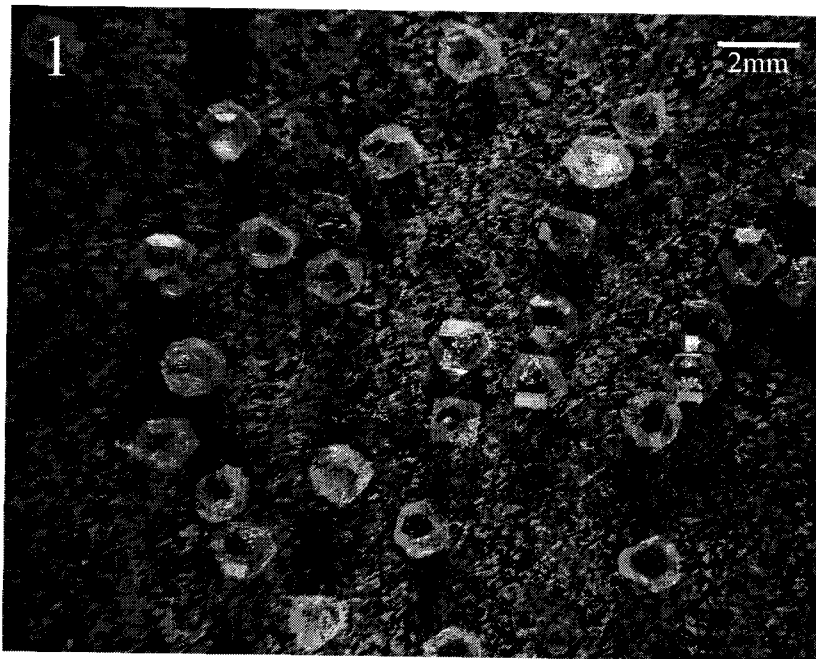
XRD-3 (below): Closeup of starting composition 8 showing no impurities.



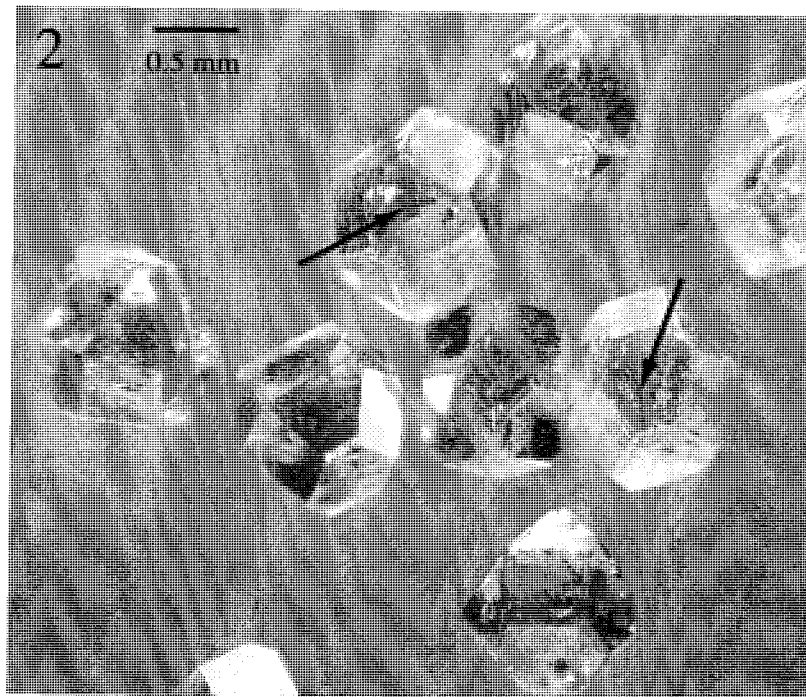


XRD 4 and 5: Red powder x-ray diffractograms represents one of the starting compositions (AJF 4-x), the black diffractogram is the results taken from an experimental run (AJF 8-14). The top shows the composition of the S/C, the lower shows how this has been changed and what has formed instead (top right corner of diffractogram)

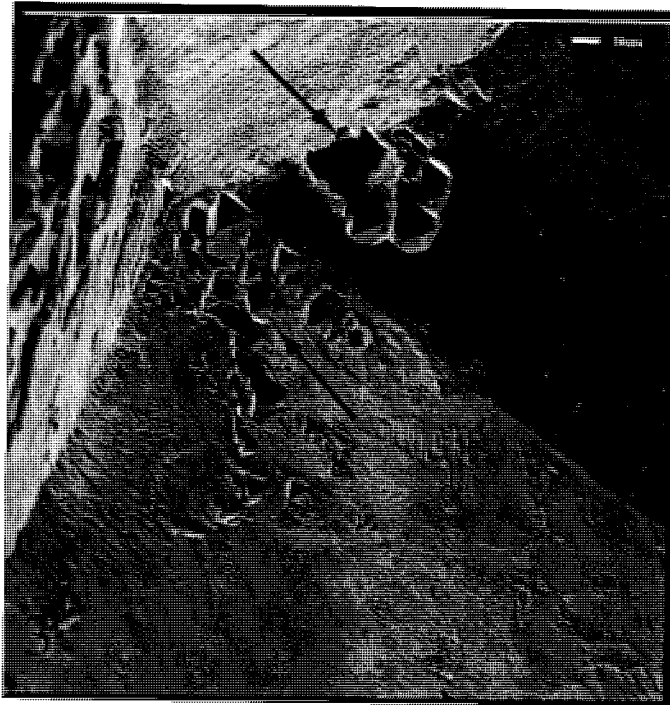




Examples of synthetic seed diamonds used in this study, obtained from Element Six. Cubo-octahedra and cubic morphology dominate. Ni and other metal catalysts can be seen as inclusion in the diamonds (arrows). No diamond with inclusions at the surface was selected to minimise the risk of contamination by these transition metals.



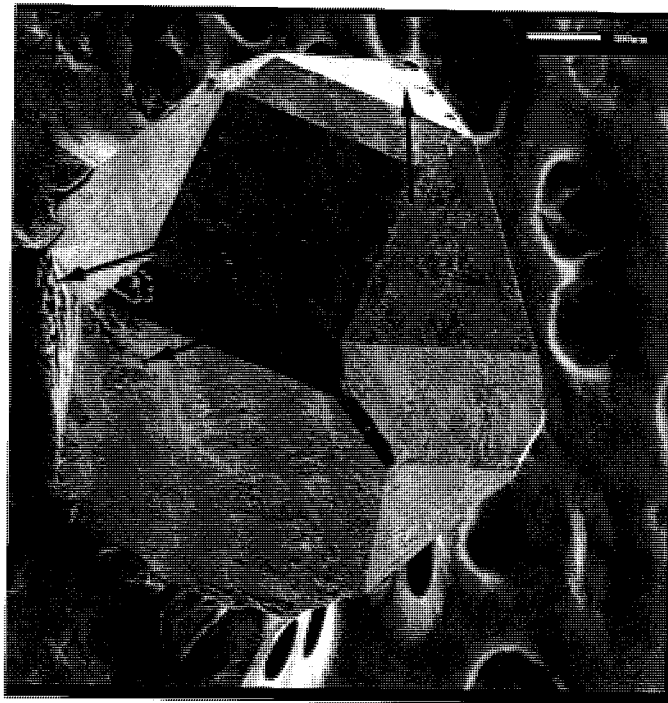
AJF 8-3



P= 7GPa
T= 1500C
t=4 hrs

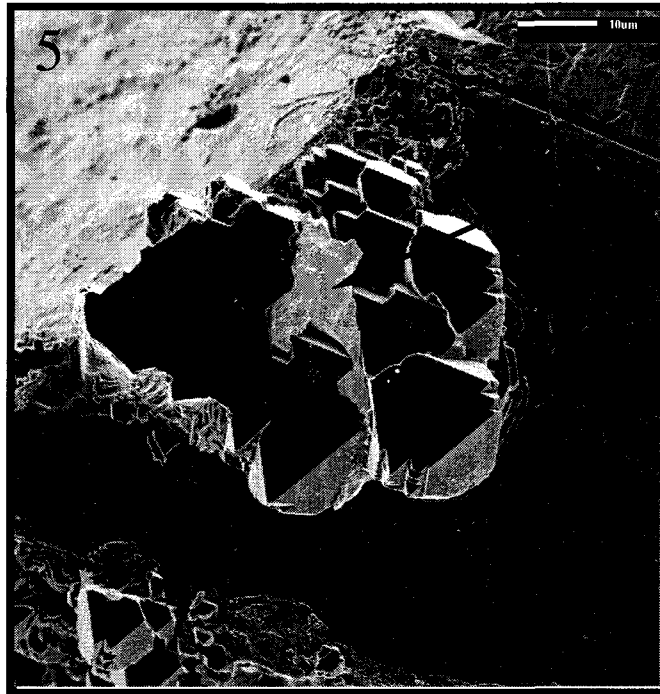
3+4: $\text{SiO}_2\text{-MgO-H}_2\text{O-KCl-C}$ system. Extensive growth observed on cubo-octahedral seed. Octahedral morphology of new growth. Wide angle of entire seed in picture 4, numerous areas of growth on one crystal.

AJF 8-3



P= 7GPa
T= 1500C
t=4 hrs

AJF 8-3

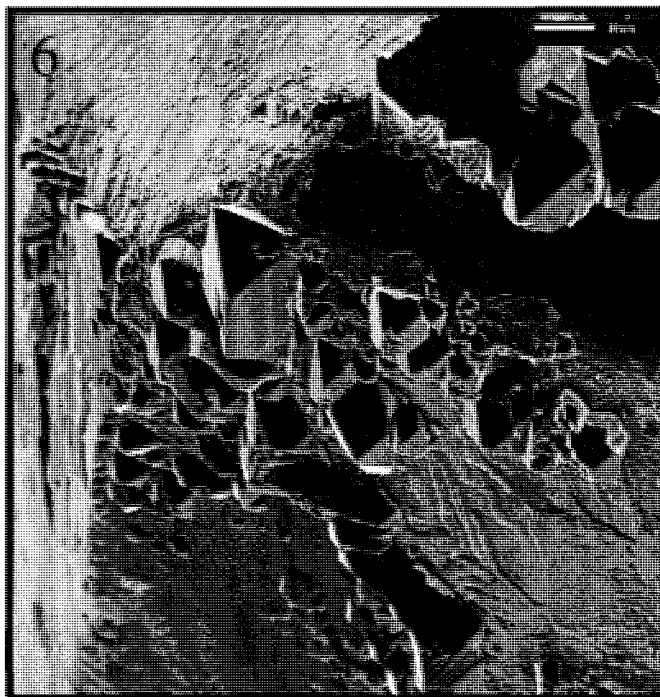


P= 7GPa
T= 1500C
t=4 hrs

SiO₂-MgO-H₂O-KCl-C system

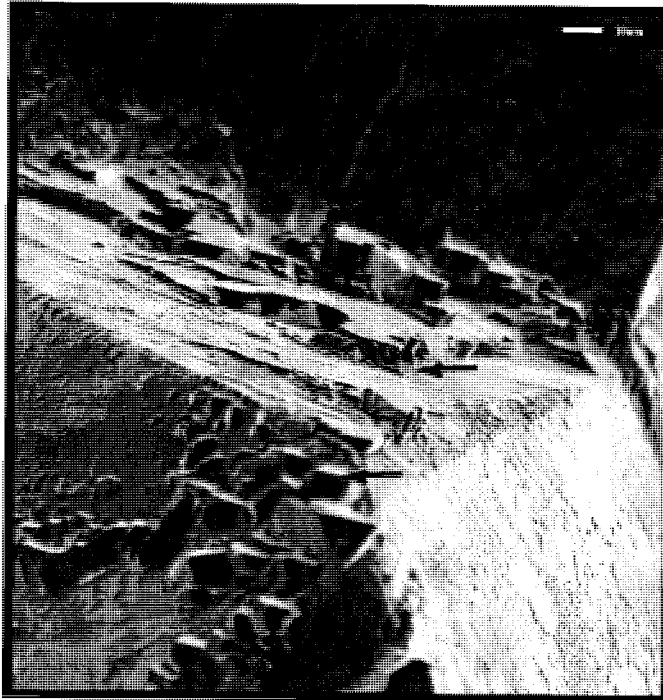
- 5: Octahedral crystals combining to form one single octahedral layer. Crystallographically aligned to seed crystal. Melt also evident.
6: Variation in growth sizes and centres. Extensive octahedral growth.

AJF 8-3



P= 7GPa
T= 1500C
t=4 hrs

AJF 8-3



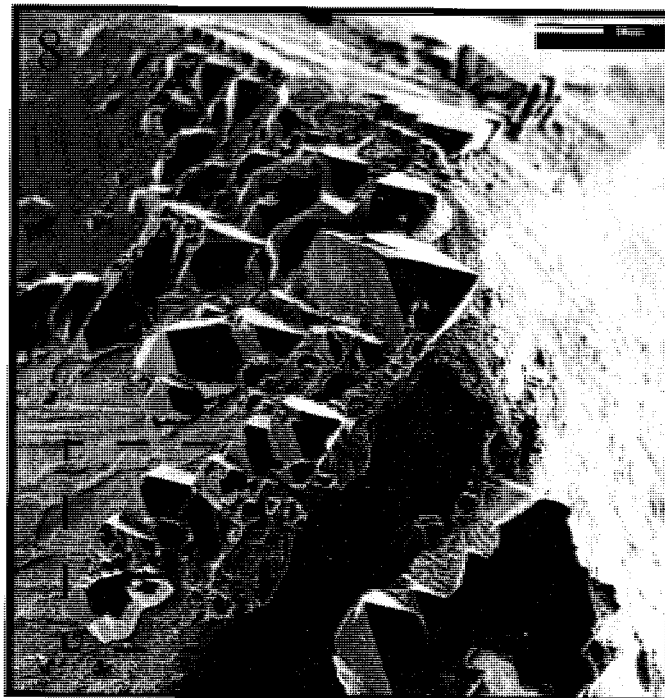
P= 7GPa
T= 1500C
t=4 hrs

SiO_2 -MgO- H_2O -KCl-C system

7: New growth layer, approx 5 microns thick caused by octahedral crystals merging.

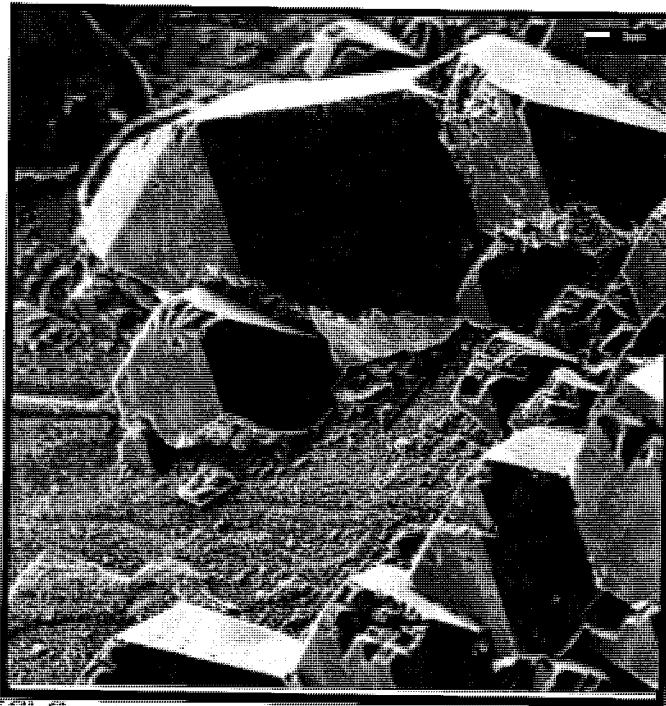
8: Spiral growth evident, dashed box. Also shown is the rough seed crystal surface

AJF 8-3



P= 7GPa
T= 1500C
t=4 hrs

AJF 8-3



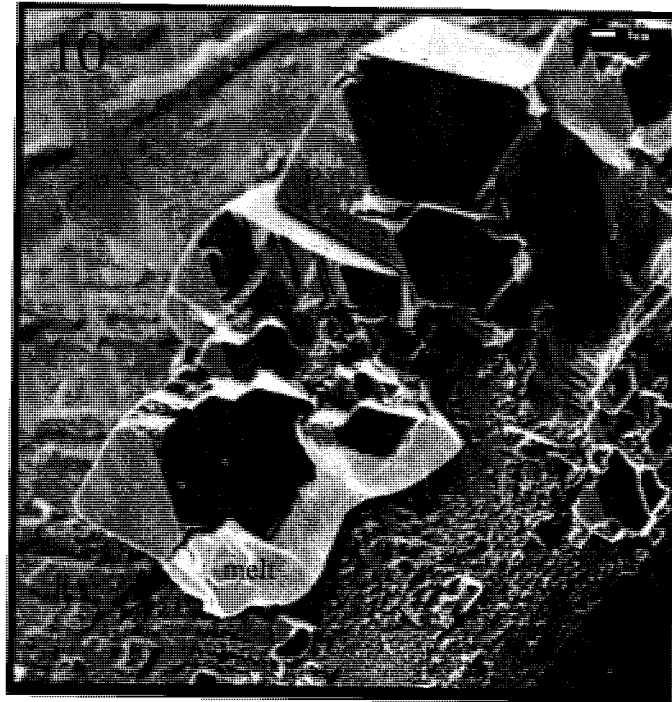
P= 7GPa
T= 1500C
t=4 hrs

SiO₂-MgO-H₂O-KCl-C system

9: Growth centers form around imperfections on seed diamond surface. Melt creates a highly reactive film around the seed surface.

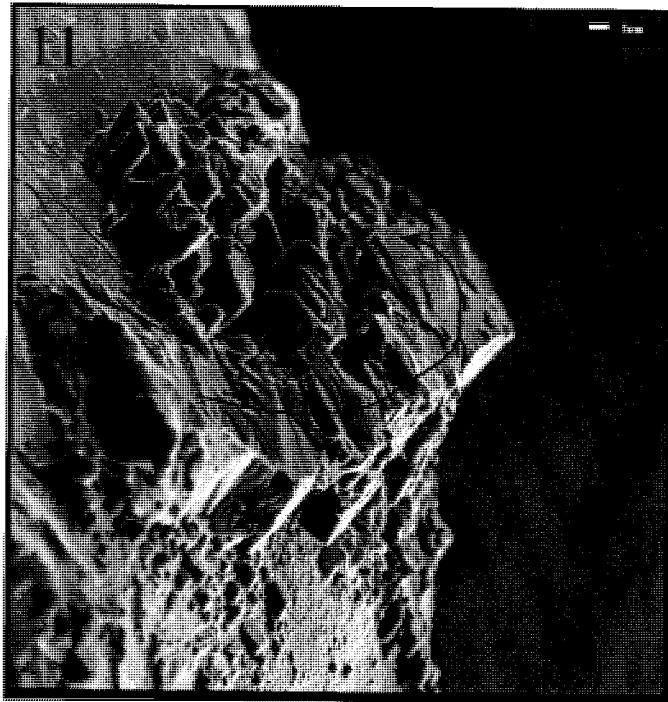
10: Layered or spiral growth, traditional crystal growth shown here (arrows). melt residue also highlighted.

AJF 8-3



P= 7GPa
T= 1500C
t=4 hrs

AJF 8-3



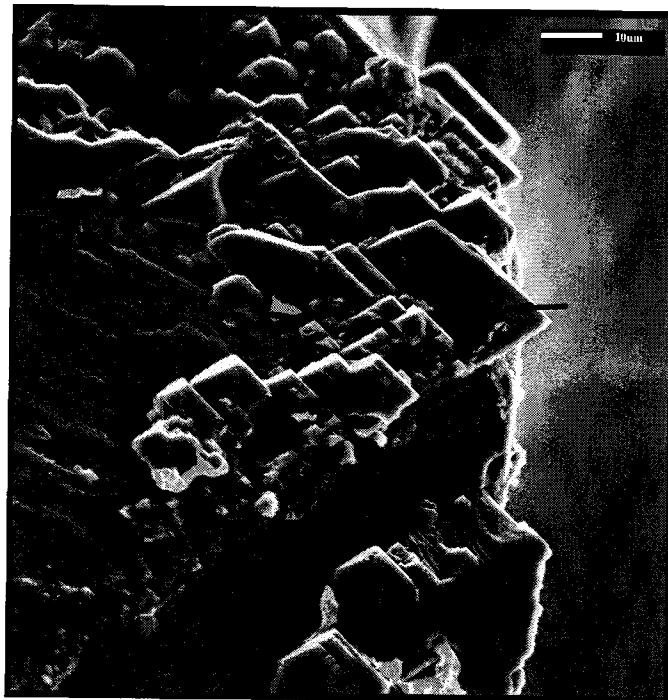
P= 7GPa
T= 1500C
t=4 hrs

SiO₂-MgO-H₂O-KCl-C system

11: Small crack in seed surface is replaced by large diamond growth feature clearly exhibiting spiral growth techniques.

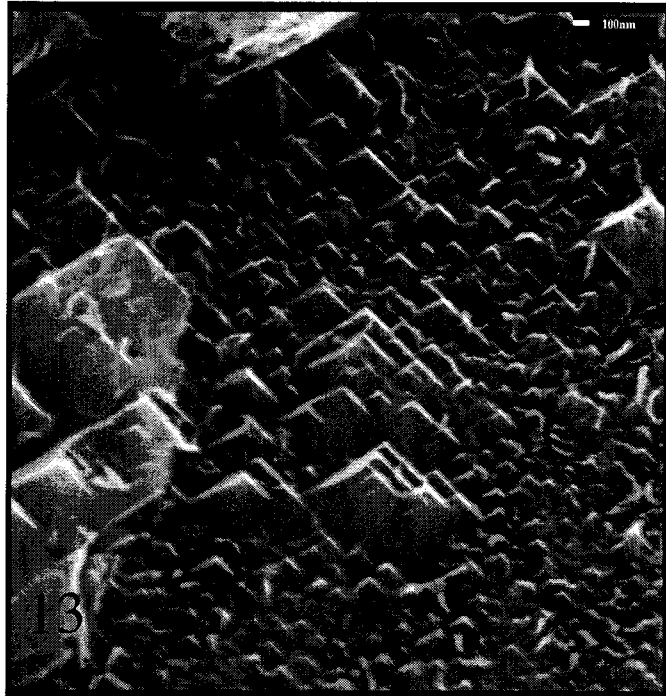
12: New octahedral diamonds.

AJF 8-3



P= 7GPa
T= 1500C
t=4 hrs

AJF 8-3



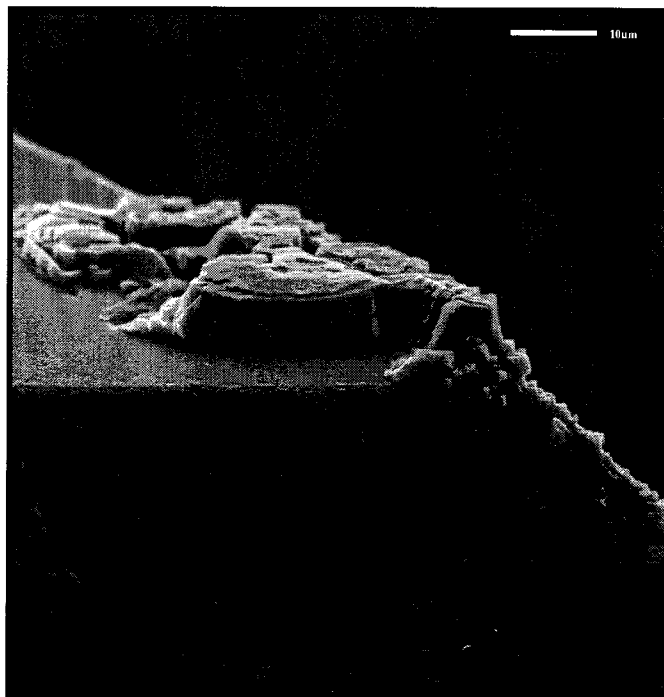
P= 7GPa
T= 1500C
t=4 hrs

SiO₂-MgO-H₂O-KCl-C system

13: Closeup shot of the diamond seed surface after experimentation.

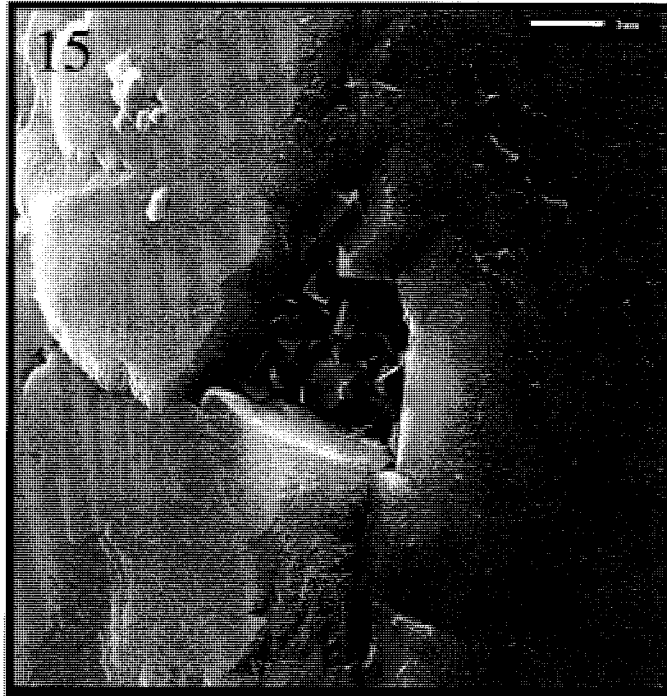
14: Edge of cubo-octahedral crystal showing growth preference on cubic faces.

AJF 8-3



P= 7GPa
T= 1500C
t=4 hrs

AJF 8-16



P= 7GPa
T= 1500C
t=4 hrs

SiO₂-MgO-H₂O-KCl-C system

15: Shows the hole in the diamond seed with smooth crystal faces either side.

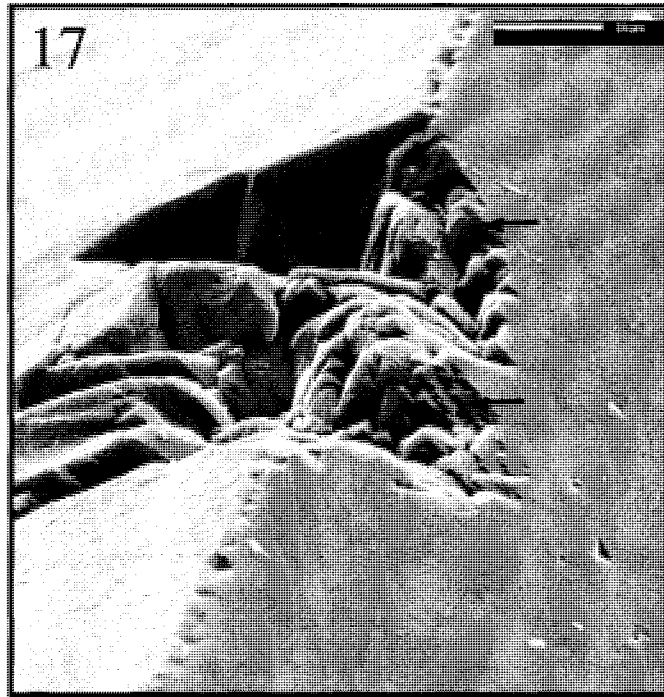
16: Hole in crystal creates ideal area for new growth to occur. Spontaneous octahedral crystals randomly oriented.

AJF 8-16



P= 7GPa
T= 1500C
t=4 hrs

AJF 8-16

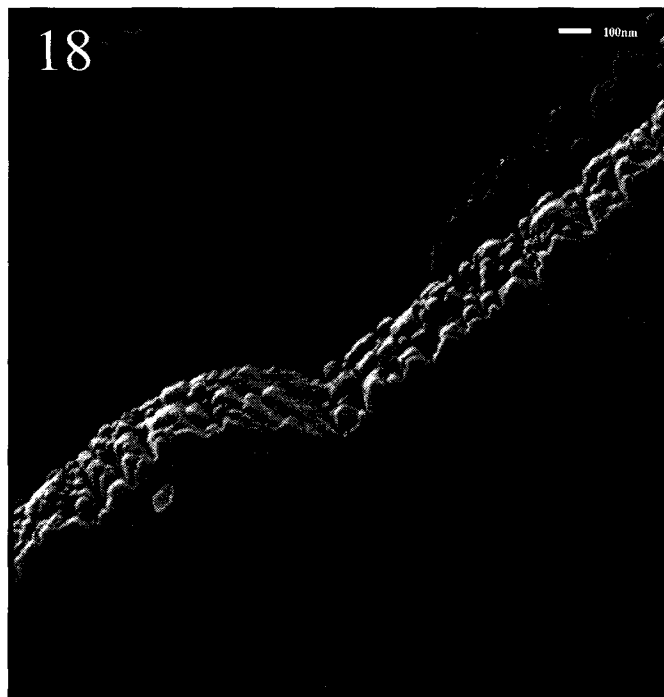


P= 7GPa
T= 1500C
t=4 hrs

SiO₂-MgO-H₂O-KCl-C system

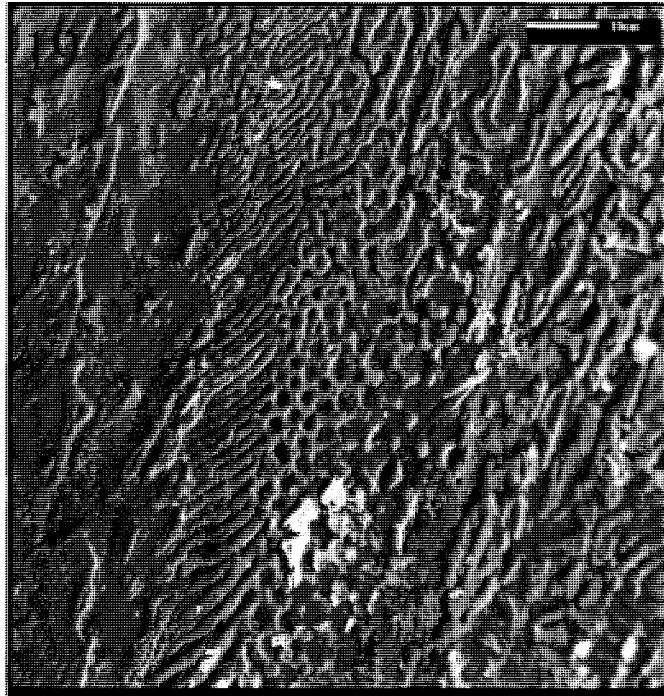
17: Pits and fractures along the crystal edges provide a place for new growth to begin.
18: Edge of a hole. This shows the growth of the diamond layers, rather than the fractured edge you would normally expect.

AJF 8-16



P= 7GPa
T= 1500C
t=4 hrs

AJF 8-14



P=7GPa
T=1500°C
t=4hrs

SiO₂-MgO-H₂O-KCl-C system

19: Non-growth surface on a seed, showing the 'dendritic' pattern which is characteristic of the rapid crystal growth used in HPHT synthesis.

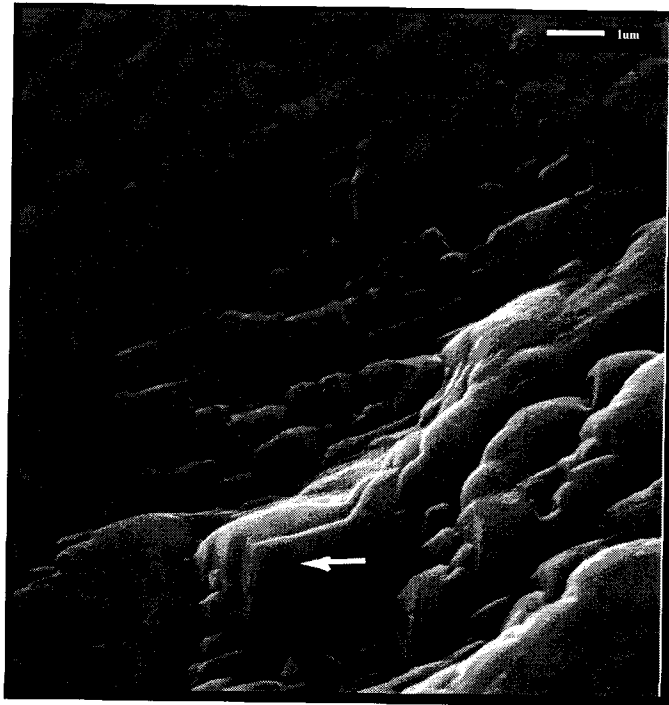
20: Extensive surface fracturing and blemishes, growth occurring where the crystal structure is rough enough .

AJF 8-14



P=7GPa
T=1500°C
t=4hrs

AJF 8-14



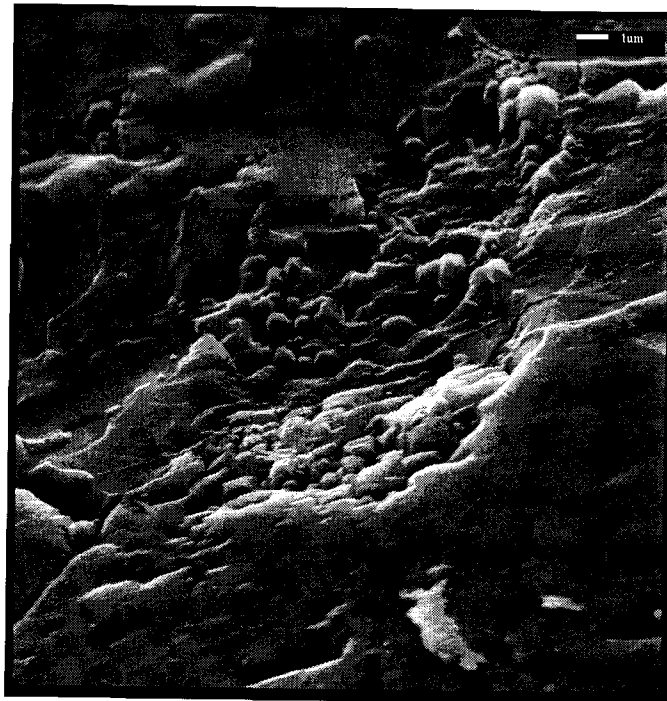
P=7GPa
T=1500°C
t=4hrs

SiO₂-MgO-H₂O-KCl-C system

21: Octahedral crystal growth alongside graphite.

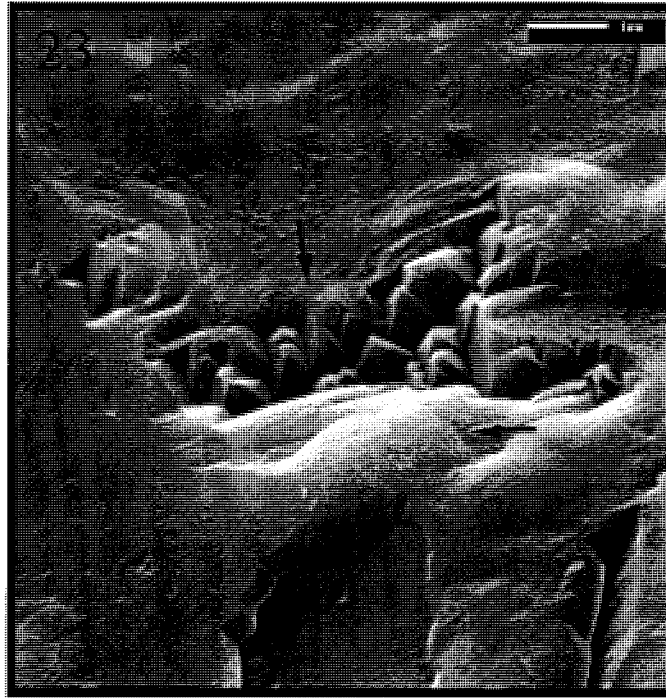
22: Irregular octahedral and cubo-octahedral growth in rough surface areas.

AJF 8-14



P=7GPa
T=1500°C
t=4hrs

AJF 8-14

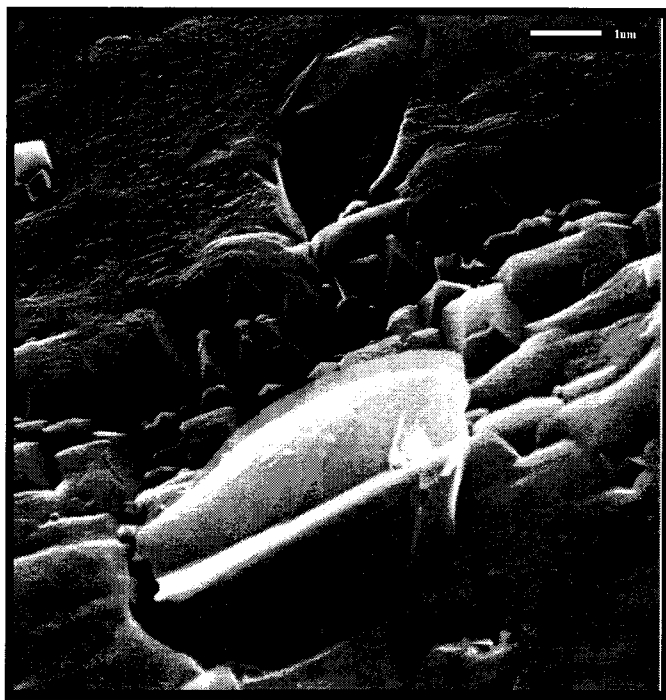


P=7GPa
T=1500°C
t=4hrs

SiO₂-MgO-H₂O-KCl-C system

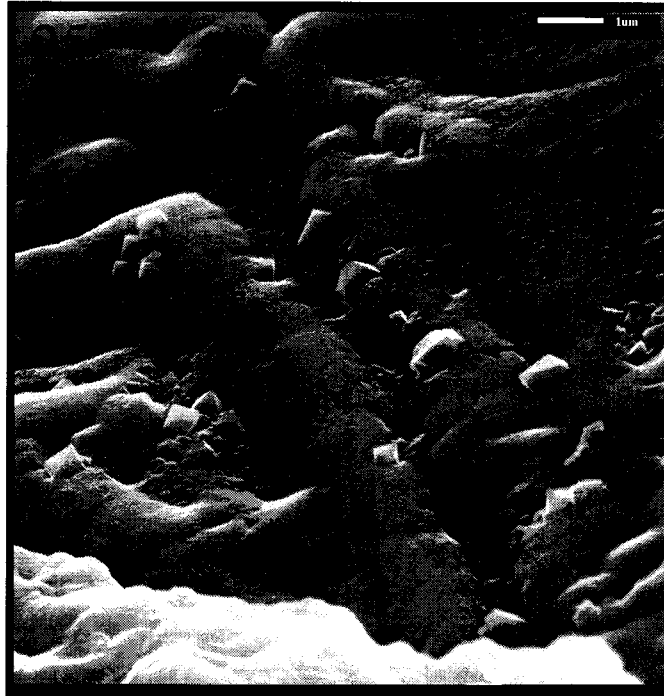
23 & 24: Smooth diamond seeds faces will not grow. However the edges of layers and in areas where the surface has been disturbed, growth can begin.

AJF 8-14



P=7GPa
T=1500°C
t=4hrs

AJF 8-14

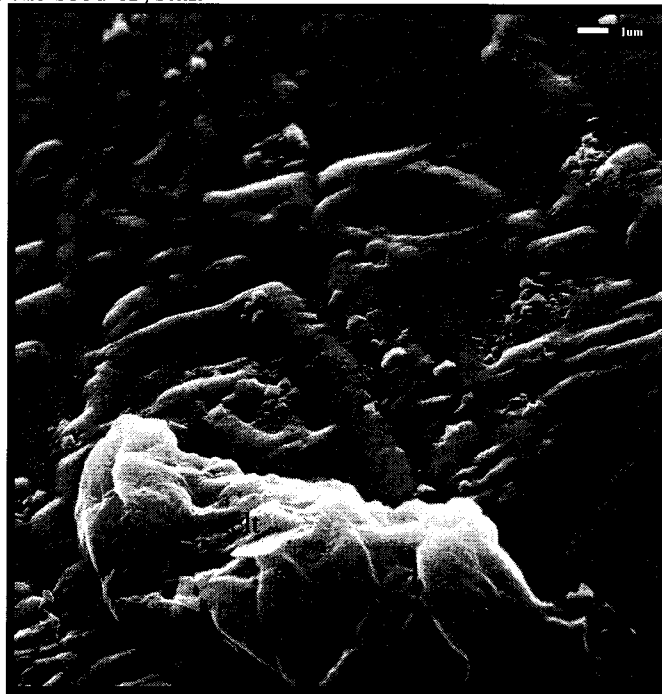


P=7GPa
T=1500°C
t=4hrs

SiO₂-MgO-H₂O-KCl-C system

25 & 26: Surfaces with pre-existing dendritic texture do nucleate and grow diamond crystals. Octahedral pits show where new diamonds have broken off the seed, leaving an indentation. It would be possible for these diamonds to then grow in the melt column after breaking off the seed crystal.

AJF 8-14



P=7GPa
T=1500°C
t=4hrs

AJF 8-14



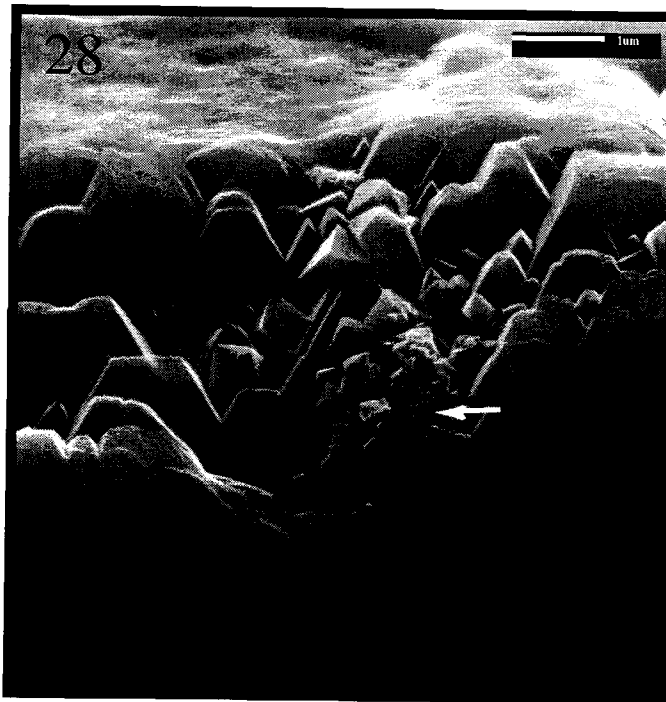
P=7GPa
T=1500°C
t=4hrs

SiO₂-MgO-H₂O-KCl-C system

27: Low magnification image of the dendritic patterns and their relationship to the new diamonds.

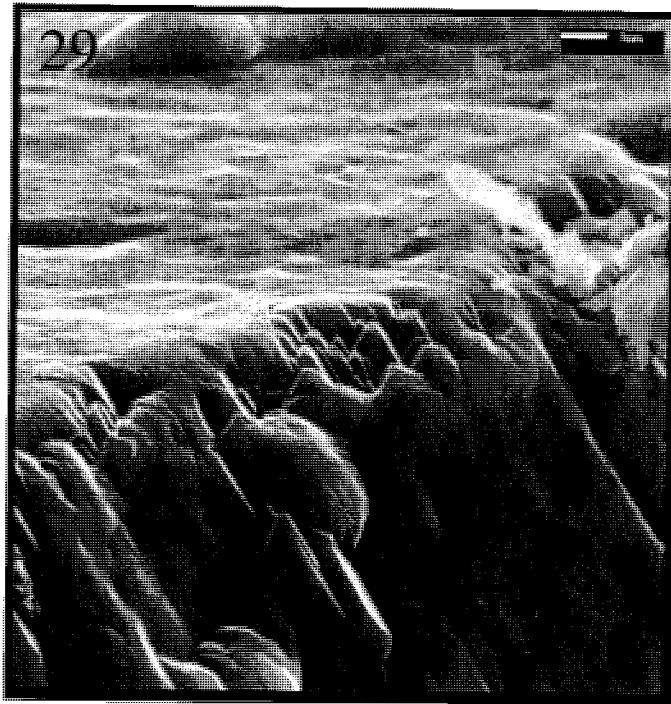
28: Edge of dendritic seed showing areas of sub-micron growth which have grown irregularly.

AJF 8-14



P=7GPa
T=1500°C
t=4hrs

AJF 8-14



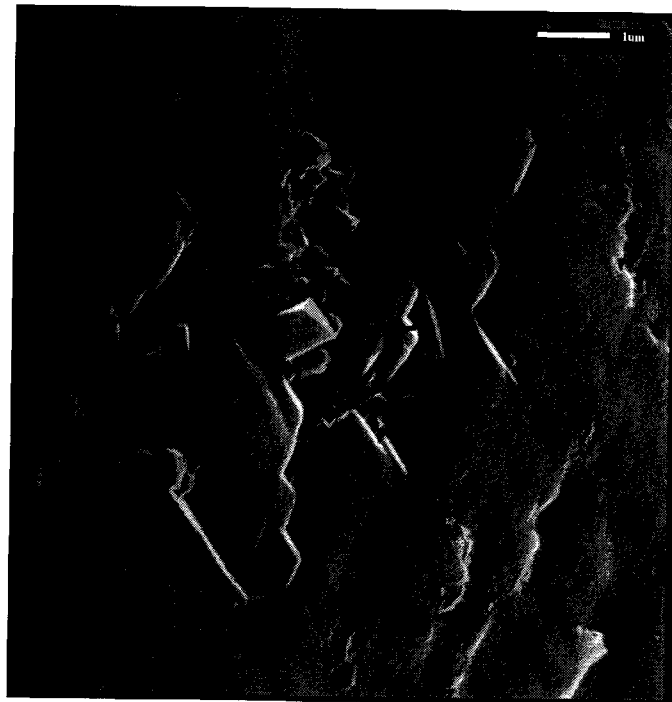
P=7GPa
T=1500°C
t=4hrs

SiO₂-MgO-H₂O-KCl-C system

29: Top and side faces of the seed crystal show smooth areas, while the edge provides a rough surface and is the easier place to start spiral-growth.

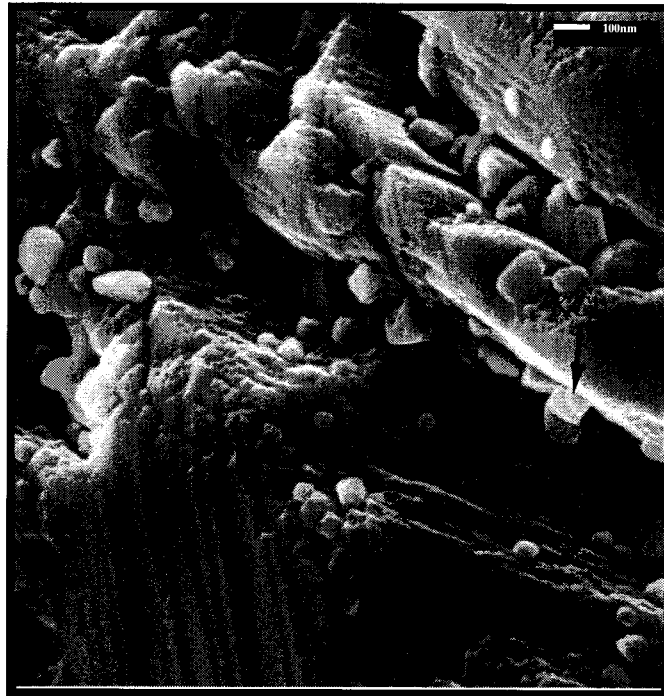
30: Octahedra crystallising in a surface irregularity.

AJF 8-14



P=7GPa
T=1500°C
t=4hrs

AJF 8-17



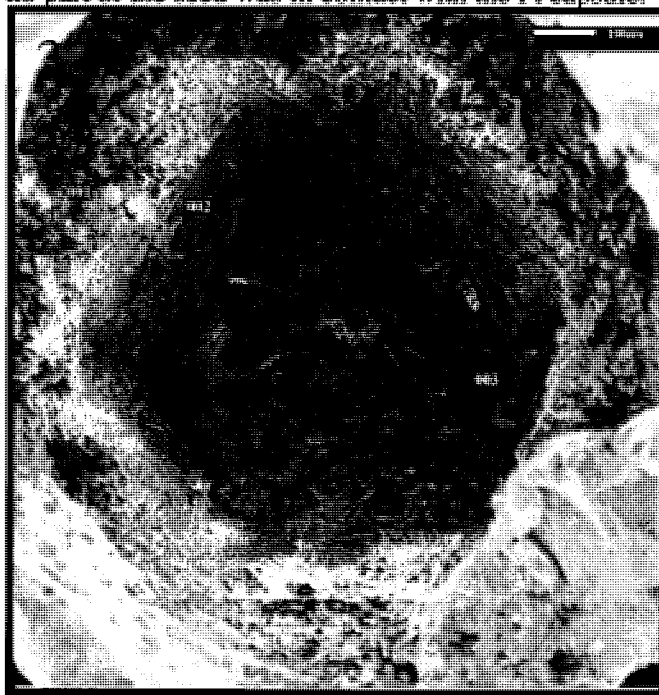
P=5.5GPa
T=1500°C
t=4hrs

SiO₂-MgO-H₂O-KCl-C system

31: Nano-layering of new diamond and KCl crystals

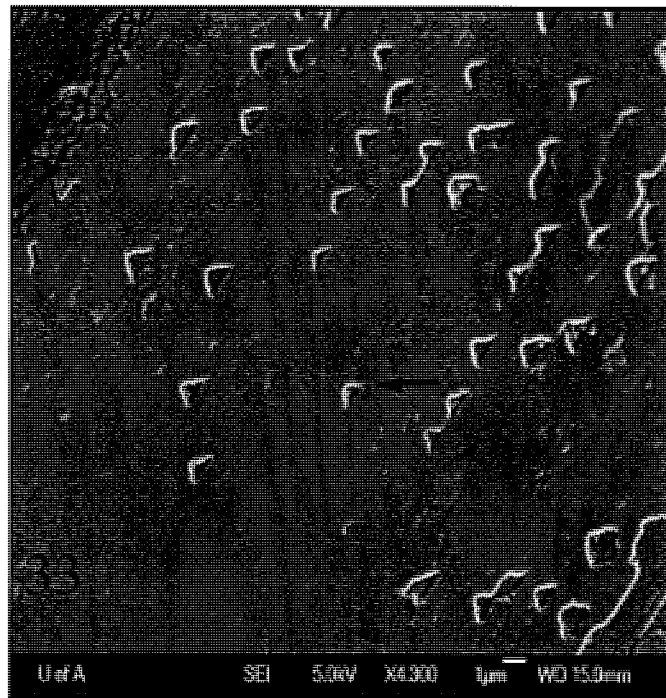
32: View inside a post-run capsule after diamond-seed removal, showing various layers. 001 layer - KCl+Silica rich, hydrous; 002 layer- mixing layer; 003 layer - mostly graphite. Upon quench no part of the seed was in contact with the Pt capsule.

AJF 11-1



P=7GPa
T=1500°C
t=4hrs

AJF 12-6

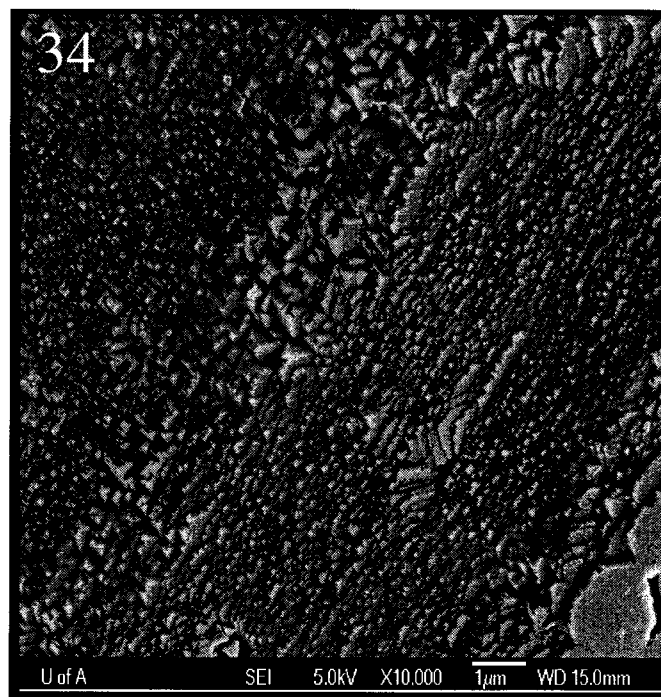


P=7GPa
T=1500C
t=4 hrs

33: MgO-SiO₂-H₂O-C-NaCl-[KCl] system. Negative trigons, aligned, resorption features in natural diamonds. This system only differs by the addition of NaCl to the starting composition.

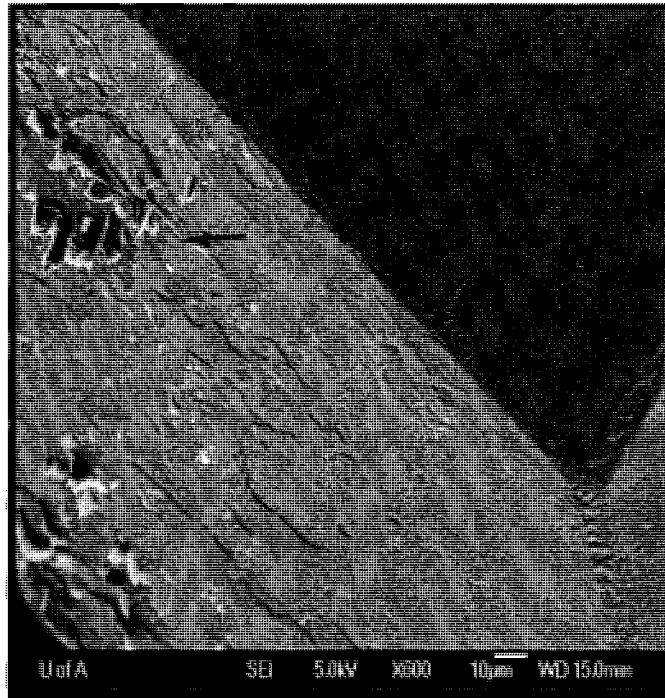
34: Very rough surface of seed crystal provides ideal nucleation points for new nm sized diamonds.

AJF 12-6



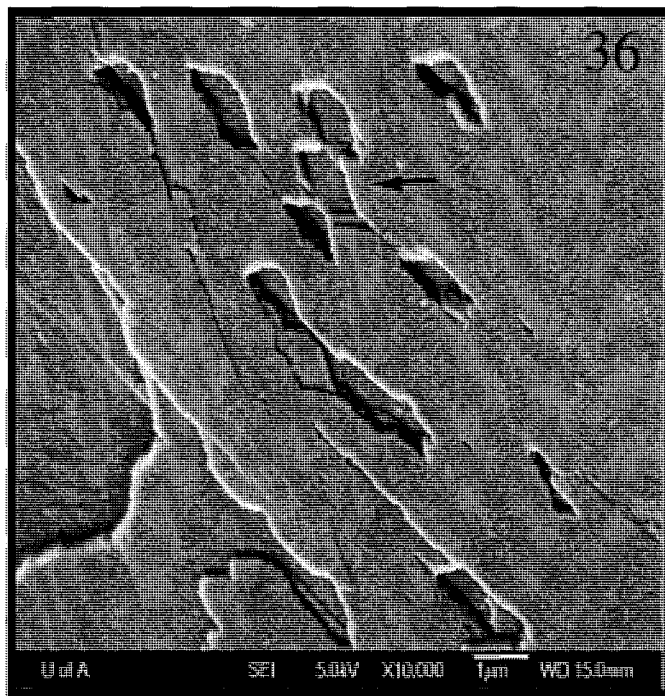
P=7GPa
T=1600C
t=4 hrs

AJF 12-6

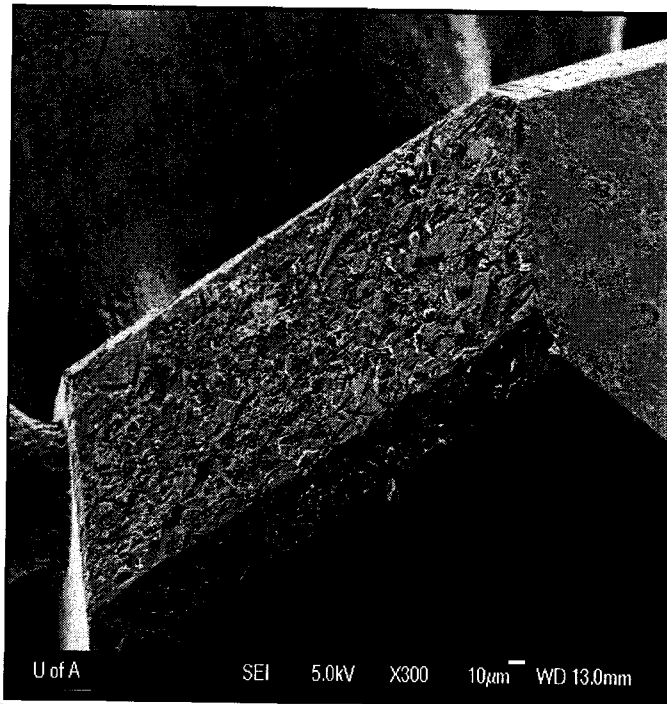


MgO-SiO₂-H₂O-C-NaCl-[KCl] system
35: No growth on smooth surface, only melt residue.
36: Dissolution hexagons, some stepped.

AJF 12-6



AJF 12-6

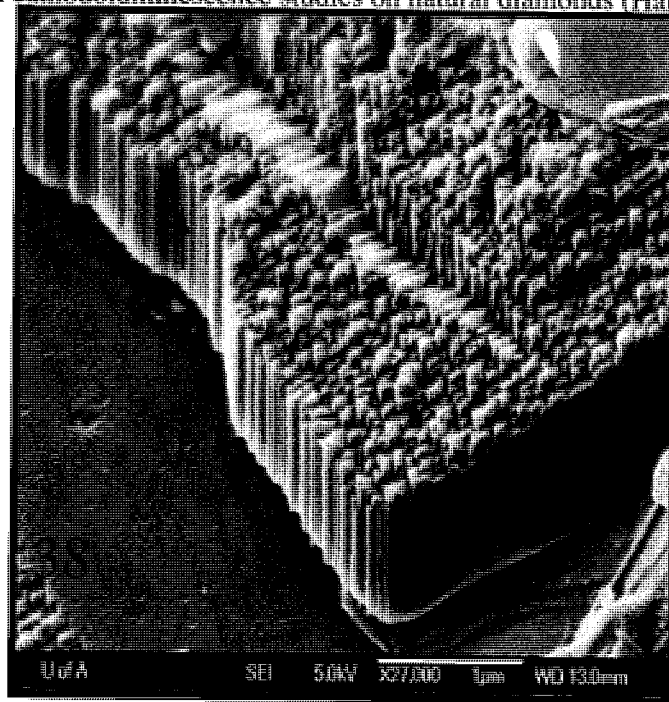


MgO-SiO₂-H₂O-C-NaCl-[KCl] system

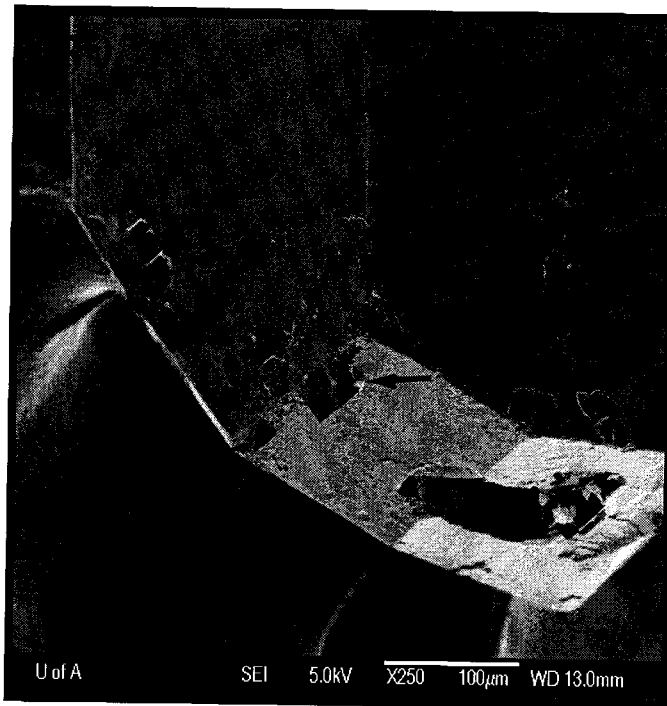
37: Graphite covering the lower face of the seed - from a layer similar to 003 in picture 32.

38: Stacked octahedral crystals make very fine nm thick layers. Similar features have been observed in cathodoluminescence studies on natural diamonds (Harte et al. 1999).

AJF 12-6



AJF 12-7



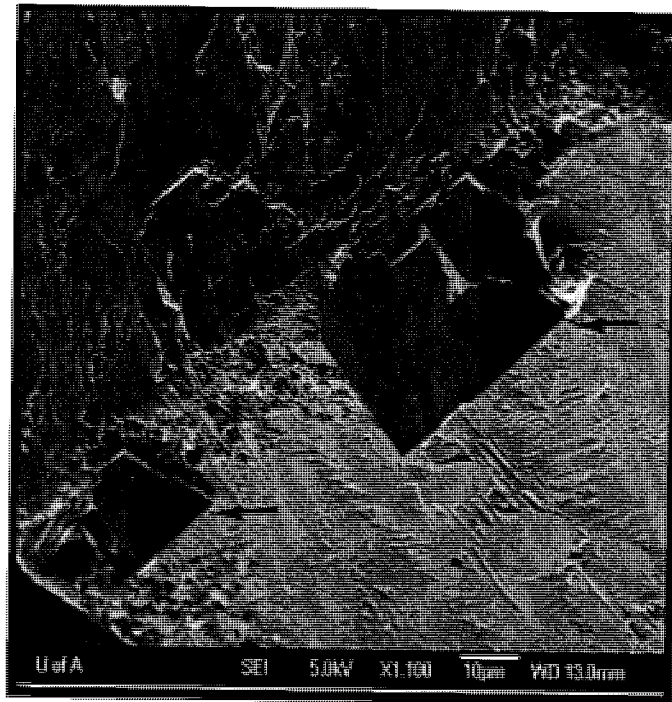
P=7GPa
T=1600C
t=4 hrs

MgO-SiO₂-H₂O-C-NaCl-[KCl] system

39: Extensive octahedral growth from a cubo-octahedral crystal edge. New octahedral layers are also shown.

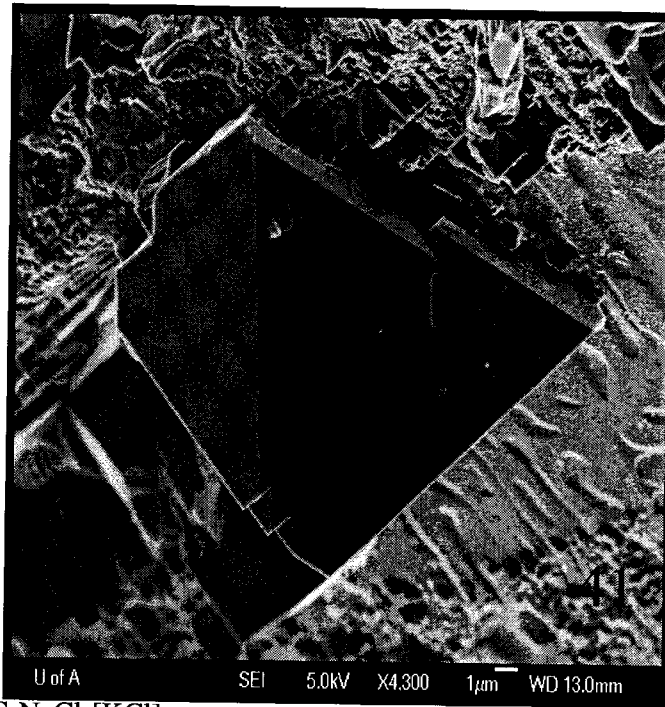
40: Closeup of the various growth styles - layering and single octahedral crystal growth.

AJF 12-7



P=7GPa
T=1600C
t=4 hrs

AJF 12-7



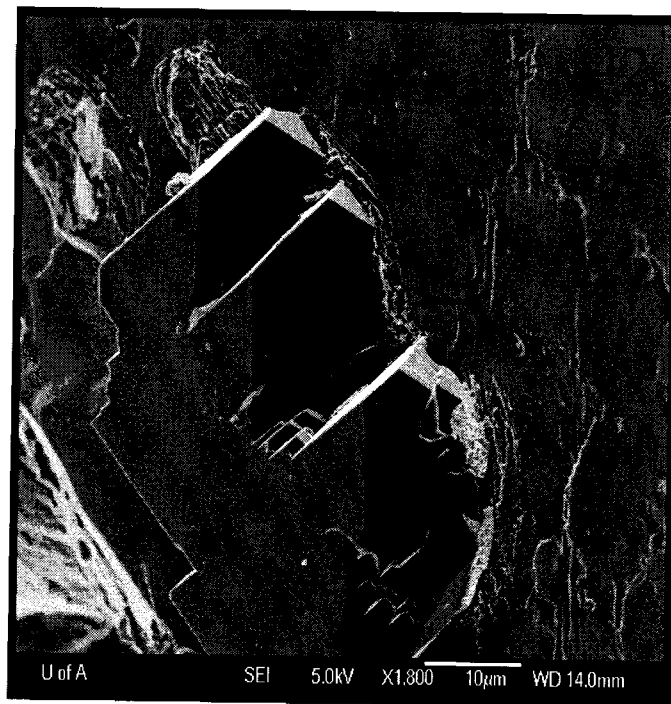
P=7GPa
T=1600C
t=4 hrs

MgO-SiO₂-H₂O-C-NaCl-[KCl] system

41: Large octahedral crystal, grown by spiral growth. Also shown is the growing diamond seed surface.

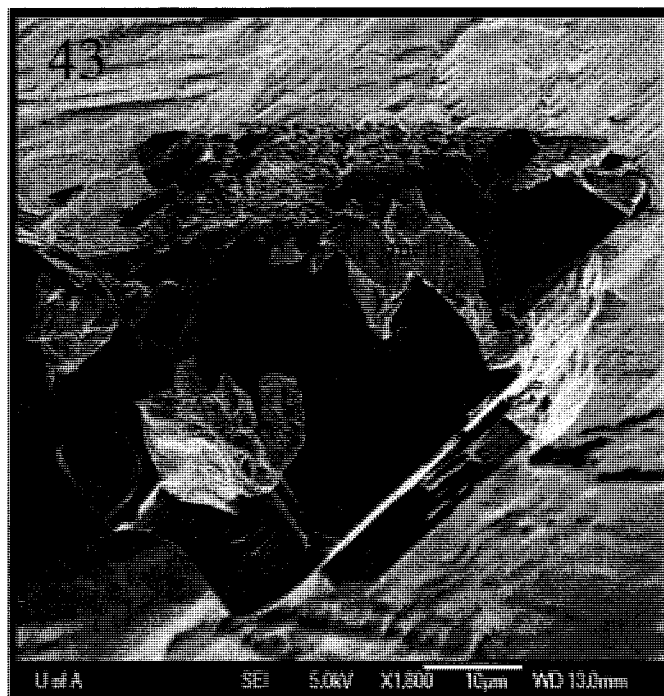
42: Layer of graphite observed around the new diamond growth area.

AJF 12-7



P=7GPa
T=1600C
t=4 hrs

AJF 12-7



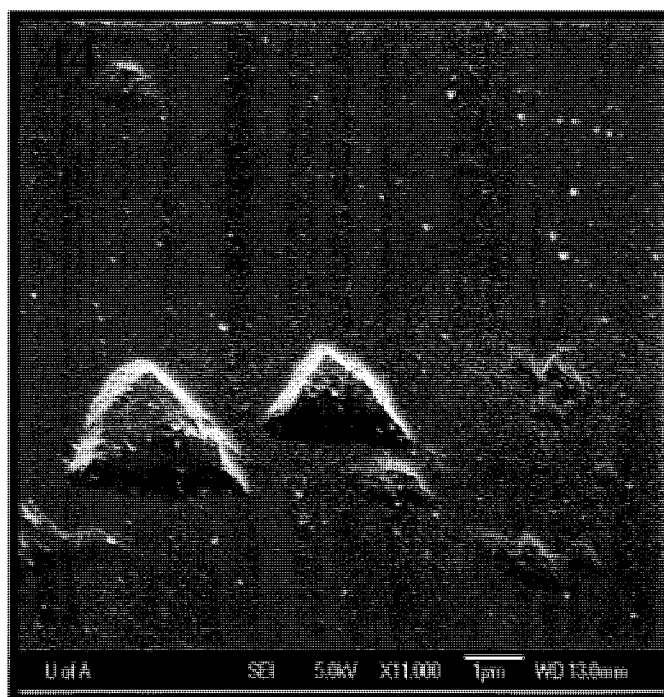
P=7GPa
T=1600C
t=4 hrs

MgO-SiO₂-H₂O-C-NaCl-[KCl] system

43: Melt/diamond interface is seen as a rough layer of misaligned octahedral crystals.

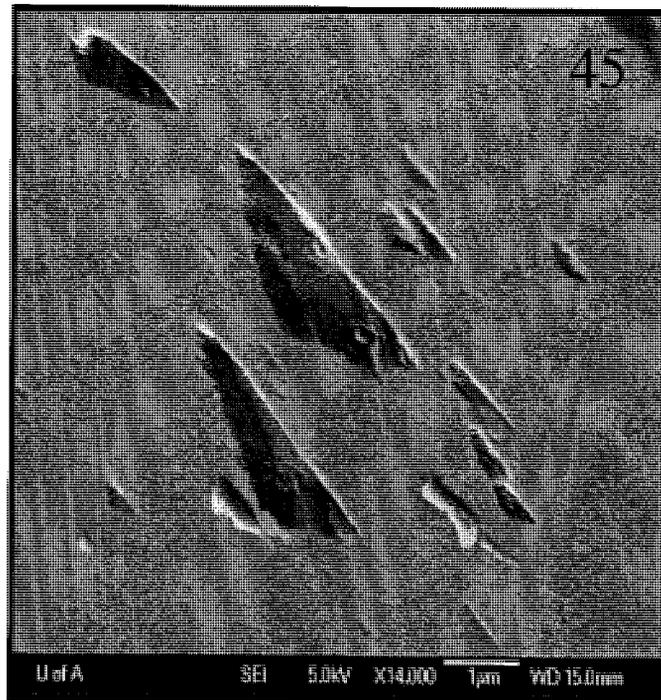
44: Negative trigons closeup - shows some of the carbon from the seed entered the melt while growth was occurring on other faces.

AJF 12-8



P=7GPa
T=1600C
t=4 hrs

AJF 12-8



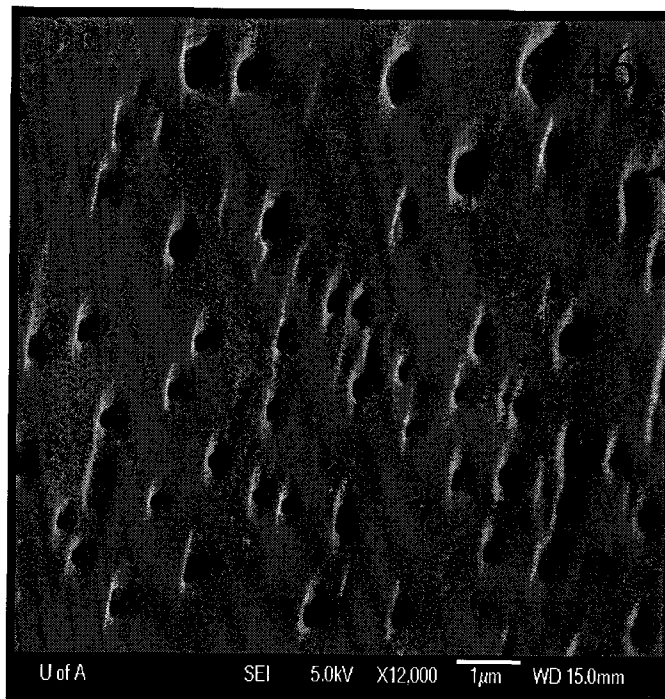
P=7GPa
T=1600C
t=4 hrs

MgO-SiO₂-H₂O-C-NaCl-[KCl] system

45: Excellent example of trigons on the seed diamond - dissolution/etch must be occurring in this system.

46: Dissolution holes.

AJF 12-8



P=7GPa
T=1600C
t=4 hrs

AJF 11-4

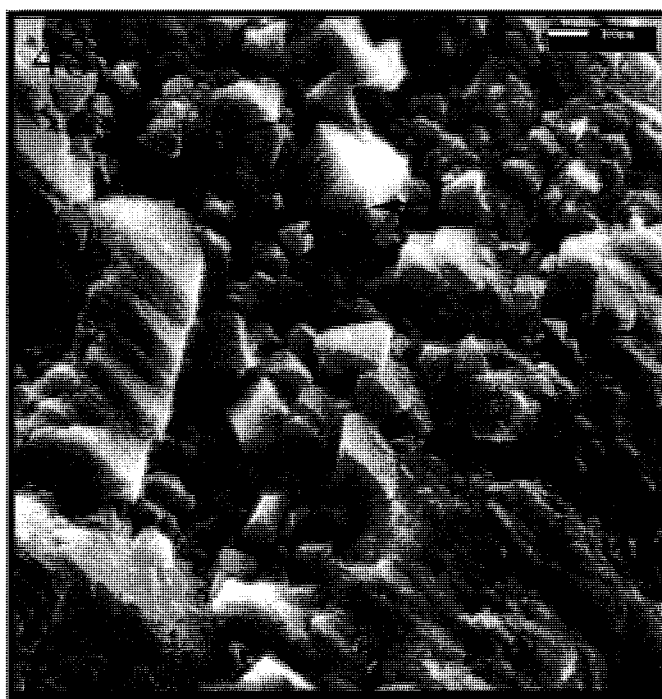


P=7GPa
T=1500C
t=4 hrs

MgO-SiO₂-H₂O-C-NaCl-[KCl] system

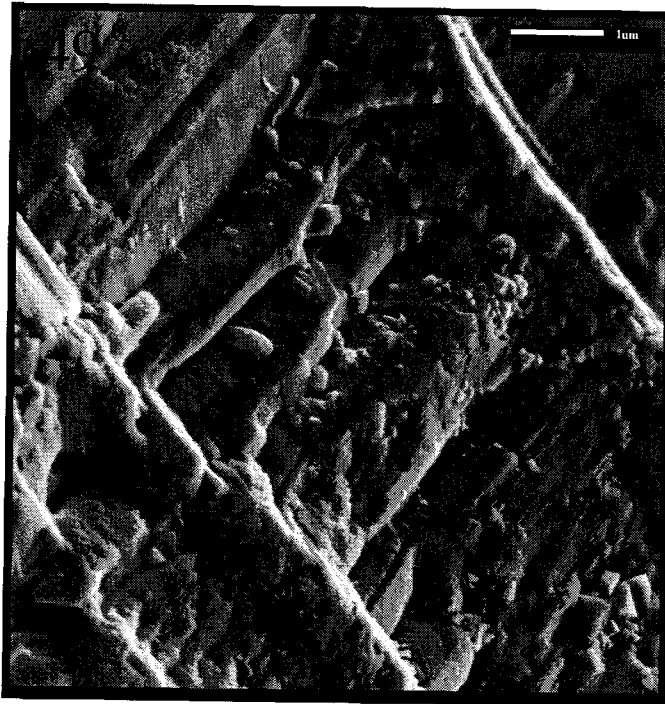
47 & 48: Stacking of octahedral crystals to form layers (top arrows). Some misaligned spontaneous octahedra are also present (lower arrow).

AJF 11-4



P=7GPa
T=1500C
t=4 hrs

AJF 11-4



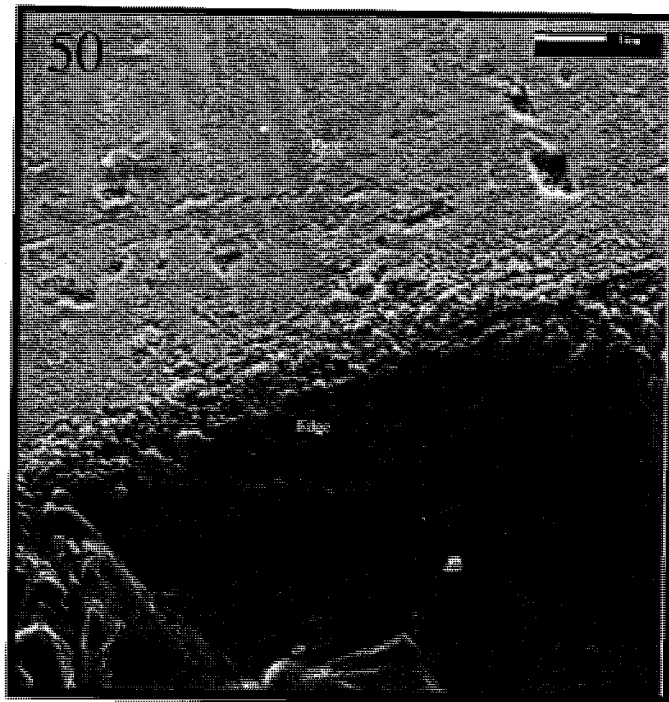
P=7GPa
T=1500C
t=4 hrs

MgO-SiO₂-H₂O-C-NaCl-[KCl] system

49: Fracture surface on the diamond seed with extensive small new diamond octahedra and layer octahedral growth.

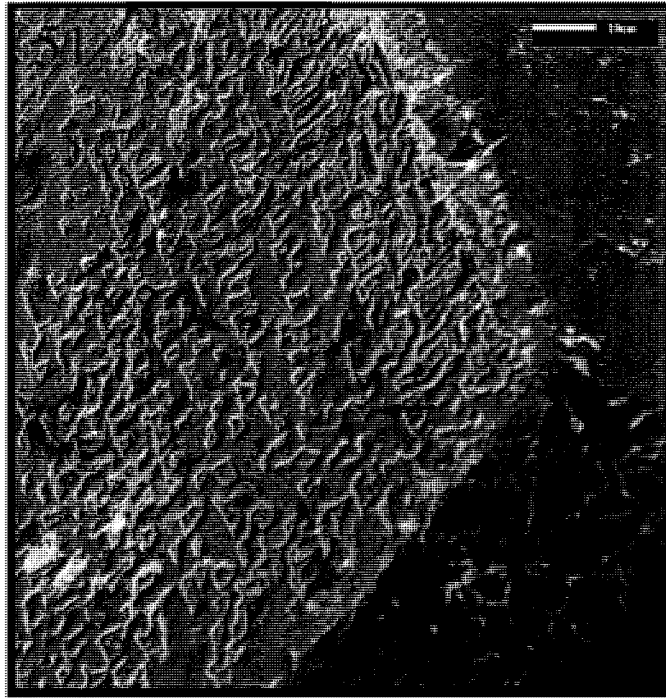
50: Growth enhancing rough surfaces on the seed crystal after experimentation

AJF 11-4



P=7GPa
T=1500C
t=4 hrs

AJF 11-4

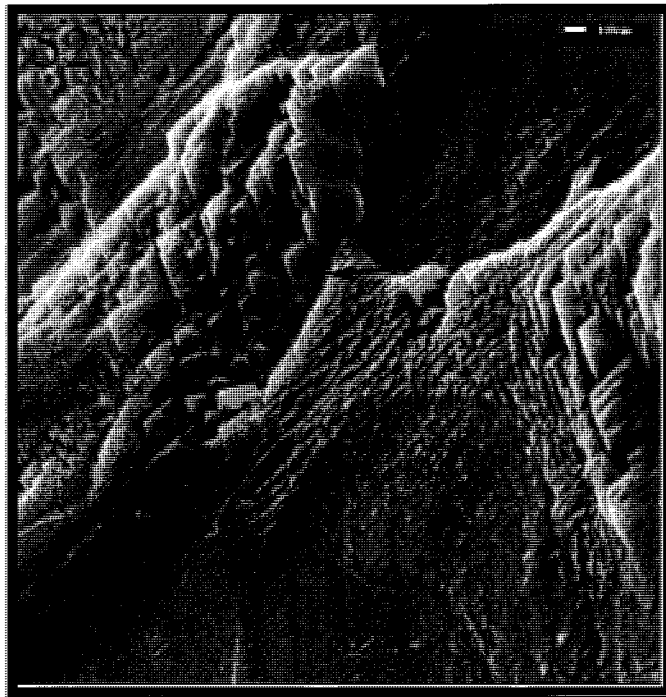


P=7GPa
T=1500C
t=4 hrs

MgO-SiO₂-H₂O-C-NaCl-[KCl] system

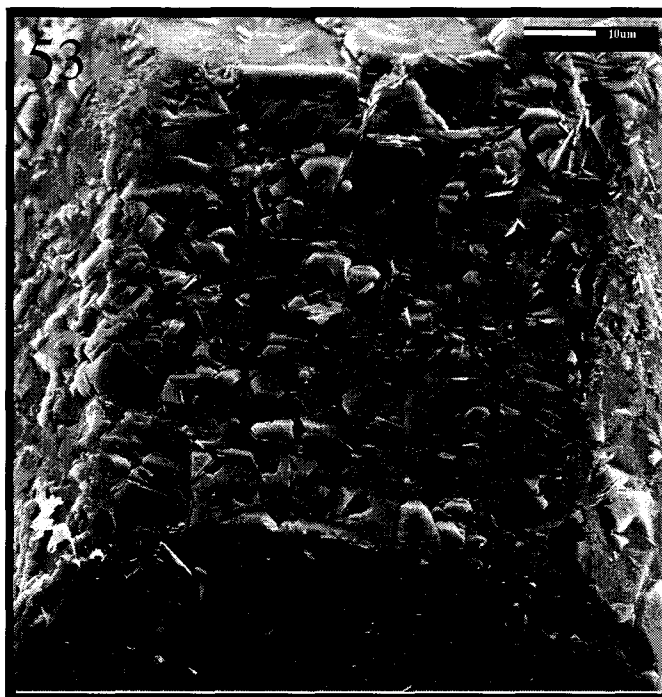
51 & 52: Stacks of Octahedral crystals (Picture 52) create isolated 'pods' that will eventually amalgamate as a new surface layer.

AJF 11-4



P=7GPa
T=1500C
t=4 hrs

AJF 11-1



P=7GPa
T=1500C
t=4 hrs

MgO-SiO₂-H₂O-C-NaCl-[KCl] system

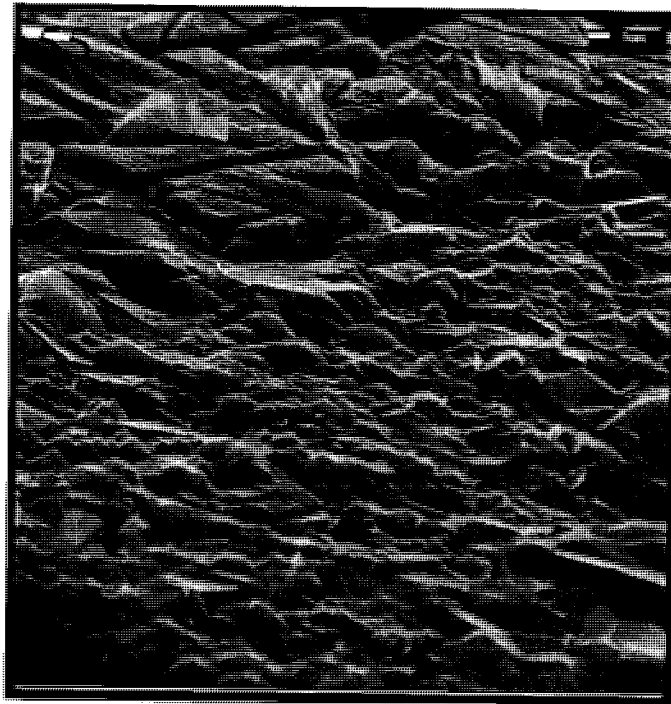
53 & 54: Mixture of diamond and graphite flakes adhering to the base of a seed. Closeup below.

AJF 11-1



P=7GPa
T=1500C
t=4 hrs

AJF 11-1



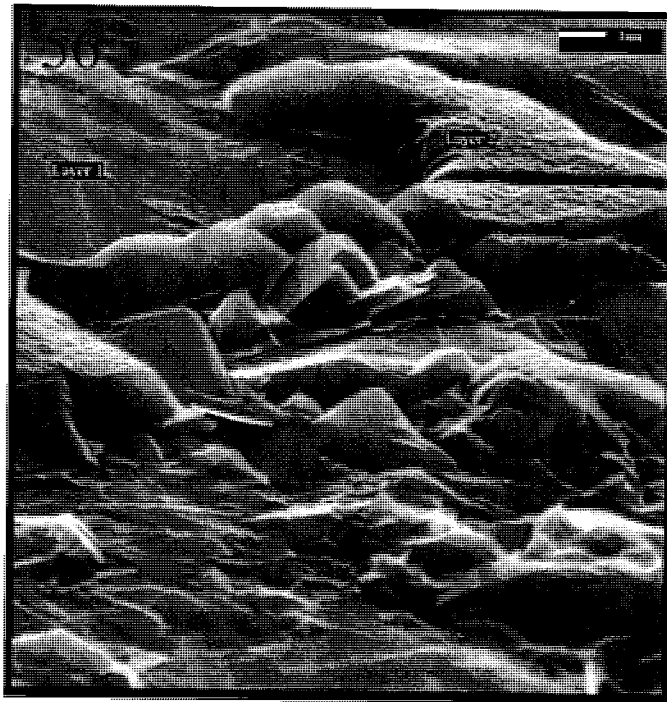
P=7GPa
T=1500C
t=4 hrs

MgO-SiO₂-H₂O-C-NaCl-[KCl] system

55: Closeup of a diamond seed surface post-run showing new layers of diamond

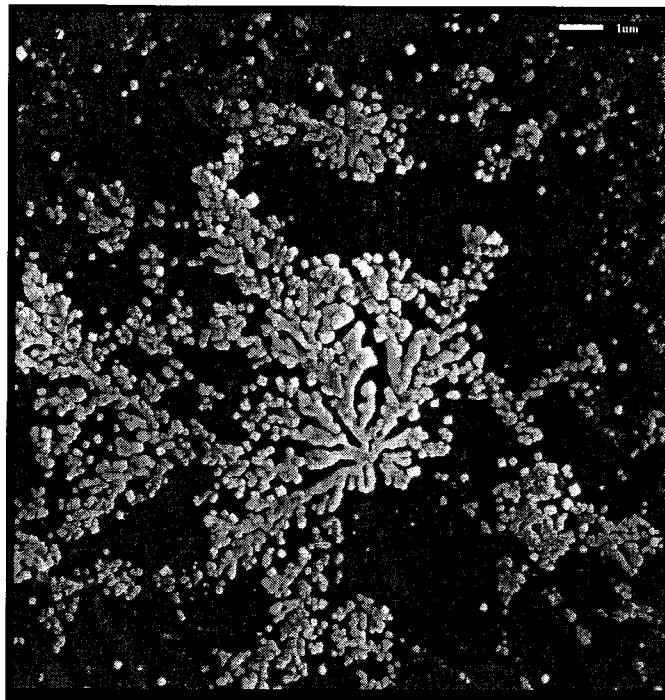
56: Two distinct layers of diamond with graphite sheets in the foreground.

AJF 11-1



P=7GPa
T=1500C
t=4 hrs

AJF 11-3



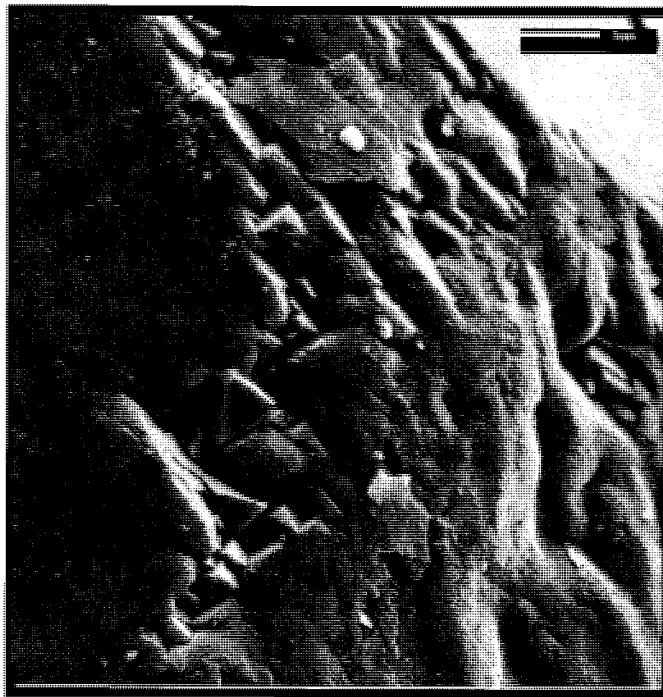
P=7GPa
T=1400C
t=4 hrs

MgO-SiO₂-H₂O-C-NaCl-[KCl] system

57: Salt (NaCl & KCl) crystals crystallised on the surface of a smooth seed face

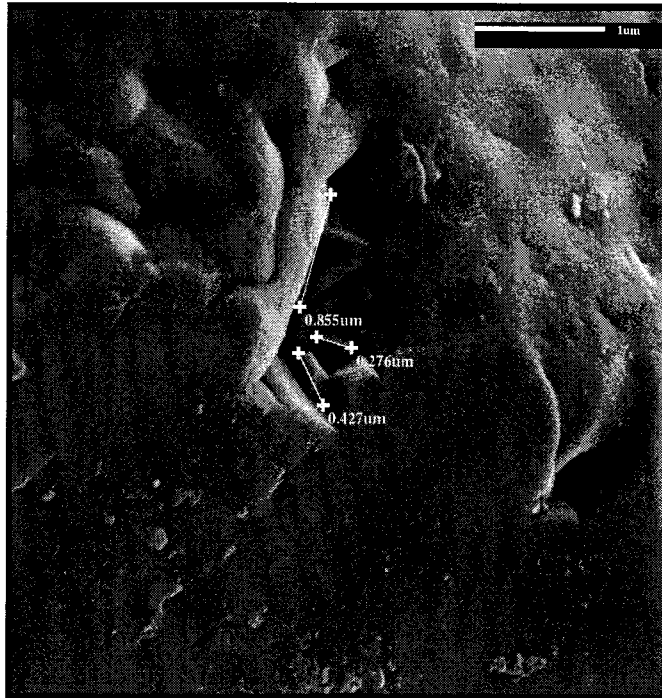
58: MgO-SiO₂-H₂O-C system - growth in a surface defect is also possible without any halide catalysts, the temperature does need to be high however.

AJF 6-3



P=7GPa
T=1500C
t=4hrs

AJF 6-3



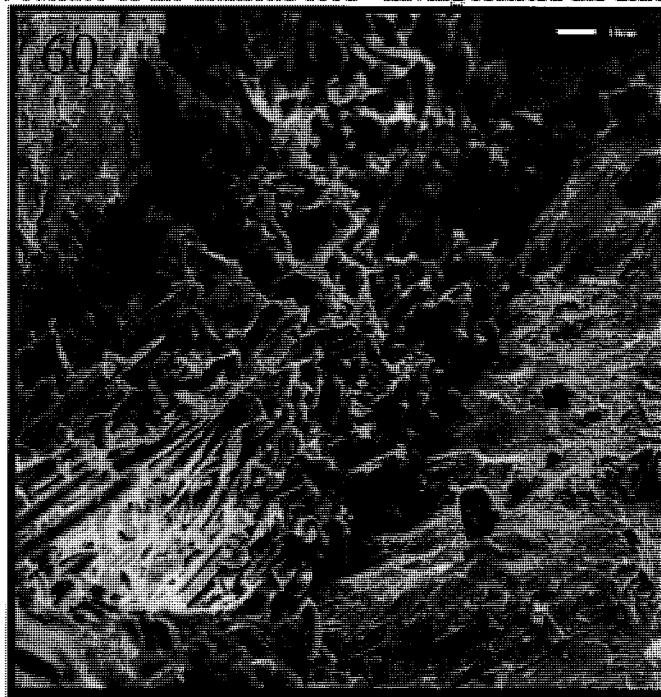
P=7GPa
T=1500C
t=4hrs

MgO-SiO₂-H₂O-C system

59: Non-Catalysed System, some measurements on the new crystal growth.

60: Melt quench crystals. Forsteritic Olivine, Enstatite OPX, an amorphous magnesian hydrous phase and carbon. Shown here is a typical quench glass, this was residing in a small crack on the surface of the diamond seed - having resisted the ultrasonic bath.

AJF 6-3



P=7GPa
T=1500C
t=4hrs

References:

Harte, B; Fitzsimons, W.C; Harris, J.W; Otter, M.L (1999) Carbon isotope ratios and nitrogen abundances in relation to cathodoluminescence characteristics for some diamonds from Kaapvaal province, S. Africa; Mineralogical magazine, 63 (6):829-856